SEISMIC FRAGILITY ESTIMATES FOR REINFORCED CONCRETE FRAMED BUILDINGS

A Dissertation

by

SATHISH KUMAR RAMAMOORTHY

Submitted to the Office of Graduate Studies of
Texas A&M University
in partial fulfillment of the requirements for the degree of

DOCTOR OF PHILOSOPHY

December 2006

Major Subject: Civil Engineering

SEISMIC FRAGILITY ESTIMATES FOR REINFORCED CONCRETE FRAMED BUILDINGS

A Dissertation

by

SATHISH KUMAR RAMAMOORTHY

Submitted to the Office of Graduate Studies of
Texas A&M University
in partial fulfillment of the requirements for the degree of

DOCTOR OF PHILOSOPHY

Approved by:

Co-Chairs of Committee,	Joseph M. Bracci
	Paolo Gardoni
Committee Members,	Mary Beth D. Hueste
	Michael Sherman
Head of Department,	David Rosowsky

December 2006

Major Subject: Civil Engineering

ABSTRACT

Seismic Fragility Estimates for Reinforced Concrete Framed Buildings.

(December 2006)

Sathish Kumar Ramamoorthy, B.E., University of Madras, India;

M.E., Indian Institute of Science, India;

M.S., University of Nebraska

Co-Chairs of Advisory Committee: Dr. Joseph M. Bracci
Dr. Paolo Gardoni

Gravity load designed (GLD) reinforced concrete (RC) buildings represent a common type of construction in the Mid-America Region. These buildings have limited lateral resistance and are susceptible to story mechanisms during earthquake loading. Fragility estimates are developed to assess the seismic vulnerability of GLD RC buildings in the Mid-America Region. Fragility is defined as the conditional probability of reaching or exceeding a performance level for a given earthquake intensity measure.

Five sample buildings of various story heights (1, 2, 3, 6, and 10 stories) are used to represent generic RC frame buildings of 1 to 10 stories tall. A Bayesian methodology is used to develop probabilistic demand models to predict the maximum inter story drift given the spectral acceleration at the fundamental period of the building. The unknown parameters of the demand models are estimated using the simulated response data obtained from nonlinear time history analyses of the structural models for a suite of synthetic ground motions, developed for Memphis, Tennessee. Seismic structural capacity values are selected corresponding to the performance levels or damage states as specified in FEMA-356 and as computed by nonlinear pushover analyses.

For the sample buildings, fragility estimates are developed using the predicted drift demands and structural capacity values. Confidence bounds are developed to represent the epistemic uncertainty inherent in the fragility estimates. In addition, bivariate

fragility estimates, formulated as a function of spectral acceleration and the fundamental building period, are developed from the fragility estimates of the individual buildings. The bivariate fragilities can be used to quantify the seismic vulnerability of GLD RC frame buildings of 1 to 10 stories. Using the Bayesian approach, a framework is developed to update the analytical fragility estimates using observed damage data or experimental test data. As an illustration of the updating framework, the analytical bivariate fragility estimates for the sample buildings in the Mid-America Region are updated using the damage data obtained from 1994 Northridge, California earthquake.

Furthermore, to investigate and demonstrate the increase in seismic performance of the GLD RC frame buildings, the columns of the 2 and 3 story buildings are retrofitted by column strengthening. Fragility estimates developed for the retrofitted buildings show the effectiveness of the retrofit technique by the improved seismic performance of GLD RC frame buildings.

ACKNOWLEDGMENTS

I would like to thank Dr. Joseph M. Bracci and Dr. Paolo Gardoni for their guidance and academic support throughout my graduate studies and research. I am especially grateful for the freedom they gave me to explore this topic while helping me maintain focus and overcome difficulties.

I am also grateful to Dr. Mary Beth Hueste and Dr. Michael Sherman for serving on my committee and for their comments and suggestions to improve my research.

Additionally, I wish to acknowledge the contributions of my professors, fellow graduate students, friends and family for their help and support. Thank you for taking the time to offer your opinions.

Finally, I would like to thank my parents, who taught me the value of education and hard work, and my wife, Narmadha, whose patience and support helped me to concentrate on research.

This work was supported in part by the Mid-America Earthquake Center through the Earthquake Engineering Research Center Program of the National Science Foundation under award number EEC-9701785. Funding was also provided by the Department of Civil Engineering and the Texas Engineering Experiment Station at Texas A&M University. The support from each of these sources is gratefully acknowledged. The opinions expressed in this paper are those of the author and do not necessarily reflect the views or policies of the sponsors.

TABLE OF CONTENTS

Chapter Page

LIST OF FIGURES

LIST OF TABLES

CHAPTER I

INTRODUCTION

1.1 BACKGROUND

Earthquakes cause significant human suffering and damage to built environment that includes buildings, water, gas, power supply, and transportation systems. This study is concerned with assessment and prediction of structural damage from an earthquake to buildings in the Mid-America Region. Estimates of structural damage are of direct value to those making decisions including engineers, city planners, emergency services, and also for optimizing the allocation of resources for maintenance, repair, and/or rehabilitation of buildings.

The relationship between earthquake ground motion intensity and structural damage can be used to obtain fragility estimates. These fragility estimates provide the conditional probability of damage exceeding a specified performance level for a structural component or system for given measures of ground motion intensity. A fragility estimate is an important element in assessing the seismic vulnerability of buildings.

1.2 SEISMIC HAZARD IN THE MID-AMERICA REGION

Moderate and high intensity earthquakes are infrequent in the Mid-America Region. However, three major earthquakes that caused significant damage and losses occurred during 1811-1812 with epicenter in New Madrid, Missouri and body-wave magnitude estimates higher than 7 mb (Nuttli 1973). Lack of detailed records related to these large events means large uncertainties on occurrence and magnitude for future high intensity events in this region.

This dissertation follows the style and format of *Journal of Structural Engineering*.

National hazards mapping conducted by the United States Geological Survey (USGS), as well as the seismologic investigations conducted on behalf of the nuclear power industry, provide clear evidence that high intensity earthquakes can occur in Central and Eastern regions of the United States. The major threats of future seismic events in Central United States come from the New Madrid Seismic Zone (NMSZ) and other areas of moderate seismicity.

Building regulation in the Central and Eastern United States generally was based on the building code developed by the Building Officials and Code Administrators International (BOCA), while regulation in the southeastern United States generally followed the recommendations of the Southern Building Code (SBC) published by the Standard Building Code Congress International (SBCCI). Uniform Building Code (UBC) published by International Conference of Building Officials (ICBO) generally served as the basis for building code regulation in the Western United States. For seismic design provisions, BOCA and SBC referred to ASCE 7 (1988), which in turn was based on UBC. After the 1971 San Fernando Earthquake, there were significant updates for seismic provisions in the UBC code. These changes were not updated in ASCE 7 until 1993. BOCA and SBC codes incorporated the updated seismic design provision only in 1993. Therefore buildings designed after 1993 in the Mid-America Region, following the revised BOCA and SBC codes were most likely designed for 10% in 50 years ground motions.

There is a wide range in return periods for maximum magnitude earthquakes throughout the United States and its territories. For example, return periods of hundreds of years in parts of California to thousands of years in Central United States. Therefore there was a need to develop a design approach that provides an approximately uniform margin against collapse throughout the United States. To address this need USGS developed national seismic hazard maps (Frankel et al. 2000) based on the probabilistic seismic hazard assessment (PSHA) presented by Cornell (1968).

Figure 1.1 provides normalized probabilistic hazard curves for seven cities in different geographic areas and different seismic zones in the United States based on the

revised USGS seismic hazard maps. These selected cities provide an indication of the variation of the different hazard curves. The slopes of the hazard curves range from relatively shallow for San Francisco and Los Angeles to relatively steep for New York and Charleston, SC. The three vertical lines correspond to the annual frequency of exceedance typically used for the USGS probabilistic maps, e.g., 10%, 5%, and 2% in 50 years. It can be observed in that the difference between the 10% in 50 years ground motion and the 2% in 50 year ground motion in the Western United States is typically less than the difference between these two probabilities in less active seismic areas such as those in the Central and Eastern United States.

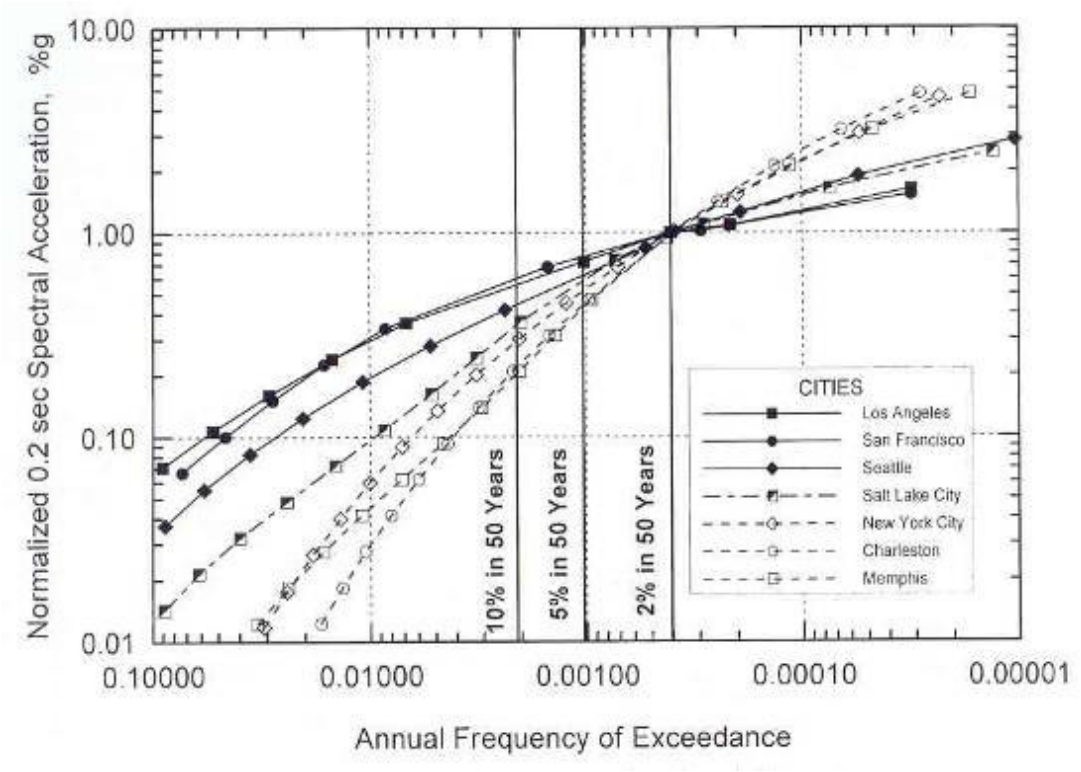

Figure 1.1 Normalized hazard curves for selected cities
(Source: Leyendecker et al. 2000)

To replace the three model building codes and provide a single series of model building code, International Code Council (ICC) published the first edition of International Building Code (IBC) in 2000. According to IBC 2005, two-thirds of the 2% in 50 year earthquakes (return period of 2475 years) should be used as the design basis ground motion for new buildings. Based on past experiences in California, these buildings should be able to resist the 2% in 50 years earthquake without collapse.

1.3 BUILDING INVENTORY

Recent awareness of seismic hazard in the Mid-America Region has led to concerns of safety and seismic vulnerability of existing buildings. Low- and mid-rise reinforced concrete (RC) frame buildings represent a common type of construction in this region (Mosalam 1996 and French 2004). Most of the buildings constructed in the Mid-America Region before the adoption of seismic provisions were primarily designed for gravity loads (GLD) with little or no consideration of seismic resistance and ductile detailing has not been provided explicitly in the design process. Therefore, RC frame buildings constructed prior to 1976 are considered as non-ductile moment resisting frames.

The reinforcement details of these non-ductile buildings are identified based on the review conducted by Beres et al. (1992) on the detailing manuals (ACI 315) and design codes (ACI 318) in use since 1940. Typical reinforcing details of GLD RC frames are: (1) little or no transverse shear reinforcement is provided within the beam-column joints; (2) beam bottom reinforcement is terminated within the beam-column joints with a short embedment length; and (3) columns have bending moment capacities close to or less than those of the joining beams, leading to column sidesway or soft story mechanisms. The damage in GLD buildings during past earthquakes (OES 1995) and previous research by Bracci et al. (1992a) showed that these buildings have poor lateral load resistance.

1.4 OBJECTIVES AND SCOPE

The purpose of this study is to quantify the seismic vulnerability of GLD RC frame buildings in the Mid-America Region. These buildings have limited seismic resistance and are vulnerable to moderate and high seismic events. Fragility estimates can be developed to quantify the seismic vulnerability, where the fragility is defined as the probability of a building reaching or exceeding a certain performance level given a specific ground motion parameter. In general, fragility estimates that are developed from actual earthquake damage data of a particular region are more representative of the building performance in that region. In the absence of actual damage data, fragility estimates can be developed from simulated data obtained from time history analysis of structural models of buildings.

The objectives of this study are to: (1) develop analytical fragility estimates to quantify the seismic vulnerability of GLD RC frame buildings in the Mid-America Region; (2) validate and update the analytical fragility estimates with actual damage data or experimental data; and (3) apply suitable retrofit technique and assess the enhanced seismic performance of GLD RC frame buildings.

1.5 REVIEW OF PAST WORK

Several researchers have developed seismic fragility estimates for RC frame buildings following different procedures and methodologies. The fragility estimates can be broadly classified into three groups; heuristic, empirical and analytical fragilities based on the damage data used in their formulation.

Heuristic fragility estimates are developed based on the estimates of the probable damage distribution of building when subjected to different earthquake intensities provided by the civil engineers with experience in the field of earthquake engineering. Probability density functions are fit to these damage estimates. Fragility estimates are obtained from the probability distributions of the damage state at each intensity level. The vulnerability assessment method prescribed in ATC-13 (1985) and ATC-40 (1996) is based predominately on expert opinion.

Empirical fragility estimates are developed using the observed damage data from past earthquake events. Fragility curves are developed by integrating the damage with the ground motion intensity parameter. Yamazaki and Murao (2000) developed fragility estimates for Japanese buildings using the damage data from the 1995 Kobe Earthquake.

Analytical fragility estimates are developed using the simulated response data obtained by time history analysis of simplified structural models of buildings for actual or synthetic earthquake ground motions. Hwang and Huo (1994), Singhal and Kiremidjian (1996), and Mosalam et al. (1997) developed analytical fragility estimates for RC frame buildings.

In general, most of the existing fragility estimates for RC frame buildings cannot be directly applied to the Mid-America Region because the earthquake ground motions used for simulation of response data do not represent the Mid-America Region. Furthermore, all the relevant uncertainties, particularly the uncertainty in the idealized mathematical model used to describe structural systems and their behavior were not incorporated in the existing fragility estimates. Furthermore, the validity of the analytical fragility estimates should be determined by comparing with field data such as observed damage data of similar buildings from earthquakes or from experimental test data. Existing analytical fragility estimates are rarely verified for field data. In addition, the existing analytical approaches do not provide a framework to update the analytical fragility estimates using observed damage data or experimental test data of similar structural systems and components. Of the reviewed fragility estimates for RC buildings, Singhal and Kiremidjian (1998) developed a Bayesian approach to update the analytical approach field data with limited success.

1.6 PROPOSED APPROACH FOR DEVELOPING FRAGILITY ESTIMATES

In this study, the analytical fragility estimates for GLD RC frame buildings are obtained by using the simulated data from the nonlinear time history analysis of structural models of buildings. Figure 1.2 shows the schematic of the proposed approach for obtaining the fragility estimates.

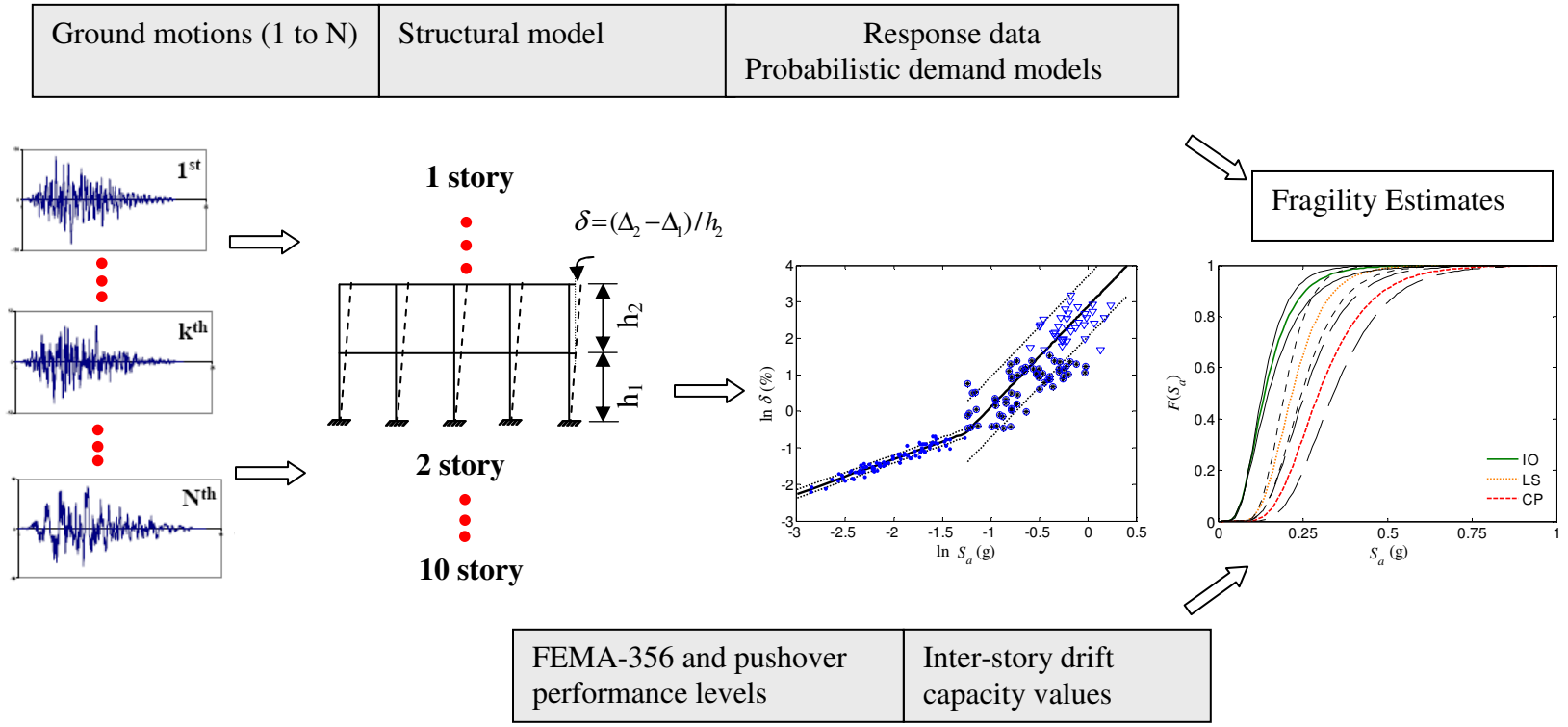

Figure 1.2. Schematic of the proposed approach for obtaining the fragility estimates for RC frame buildings

The uncertainty in each element of the chain of events from the ground motions, structural modeling, structural response, and to demand models and their propagation should be accounted for.

For rapid seismic vulnerability assessment, fragility estimates are developed for generic buildings that represent, in an average the building inventory in a particular region. In this study, based on the building inventory data compiled by French (2004) 1, 2, 3 story (low-rise) and 6 and 10 story (mid-rise) RC frame buildings are selected to represent the generic buildings in the Mid-America Region.

Structural demand is defined as the peak inter story drift (δ) imposed due to an earthquake ground motion. A Bayesian methodology is used to develop probabilistic demand models to predict δ for a given scalar intensity measure. A practical approach is to select a scalar intensity measure of the ground motion that can be correlated well with the structural response. Several studies (Luco and Cornell 2000, and Gardoni et al. 2003) have shown that the 5% damped elastic spectral acceleration, S_a , at the fundamental period of the building, T_1, gives good correlation of the structural damage. In addition, the elastic spectral acceleration can be conveniently obtained from the USGS National earthquake maps (2002). Simulated response data obtained from the nonlinear time history analyses of structural models of sample buildings for the synthetic ground motions are used to for statistical analysis. The Bayesian approach properly accounts for all the prevailing uncertainties.

Structural capacity is also defined as the inter story drift value that will satisfy a specified performance level. These performance levels qualitatively define the damage levels in the buildings. In this study, structural capacity values are identified corresponding to the performance levels specified in FEMA-356 (FEMA, 2000), and also for the damage levels obtained from nonlinear pushover analyses.

By using the estimated demand and capacity values, fragility estimates are then given for the selected low- and mid-rise RC frame buildings. These fragility estimates can be used to quantify the seismic vulnerability of GLD RC frame buildings. The choice made for the analysis method, structural idealization, seismic hazard, and damage

models strongly influences the fragility estimates and cause significant differences in the fragility estimates made by different authors for the same location, same structure type, and seismicity (Priestley 1998). Therefore to develop more robust fragility estimates, the analytical fragility estimates are updated with actual damage data of similar RC frame buildings from other regions.

1.7 OUTLINE OF DISSERTATION

Following the general introduction presented in this chapter, Chapter II discuses the Bayesian approach for the statistical analysis. The problem of constructing a prior distribution that properly reflects the present state of knowledge is discussed.

Chapter III discusses the selection of generic buildings representative of building inventory data in the Mid-America Region. Design, member details and analytical modeling of buildings are also discussed. In Chapter IV, probabilistic demand models are developed to predict the inter story drift. The unknown parameters of the demand model are estimated by using the response data obtained from nonlinear time history analyses. Seismic structural capacity values corresponding to the performance levels or damage specified in FEMA-356 and nonlinear pushover analyses are presented in Chapter V.

In Chapter VI, fragility estimates of all buildings are determined using the predicted demand and capacity values presented in Chapters IV and V, respectively. Confidence bounds are also developed around the median fragility estimates to represent the epistemic uncertainties in the fragility estimates. Bivariate fragility estimates, formulated as a function of spectral acceleration and the fundamental building period, are developed from the fragility estimates of individual buildings.

Chapter VII presents the Bayesian methodology to update the analytical fragility estimates using observational and experimental data. As an illustration of the methodology, the bivariate fragility estimates are updated by using the actual damage data of RC frame buildings during the 1994 Northridge earthquake in California.

Chapter VIII presents the fragility estimates of the retrofitted GLD RC frame buildings. In general, the GLD RC frame buildings are susceptible to soft story mechanism due to low moment capacities of columns compared to that of the beams at a beam column joint. To deter the soft story mechanism and improve the seismic performance of these buildings, the buildings are retrofitted by strengthening the columns.

Chapter IX documents the summary, contributions, and conclusions of this dissertation and also future research.

CHAPTER II

STATISTICAL ANALYSIS

2.1 INTRODUCTION

The statistical analysis of simulated data presented in this dissertation is based on the Bayesian notion of probability. In order develop more robust fragility estimates and to validate and update the analytical fragility estimates, it is essential for the statistical approach to be capable of incorporating all types of available information and explicitly account for all the relevant uncertainties. The Bayesian approach used in this study is ideally suited for the above purpose. This chapter presents the details of the Bayesian approach.

2.2 BAYESIAN METHODOLOGY

The fundamental concepts of Bayesian inference, closely following Box and Tiao (1992) and Gardoni et al. (2002a), is presented in this section. Suppose that $\mathbf{y}' = (y_1, y_2, \ldots, y_n)$ is a vector of n observations, and that its conditional probability density function, $p(\mathbf{y} \mid \boldsymbol{\theta})$, depends on the values of m unknown parameters $\boldsymbol{\theta}' = (\theta_1, \theta_2, \ldots, \theta_m)$ having a probability distribution $p(\boldsymbol{\theta})$. Then

$$p(\mathbf{y} \mid \boldsymbol{\theta})\, p(\boldsymbol{\theta}) = p(\mathbf{y}, \boldsymbol{\theta}) = p(\boldsymbol{\theta} \mid \mathbf{y})\, p(\mathbf{y}) \tag{2.1}$$

where $p(\mathbf{y}, \boldsymbol{\theta})$ represents the joint probability distribution of $\mathbf{y}$ and $\boldsymbol{\theta}$.

For given observed data $\mathbf{y}$, the conditional probability distribution of $\boldsymbol{\theta}$ can be written as

$$p(\boldsymbol{\theta} \mid \mathbf{y}) = \frac{p(\mathbf{y} \mid \boldsymbol{\theta})\, p(\boldsymbol{\theta})}{p(\mathbf{y})} \text{ with } p(\mathbf{y}) \neq 0 \tag{2.2}$$

and

$$p(\mathbf{y}) = E_{\boldsymbol{\theta}}\left[p(\mathbf{y}\mid\boldsymbol{\theta})\right] = \kappa(\mathbf{y})^{-1} = \begin{cases} \int p(\mathbf{y}\mid\boldsymbol{\theta})\, p(\boldsymbol{\theta})\, d\boldsymbol{\theta} & \boldsymbol{\theta} \text{ continuous} \\ \sum p(\mathbf{y}\mid\boldsymbol{\theta})\, p(\boldsymbol{\theta})\, \Delta\boldsymbol{\theta} & \boldsymbol{\theta} \text{ discrete} \end{cases} \tag{2.3}$$

where the sum or the integral is taken over the admissible range of $\boldsymbol{\theta}$, and where $E_{\boldsymbol{\theta}}[f(\boldsymbol{\theta})]$ is the mathematical expectation of $f(\boldsymbol{\theta})$ with respect to the distribution $p(\boldsymbol{\theta})$. Therefore, Eq. (2.2) can be written as

$$p(\boldsymbol{\theta}\mid\mathbf{y}) = \kappa p(\mathbf{y}\mid\boldsymbol{\theta})\, p(\boldsymbol{\theta}) \tag{2.4}$$

Eq. (2.2), or its equivalent Eq. (2.4) is referred to as *Bayes' theorem*, where $p(\boldsymbol{\theta})$ can be viewed as the prior distribution reflecting the state of knowledge about $\boldsymbol{\theta}$ prior to obtaining the data. $p(\boldsymbol{\theta}\mid\mathbf{y})$ is the posterior distribution of $\boldsymbol{\theta}$ given $\mathbf{y}$, which represents the knowledge gained about $\boldsymbol{\theta}$ from the observed data. The quantity κ is a normalizing factor necessary to ensure that the posterior distribution $p(\boldsymbol{\theta}\mid\mathbf{y})$ integrates or sums to one. Following Fisher (1922), $p(\mathbf{y}\mid\boldsymbol{\theta})$ in Eq. (2.4) is called as the likelihood function of $\boldsymbol{\theta}$, for given data $\mathbf{y}$ and is written as $L(\boldsymbol{\theta}\mid\mathbf{y})$. Therefore, the Bayes' formula is written as

$$p(\boldsymbol{\theta}\mid\mathbf{y}) = \kappa L(\boldsymbol{\theta}\mid\mathbf{y})\, p(\boldsymbol{\theta}) \tag{2.5}$$

The Bayes' theorem states that the probability distribution for $\boldsymbol{\theta}$ posterior to the data $\mathbf{y}$ is proportional to the product of the distribution for $\boldsymbol{\theta}$ prior to obtaining the data and the likelihood for $\boldsymbol{\theta}$ given $\mathbf{y}$. The data modifies the prior information through the likelihood function. Therefore, the likelihood function plays a very important role in Bayes' theorem.

In addition, the Bayes' theorem can be used to continuously update the present knowledge every time new knowledge becomes available. For example, if an initial sample of observations, $\mathbf{y}_1$, is originally available, then application of the Bayes formula gives

$$p(\boldsymbol{\theta}\mid\mathbf{y}_1) \propto L(\boldsymbol{\theta}\mid\mathbf{y}_1)\, p(\boldsymbol{\theta}) \tag{2.6}$$

Suppose, if a second sample of observations, $\mathbf{y}_2$, distributed independently of the first sample, becomes available, $p(\boldsymbol{\theta} \mid \mathbf{y}_1)$ can be updated to account for the new information such that

$$\begin{aligned} p(\boldsymbol{\theta} \mid \mathbf{y}_1, \mathbf{y}_2) &\propto p(\boldsymbol{\theta}) L(\boldsymbol{\theta} \mid \mathbf{y}_1) L(\boldsymbol{\theta} \mid \mathbf{y}_2) \\ &\propto p(\boldsymbol{\theta} \mid \mathbf{y}_1) L(\boldsymbol{\theta} \mid \mathbf{y}_2) \end{aligned} \tag{2.7}$$

Eq. (2.7) is of the same form as Eq. (2.6) except that $p(\boldsymbol{\theta} \mid \mathbf{y}_1)$, the posterior distribution for $\boldsymbol{\theta}$ given $\mathbf{y}_1$ acts as the prior distribution for the second sample. This updating process can be applied any number of times. Repeated applications of Bayes's theorem can then be seen as a learning process, where the present knowledge about the unknown parameters $\boldsymbol{\theta}$ is continuously modified as new data becomes available.

2.2.1 Prior Distribution of Parameters

A prior distribution, which is supposed to represent what is known about unknown parameters before the data is available, plays an important role in Bayesian analysis. Such a distribution can be used to represent prior knowledge or relative ignorance. For this reason, it is essential to construct prior distributions that could reflect a situation where little is known a priori. Bayes suggested that in case of lack of previous knowledge one could use a uniform distribution. This is usually referred to as "Bayes's postulate."

In refutation of Bayes's postulate, it is argued that if the distribution of a continuous parameter θ is taken locally uniform, then the distribution of a transformation of θ, e.g., $\ln\theta$ or θ^{-1}, would not be locally uniform. Thus application of Bayes' postulate to different transformations of θ would lead to inconsistent posterior distribution even for the same data. This inconsistency does not mean that Bayes' postulated should not be used in practice. In general, the inconsistency is unacceptable only if it produces results outside acceptable limits of approximation. For example, if the range of uncertainty for θ is not large compared to the mean value, then over this range, transformations such as

$\ln\theta$ or θ^{-1} would be nearly linear. Thus approximate uniformity for θ would imply approximate uniformity for the transformed θ.

For large or even moderate-sized samples, fairly drastic changes in the prior distribution may only lead to minor modifications of the posterior distribution. Thus, for independent observations $y_1, y_2, \ldots, y_n$, the posterior distribution is given as

$$p(\theta \mid y_1, y_2, \ldots, y_n) \propto p(\theta) \prod_{i=1}^{n} p(y_i \mid \theta) \tag{2.8}$$

Therefore, for sufficiently large n, the information content introduced by the likelihood tend to overwhelm the contribution of the prior. An illustration of the robustness of inference, under sensible modification of the prior, is provided by the study of Mosteller and Wallance (1964). The above arguments suggest that arbitrariness in the choice of the transformation in terms of which the prior is locally uniform is often acceptable. The degree of arbitrariness will have an appreciable effect for sample sizes than for the large sample sizes.

2.2.2 Non-informative Prior

This section describes how to construct a non-informative prior for probabilistic models that are used later in this study. For example, for constructing a non-informative prior distribution for the parameter $\boldsymbol{\Theta} = (\boldsymbol{\theta}, \boldsymbol{\Sigma})$, where $\boldsymbol{\theta} = (\theta_1, \ldots \theta_n)$ represents a vector of parameters and $\boldsymbol{\Sigma}$ represents the variance-covariance matrix, it is assumed that $\boldsymbol{\theta}$ and $\boldsymbol{\Sigma}$ are approximately independent. Therefore the prior distribution of $\boldsymbol{\Theta}$ is given as

$$p(\boldsymbol{\Theta}) \approx p(\boldsymbol{\theta})\, p(\boldsymbol{\Sigma}) \tag{2.9}$$

It is also assumed that the parameterization in terms of $\boldsymbol{\theta}$ is such that it is appropriate to take $\boldsymbol{\theta}$ as locally uniform,

$$p(\boldsymbol{\theta}) = \text{constant} \tag{2.10}$$

Following Gardoni et al. (2002a),

$$p(\boldsymbol{\Sigma}) \propto |\mathbf{R}|^{-(n+1)/2} \prod_{i=1}^{n} \frac{1}{\sigma_i} \tag{2.11}$$

where, σ_i^2 represents the variances, $\mathbf{R} = [\rho_{ij}]$ represents the $n \times n$ correlation matrix. For a single parameter Eq. (2.11) can be written as

$$p(\sigma) \propto \frac{1}{\sigma} \tag{2.12}$$

2.2.3 Likelihood Function

As mentioned earlier, the likelihood function $L(\boldsymbol{\theta} \mid \mathbf{y})$ plays a very important role in Bayes' formula. The likelihood function is defined up to a multiplicative constant. This is in accord with the role it plays in Bayes' formula, since multiplying the likelihood function by an arbitrary constant will have no effect on the posterior distribution of $\boldsymbol{\theta}$. Formulation of the likelihood function depends on the type and form of the available information (Gardoni et al. 2002a).

2.2.4 Posterior Distribution

Combining the likelihood function and the prior distribution, the posterior distribution of the parameters are obtained. However computation of the posterior statistics is not a trivial one. It requires multifold integration over the Bayesian integrand $L(\boldsymbol{\theta} \mid \mathbf{y})\, p(\boldsymbol{\theta})$. In this study, an importance sampling algorithm developed by Gardoni et al. (2002a) is used to compute the posterior statistics of the parameters.

CHAPTER III

BUILDING SYSTEMS AND SIMULATION OF RESPONSE DATA

3.1 INTRODUCTION

For rapid seismic vulnerability assessment of buildings in a region, seismic fragility estimates are developed for generic buildings that represents, in an average sense, the building inventory in that region. These fragility estimates can be used to quantify the seismic vulnerability of the entire building inventory. The fragility estimates are developed using the simulated response data of the structural models of the generic buildings. The key aspects in the simulation procedure are: selection of ground motions, definition of generic buildings, and nonlinear analysis of structural models of generic buildings. This chapter presents in detail the three key aspects mentioned above.

3.2 SYNTHETIC GROUND MOTIONS

As explained in Section 1.2, Mid-America is a region of moderate seismicity, where infrequent moderate to large earthquakes have occurred in the past. However, strong motion records of engineering interest are non-existent. Therefore, synthetic ground motions generated for Memphis, TN, by Wen and Wu (2001) and Rix and Fernandez (2004) are used in this study. Wen and Wu (2001) provided two suites of 10 uniform ground motions; with probabilistic intensities of 10% in 50 years and 2% in 50 years, for both hard rock and representative soil sites. From the ground motions developed by Rix and Fernandez (2004), 20 scenario-based records using two different source models, Atkinson and Boore (1995) and Frankel et al. (1996), and moment magnitudes of 5.5 at hypo-central distances of 10 km, of 6.5 at 10 and 50 km, and of 7.5 at 20 km are considered. A total of 180 earthquake records are used in the inelastic time history analyses. Figure 3.1 shows the sample 5% damped elastic response spectra of the synthetic ground motions. For a particular ground motions, the S_a corresponding to the

fundamental period of the building is used as the seismic demand. The S_a values are normalized with the acceleration due to gravity (g).

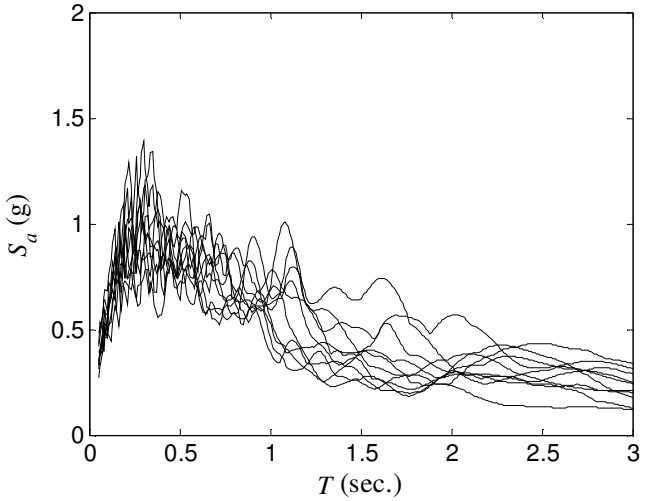

(a) 2% in 50 years records for soft soil (Wen and Wu 2001)

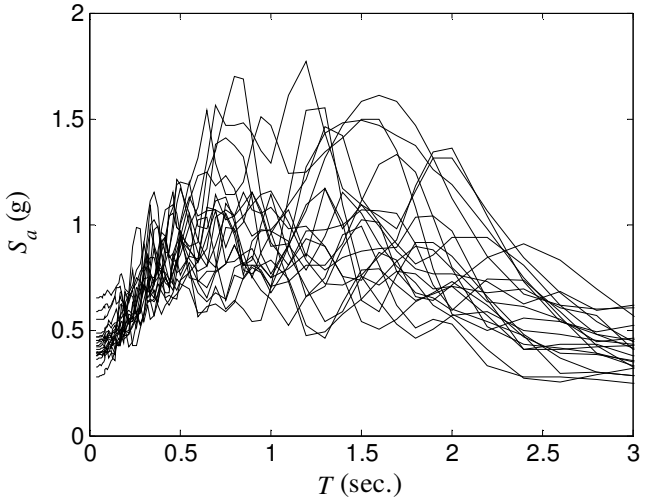

(b) Moment magnitude 7.5, hypo-central distance 20 km, Frankel et al. (1996) model (Rix and Fernandez 2004)

Figure 3.1 Sample response spectra of synthetic ground motions used in this study

3.3 GENERIC BUILDINGS

Generic buildings are defined by structural geometry, typical structural components and methods of design. Sample structures that are defined by specific geometry and design parameters, are selected to represent the generic buildings. French (2004) compiled building inventory data for Memphis, TN. A brief summary of the database is presented here. Table 3.1 shows the classification of buildings based on the structural type. Tables 3.2 and 3.3 list the classification of buildings based on year of construction and number of stories, respectively. It is evident from this inventory data that significant number of existing RC frame buildings (classified as C1 and highlighted in Tables 3.1-3.3) were designed and constructed prior to the adoption of seismic provisions in the building codes. Also, most of the RC frame buildings are in the 1 to10 story range. Based on the number of stories, buildings are classified as low-rise (1 to 5 story) and mid-rise (6 to 10 story).

Based on this inventory data, 1, 2, 3, 6, and 10 story RC frame buildings are selected to represent the generic GLD RC frame buildings in the Mid-America Region. Since seismic fragility estimates are developed for generic buildings that represents, in an average sense, the building inventory in that region, a regular and symmetric distribution of mass and stiffness are selected for all sample buildings. All buildings are assumed to have 4 equal bays with a spacing of 26 ft in the longitudinal and transverse directions with an individual story height of 12 ft. Figure 3.2 shows the plan and elevation details of the sample buildings.

It is assumed for simplicity that the slabs, beams and columns will have constant cross-sections throughout the height of each building and that the bases of the lowest story segments are fixed. Floor and roof elements (diaphragms) are assumed to be rigid. In the rest of this section loading details, analysis, and design of sample buildings are presented.

Table 3.1 Classification of buildings based on the structure type for Memphis, TN (French 2004)

Structure Type	Code	No. of buildings
Concrete MRF	C1	461
Concrete Shear Wall	C2	115
Concrete Tilt-up	PC1	1060
Precast Concrete Frame	PC2	140
Reinforced Masonry	RM	1524
Steel Frame	S1	479
Light Metal Frame	S3	7364
Unreinforced Masonry	URM	6033
Wood Frame	W	269475
Unknown	Unknown	406

Table 3.2 Classification of buildings based on year of construction (French 2004)

Code	Pre 1939	1940-49	1950-59	1960-69	1970-79	1980-89	Post 1990	Total
C1	103	11	16	35	76	131	89	461
C2	6	6	32	38	24	5	3	115
PC1		2	38	153	250	365	252	1060
PC2	3	2	81	40	2	7	5	140
RM	3	0	4	35	173	625	684	1524
S1	7	2	9	25	52	335	49	479
S3	47	48	720	1016	820	2056	2657	7364
URM	2193	1401	851	806	755	20	7	6033
W	29370	23248	49929	36848	45333	35176	49571	269475
Unknown	3	0	1	0	5	4	4	406
Totals	212768	71913	1786	135	53	13	389	287057
Percent	74.12	25.05	0.62	0.05	0.02	0.00	0.14	100

Table 3.3 Classification of buildings based on number of stories for Memphis, TN (French 2004)

Code	1	2	3-5	6-10	11-20	Over 21	Unknown	Total
C1	125	74	191	44	24	3	0	461
C2	13	18	31	30	16	7	0	115
PC1	977	71	10	1	1	0	0	1060
PC2	78	35	19	7	1	0	0	140
RM	1131	323	69	1	0	0	0	1524
S1	58	192	196	22	9	2	0	479
S3	6170	962	231	1	0	0	0	7364
URM	4487	942	577	25	1	1	0	6033
W	199725	69293	456	1	0	0	0	269475
Unknown	4	3	6	3	1	0	389	406
Totals	212768	71913	1786	135	53	13	389	287057
Percent	74.12	25.05	0.62	0.05	0.02	0.00	0.14	100

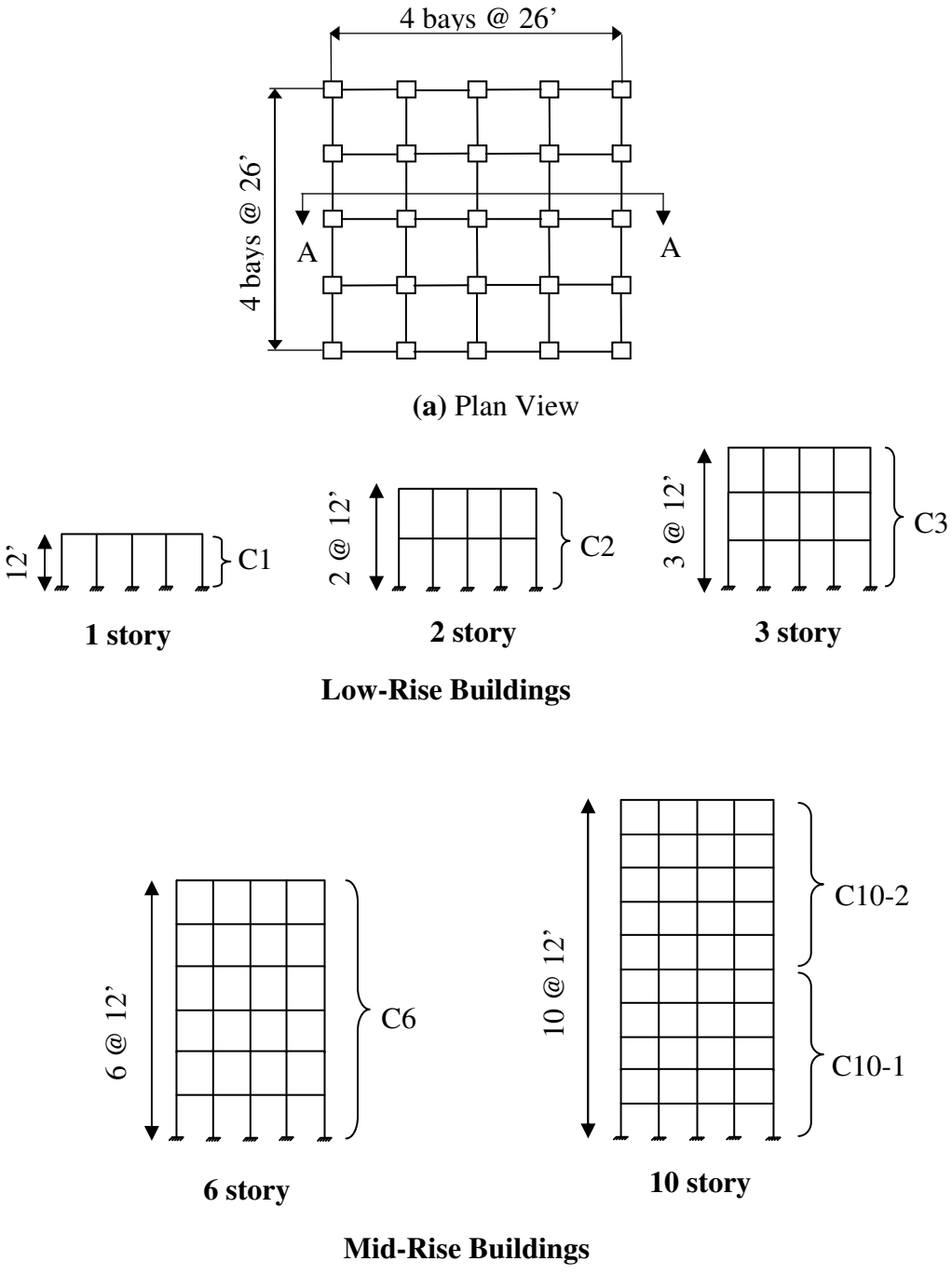

Figure 3.2 Plan and elevation of low- and mid-rise GLD RC frame buildings

3.3.1 Loading Details

The gravity loads consist of the structural self weight; 20 psf superimposed dead loading for electrical, mechanical, plumbing, and floor and ceiling fixtures; 250 lb/ft for exterior cladding; and 50 psf for live loads for a typical office building.

The buildings are assumed to be located in Memphis, TN, therefore the design wind speed is determined to be 90 mph. Since wind load seldom govern the design of low-rise buildings, wind load forces are determined only for the 6 and 10 story buildings in accordance with the analytical procedure (Method 2) given in ASCE-7 (2002). A summary of the design wind forces at all floor levels for a frame of the 6- and 10 story building is listed in Tables 3.4 and 3.5, respectively.

Table 3.4 Design wind forces for a frame of the 6 story building

Level	Height above ground level, *Z* (feet)	Design wind force		Total force (kips)
		Windward (kips)	Leeward (kips)	
6	72	1.68	-1.05	2.73
5	60	3.19	-2.00	5.19
4	48	3.00	-1.87	4.87
3	36	2.76	-1.72	4.48
2	24	2.46	-1.54	3.99
1	12	2.02	-1.26	3.28

Table 3.5 Design wind forces for a frame of the 10 story building

Level	Height above ground level, Z (feet)	Design wind force		Total force (kips)
		Windward (kips)	Leeward (kips)	
10	120	1.95	-1.22	3.16
9	108	3.78	-2.36	6.14
8	96	3.65	-2.28	5.94
7	84	3.52	-2.20	5.71
6	72	3.36	-2.10	5.47
5	60	3.19	-2.00	5.19
4	48	3.00	-1.87	4.87
3	36	2.76	-1.72	4.48
2	24	2.46	-1.54	3.99
1	12	2.02	-1.26	3.28

3.3.2 Load Combinations

The non-seismic load combinations of ASCE-7 (2002) are used in the design of the structural members. The following load combinations are used to determine the critical member forces

1. $1.2D+1.6L$
2. $1.2D+1.0L+1.6W$
3. $0.9D+1.6W$

where D, L, and W are the effects due to dead loads, live loads, and wind forces, respectively.

3.3.3 Method of Analysis

Due to regular plan and symmetric distribution of mass and stiffness, torsion effects will be negligible for these buildings. Therefore, these regular buildings can be analyzed independently in the two lateral directions. A two-dimensional analysis of the typical interior frame of the building is performed for the gravity and wind loads using ETABS (CSI 2006). In the ETABS model, rigid-end offsets are defined at the ends of the horizontal members so that results are automatically obtained at the faces of the supports. The stiffness properties of the members are input by using the effective moment of inertia of the section. Based on the experimental results obtained by Bracci et al. (1995a) for GLD RC frame buildings the effective section properties are defined as follows

- Beams: $I_{eff} = 0.5 I_g$
- Columns: $I_{eff} = 0.70 I_g$

where I_g and I_{eff} are the gross and effective moment of inertia of the section, respectively. The concrete is assumed to have an unconfined compressive strength of 4000 psi, while steel reinforcement is assumed to have yield strength of 60,000 psi.

To determine the maximum positive and negative moment, dead load is applied to all the spans whereas checkerboard patterns and loading on all spans are used for live loads. Except for the roof level, the cladding load is applied to the exterior beam at each floor level.

3.3.4 Design Details and Member Sections of Buildings

All components of the sample buildings are designed according to the ACI 318 (2005) non-seismic design provisions. Since gravity load forces governed over the wind load forces, typical slabs, beams, and columns are designed and detailed for gravity load effects.

Column spacing is determined and maximized based on using an 8 in. thick reinforced concrete two-way slab designed according to the Direct Design Method specified in ACI-318 (2005). Based on these gravity loadings, the minimum required slab reinforcement, #4 bars @ 12" cc., governs the design for both the column and middle strip regions. Since floor loads are approximately the same for all buildings, slab and beam cross-section and reinforcement profiles are identical regardless of the story level and building. Beams are designed as T-beam sections according to ACI-318 (2005), with an effective slab flange widths of 78 in. and 42 in. for the interior and exterior spans, respectively. The final beam sections at the beam-column joint faces are 16 in. wide and 24 in. deep from the top of the slab to the soffit of the beam. Table 3.6 lists the required flexural reinforcement. For negative moment at the supports, 5-#7 bars and 2-#7 bars for top and bottom bars, respectively are used. #3 bars @ 10" are used for shear reinforcement. At the mid-span, 2-#7 bars and 4-#7 bars are used for top and bottom bars, respectively. Figure 3.3 shows the reinforcement profiles and beam cross-sections at the critical locations.

Table 3.6 Flexural reinforcement details for beam

Location	M_u (ft-kips)	A_s^* (in.^{2})	Reinforcement	ϕM_n (ft-kips)
Support	–233	2.46	5-#7	268
Midspan	198	1.98	4-#7	218

$$^*A_{s,\min} = \frac{3\sqrt{f_c'}\,b_w d}{f_y} = \frac{3\sqrt{4,000}\times 16\times 21.5}{60000} = 1.08 \text{ in.}^2$$

$$= \frac{200 b_w d}{f_y} = \frac{200\times 16\times 21.5}{60000} = 1.15 \text{ in.}^2$$

$$A_{s,\max} = \rho_{\max} b_w d = 0.0214\times 16\times 21.5 = 7.36 \text{ in.}^2$$

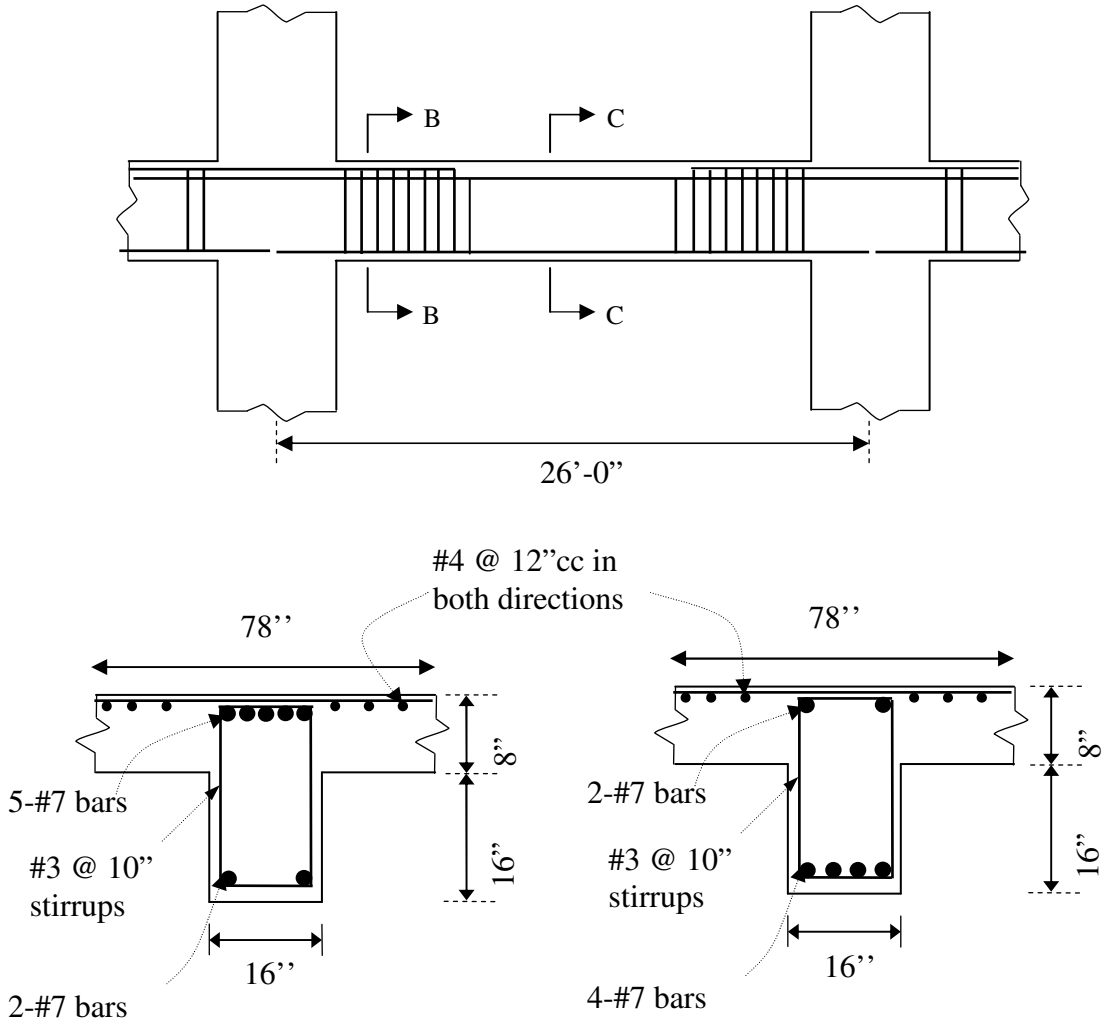

Figure 3.3 Cross-section and reinforcement details of beams
(Not to scale)

Columns are also designed to resist combinations of moment and axial load occurring from the governing combinations of factored wind and gravity loads. In Figure 3.2, C1, C2, C3, and C6 represent the columns in 1, 2, 3 and 6 story building, respectively. As mentioned earlier, the column cross-section and reinforcement details

for a sample building are assumed to be same for all floor levels. For 10 story building, the column cross-section is kept constant for all floor levels, but the reinforcement details are changed at the fifth floor level. C10-1 and C10-2 represents the columns in floors 1 to 5 and 6 to 10, respectively. Figure 3.4 shows the general profile of the column and Table 3.7 lists the cross-section and reinforcement details of the columns in low- and mid-rise buildings. The member details of the buildings are representative of the non-seismic provisions of ACI-318 (2005).

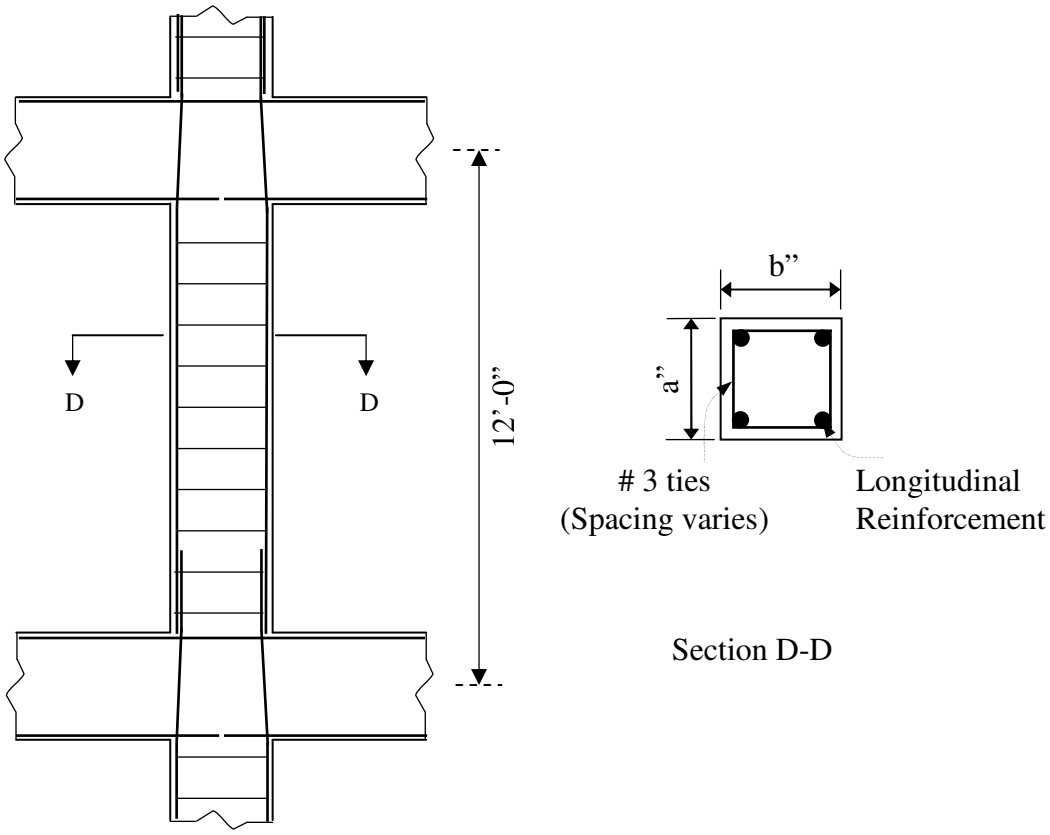

Figure 3.4 Cross-section and reinforcement details of columns
(Not to scale)

Table 3.7 Cross-section and reinforcement details of columns in low- and mid-rise buildings

Building	Column	Section (a" × b")	Reinforcement details	
			Longitudinal Bars	Ties
1 story	C1	12" × 12"	4-#8 bars	#3 @ 12 in
2 story	C2	16" × 16"	4-#8 bars	#3 @ 16 in
3 story	C3	16" × 16"	4-#8 bars	#3 @ 16 in
6 story	C6	20" × 20"	4-#9 bars	#3 @ 16 in
10 story	C10-1	20" × 20"	8-#9 bars	#3 @ 16 in
	C10-2	20" × 20"	4-#9 bars	#3 @ 16 in

3.4 NONLINEAR ANALYSIS

The simulated damage data obtained from the nonlinear time history analyses of structural models of the generic buildings are used for developing the fragility estimates. The importance of choosing a nonlinear analysis tool and understanding its limitations cannot be underestimated. This tool should enable sufficiently accurate modeling of the structures under investigation and provide stable nonlinear time history analysis of the structure. In addition, this analysis tool must be calibrated to give a level of confidence in the response quantities provided.

3.4.1 IDASS Models

A typical interior frame of the building is modeled as a two-dimensional frame in IDASS (Kunnath 2003). IDASS is a nonlinear analysis program for frame and frame-wall structures subjected to seismic excitations. The program requires specification of member behavior in terms of moment curvature envelopes and an associated hysteretic rule. For each component cross-section, the moment curvature relation is specified as a non-symmetric tri-linear envelope with three degrading hysteretic parameters, as shown in Figure 3.5. Table 3.8 lists the parameters of and description of the moment curvature envelope for components (beams and columns) of sample buildings. The three main

characteristic represented in the hysteretic model are stiffness degradation, strength deterioration and pinching effect.

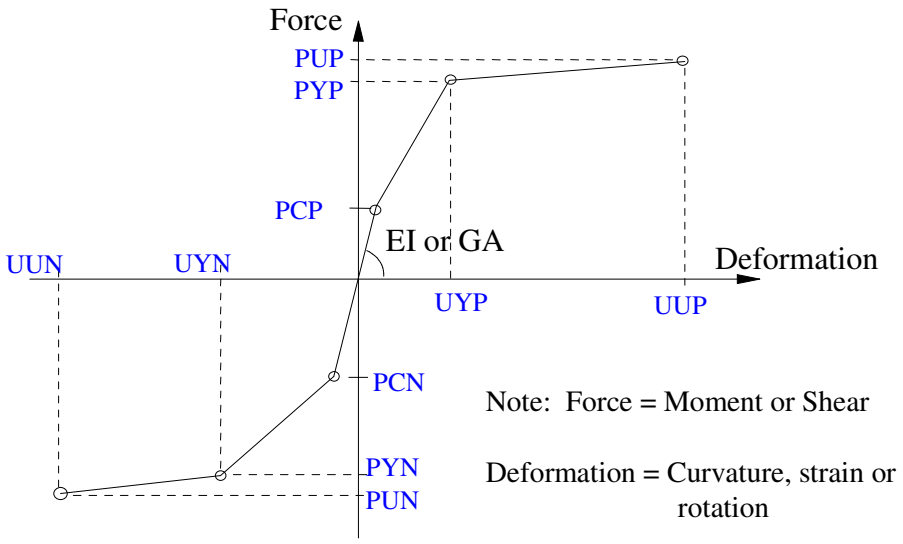

Tri-linear moment curvature envelope

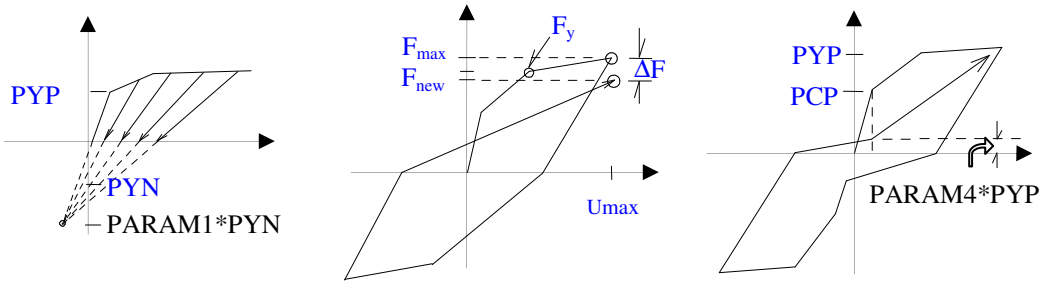

1. Modeling of stiffness degradation

2. Modeling of strength deterioration

3. Modeling of slip

Figure 3.5 Modeling of degrading hysteretic behavior of RC members in IDASS (Kunnath 2003)

Table 3.8 Parameters for moment curvature envelope for components of RC frame buildings

Parameter	Description
EI	Initial flexural rigidity
GA	Shear stiffness (Shear modulus*shear Area)
PCP	Cracking moment (positive)
PYP	Yield moment (positive)
PUP	Ultimate moment (positive)
UYP	Yield curvature (positive)
UUP	Ultimate curvature (positive)
PCN	Cracking moment (negative)
PYN	Yield moment (negative)
PUN	Ultimate moment (negative)
UYN	Yield curvature (negative)
UUN	Ultimate curvature (negative)

Lack of transverse reinforcement within the joint region is characteristic of GLD RC buildings. This lack of shear-resistance mechanism can lead to nonductile failures once the shear capacity of concrete has been exceeded. Previous experimental research on the seismic performance of the beam-column joints that have no transverse reinforcement in the joint region (Beres et al. 1996, Walker 2001, Alire 2002, and Pantelides et al. 2002) revealed that the joint shear stress-strain response typically has a degrading envelope and a highly pinched hysteresis.

Most nonlinear dynamic analyses programs assume infinite rigidity of the beam-column joint in concrete frame regardless of the reinforcement details. Celik and Ellingwood (2006) showed that the rigid joint model is inadequate in representing the highly pinched hysteretic character. To avoid the complexity of modeling the nonlinear degrading inelastic behavior of a joint, an approximate approach is used in IDASS to model the joint behavior. Flexural properties of the members framing into a joint are

adjusted to reflect the joint behavior. Also, to model the non-ductile detailing of the GLD RC frame building, the moment curvature envelope is modified for stiffness degradation, target slip, and pinching effect.

3.4.2 Validation of IDASS

Bracci et al. (1992a) conducted shake table tests on a one-third scale model of a GLD RC frame subjected to simulated earthquake events. Aycardi et al. (1992) conducted companion component and subassembly testing of members and connections of the scaled model using quasistatic reversed cyclic loading. These experimental results were used to calibrate the hysteretic degrading parameters in IDASS. Using these calibrated values, the stiffness degrading, target slip or crack closing, and energy based strength decay parameters for GLD buildings are set to 0.7, 0.7, and 0.05, respectively.

In addition, the inter story drift responses from these experimental studies were up to peak drifts between 3% and 5%, and thus IDASS was calibrated up to these drift levels. Further discussion and details of the calibrations are presented in Hoffman et al. (1992) and Bracci et al. (1992a).

3.4.3 Fundamental Building Period

An eigenvalue analysis of the structural model is performed in IDASS to determine the important elastic dynamic properties of the building, such as the fundamental periods and the mode shapes of the building. As mentioned earlier, an important parameter for quantifying seismic demand in this work is the first mode period of the structure, T_1. For the 1, 2, 3, 6, and 10 story buildings, T_1 is equal to 0.61, 0.58, 0.87, 1.38, and 2.35 sec., respectively. It should be emphasized that these values are obtained by assuming reduced member sections according to recommendations in ACI-318 (2005). It is important to note that the fundamental period of a building is sensitive to design and construction practices. However, the values used are considered, on the average, to represent the fundamental periods of the 1to 10 story RC frame building inventory in the Mid-America Region.

To estimate the fundamental period of a 1 to10 story building of general height, h, the building period T_1 is expressed as a function of h. According to FEMA-356 (2000) and ASCE 7-02 (2002), T_1 can be estimated using an empirical relation:

$$T_1 = C_t \left(h\right)^x \tag{3.1}$$

where $C_t = 0.018$ (FEMA-356 2000) or $C_t = 0.016$ (ASCE 7-02 2002) for concrete moment-resisting frame buildings, h represent the height (in feet) from the base to the roof level of the building, and $x = 0.9$. The empirical relation given in Eq. (3.1) intentionally underestimates the actual building period and generally results in conservative estimates of lateral load for design purposes.

For a probabilistic approach, an unbiased estimate of the fundamental period of the building is required. An unbiased probabilistic model similar to the empirical relation given in Eq. (3.1) is developed to estimate the T_1 of RC frame buildings from 1 to 10 story height with no systematic error. The general model form is written as:

$$T_1 = \eta_1 \left(h\right)^{\eta_2} e \tag{3.2}$$

where η_1 and η_2 are the unknown parameters of the model, and e is the unit-median error term that describes the uncertainty in the relationship. A logarithmic transformation of the model given in Eq. (3.2) is written as:

$$\ln\left(T_1\right) = \ln\left(\eta_1\right) + \eta_2 \ln\left(h\right) + \sigma_{T_1}\varepsilon \tag{3.3}$$

where $\sigma_{T_1}\varepsilon$ represents the model error, σ_{T_1} represents the unknown standard deviation of the model error, and ε is a normal random variable with zero mean and unit standard deviation. A Bayesian statistical analysis is used to estimate the unknown parameters of the model $(\eta_1, \eta_2, \sigma_{T_1})$. The building period values obtained from the eigenvalue analysis of 1, 2, 3, 6, and 10 story buildings are used as data. The posterior mean values of the parameters are $\eta_1 = 0.097$, $\eta_2 = 0.624$, and $\sigma_{T_1} = 0.188$.

Figure 3.6 shows the estimated median fundamental building period, $\hat{T}_1$, computed by substituting the posterior mean of the model parameters in Eq. (3.2), along with the

one standard deviation confidence bounds. Points of type (◊) represent the T_1 of the buildings obtained by eigenvalue analysis. The dashed and dotted lines represents the period estimates from the FEMA-356 and ASCE 7-02 empirical relation, respectively. Figure 3.6 shows that the FEMA and ASCE fundamental building period estimates are biased approximately by a factor of 2σ from the median $\hat{T}_1$. The developed probabilistic model corrects for this bias.

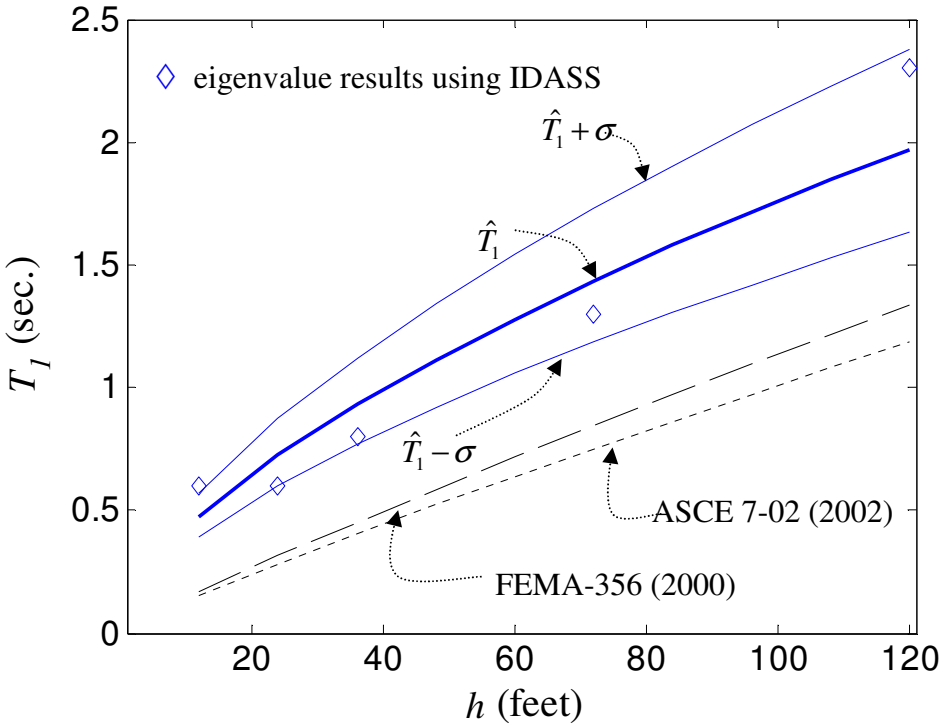

Figure 3.6 Fundamental building period estimates for 1 to 10 story GLD RC frame buildings

3.5 SIMULATED RESPONSE DATA

Nonlinear time history analyses of the structural models are carried out in IDASS using the 180 synthetic ground motions mentioned earlier. Figure 3.7 shows the diagnostic

plots of peak inter story drift, δ, versus S_a for sample buildings. The response data have a large scatter due to record-to-record variation in the intensity of synthetic ground motions. The structural system generally goes into inelastic range under severe ground excitations.

3.5.1 Categorization of Response Data

Based on the trends in the response data, they are categorized into three different types. A datum is of Type I when $\delta \le \delta_1\%$ where $\delta_1 = 0.6\%$, which is established based on the response data. Type I data represents the elastic response of the system. A datum is of Type II data when $\delta_1 < \delta \le \delta_2$ and a datum is of Type III data when $\delta > \delta_2$ where, δ_2 represents the maximum inter story drift value used in validating IDASS for GLD RC frame buildings. Note that the response predictions from IDASS beyond $\delta_2 = 5\%$ might be inaccurate due to lack of model verification and potential higher order analysis effects and are considered to be uncertain. Types I and II data are categorized as 'equality' data. Type III data are categorized as 'lower bound' data, where the information used in the statistical analysis is that $\delta > \delta_2$, instead of the actual response from the dynamic analysis as it is for data Types I and II. For example if the IDASS provides an inter story drift of 8%, this value is beyond the validation limit (i.e. 5%). In this case, the information used in the statistical analysis is that $\delta > 5\%$.

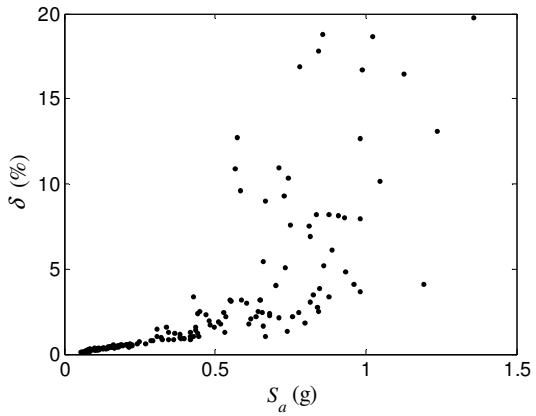

(a) 1 story

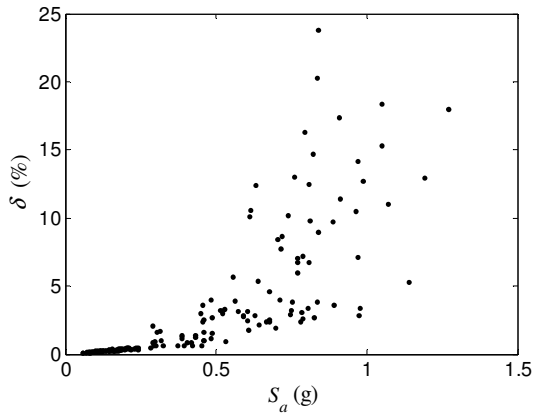

(b) 2 story

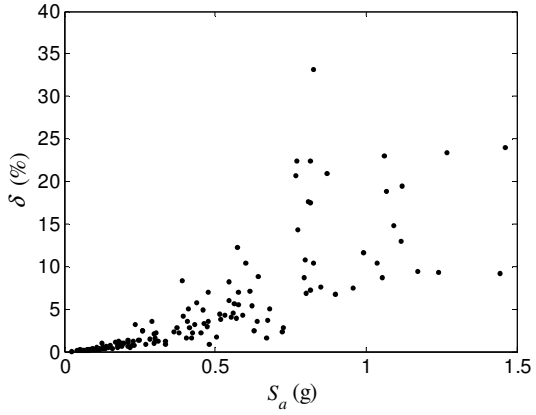

(c) 3 story

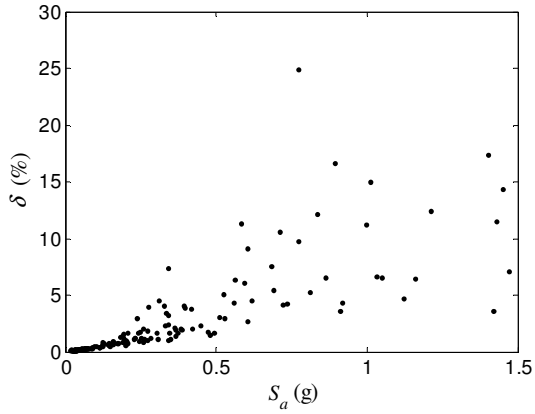

(d) 6 story

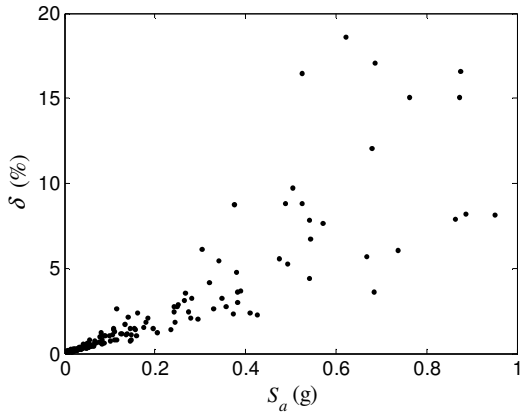

(e) 10 story

Figure 3.7 Simulated response data from nonlinear time history analyses

3.6 SUMMARY

The key aspects in obtaining the simulated response data are: selection of ground motions, definition of generic buildings, and nonlinear analysis of structural models of generic buildings. Synthetic ground motions developed for Memphis, TN, are selected for time history analyses. Sample buildings are selected to represent generic low- and mid-rise RC frame buildings representative of the Mid-America Region. These sample buildings are designed and detailed in accordance with the nonseismic provisions in ACI 318 (2005). Typical interior frames of the sample buildings are modeled as two-dimensional frame in IDASS. Nonlinear time history analysis of these structural models is carried out to obtain the response data for buildings. The response data have large scatter for high intensity ground motions.

CHAPTER IV

PROBABILISTIC DEMAND MODELS

4.1 INTRODUCTION

Unbiased estimates of the structural demand and capacity are required for obtaining the fragility estimates. Therefore, it is essential to develop probabilistic demand models that are unbiased that is, on average, correctly predict the mean structural demand and accounts for all prevailing uncertainties (Ramamoorthy et al. 2006a). This chapter presents a Bayesian framework for developing probabilistic demand models for GLD RC frame buildings that accounts for model errors that arise from using an inaccurate model form and statistical uncertainty.

4.2 DEMAND MODELS

In this study, a probabilistic seismic demand model relates ground motion intensity measures to structure specific demand measures. Selecting an intensity measure and demand measure pair for a practical sufficient, effective, and efficient probabilistic demand models is not easy (Mackie and Stojadinovic 2001). Thus, the choice of intensity and demand measure and the relationship between these measures are critical for a successful probabilistic demand model. Based on extensive regression analyses of response of steel structures Cornell et al. (2002) proposed that for a given S_a, the peak inter story drift demand can be predicted using the power model:

$$\delta = \gamma_0 \left(S_a\right)^{\gamma_1} e \tag{4.1}$$

where e is the unit-median error term that describes the uncertainty in the relationship; and the unknown parameters, γ_0 and γ_1 can be determined by regression analysis. This relationship is approximate and there can have large scatter around the regression line. The predicted demand is therefore the estimate of the mean inter story drift demand

conditional on a given value of S_a. The scatter in terms of the coefficient of variation, $\sigma_{\delta|S_a}$, also depends, in principle, on S_a. Other demand models, with multiple regressors like peak ground acceleration (PGA), spectral velocity (S_v), spectral displacement (S_d) and duration of the earthquake, can also be used to as the seismic intensity variable. However, the demand model given in Eq. (4.1) is simple and accurate. Also, Gardoni et al. (2003) showed that S_a correlates well with the structural response.

Following Gardoni et al. (2002b), a logarithmic transformation of Eq. (4.1) gives a linear regression model

$$\ln(\delta) = \ln(\gamma_0) + \gamma_1 \ln(S_a) + \sigma_{\ln(\delta)|S_a}\varepsilon \tag{4.2}$$

where ε is a random variable representing the unknown errors in the model with zero mean and unit standard deviation; $\sigma_{\ln(\delta)|S_a}$ represents the standard deviation of the model error. Diagnostic plots of the data or the residuals against model predictions or individual regressor can be used to verify the suitability of an assumed transformation (Rao and Toutenburg, 1997).

By defining $D = \ln(\delta)$, $\theta_0 = \ln(\gamma_0)$, and $\theta_1 = \gamma_1$, Eq. (4.2) can be written as:

$$D(S_a;\boldsymbol{\Theta}) = \theta_0 + \theta_1 \ln(S_a) + \sigma_{D|S_a}\varepsilon \tag{4.3}$$

where $\boldsymbol{\Theta} = (\theta_0, \theta_1, \sigma_{D|S_a})$ are unknown parameters that need to be estimated, $\sigma_{D|S_a}\varepsilon$ represents the error of the model in logarithmic form. Bayes' theorem can be used to estimate the parameters of the model in Eq. (4.3) under the following assumptions: (1) the model error ε is normally distributed (normality assumption); and (2) the model variance is independent of S_a (homoskedasticity assumption). Figure 4.1 shows the plots of response data in logarithmic space, $\ln(\delta)$ versus $\ln(S_a)$ for all buildings. The solid dots ($\bullet$) represent Type I data, the stars ($\circledast$) represent Type II data, and the triangles ($\triangledown$) represent the 'lower bound' data (Type III).

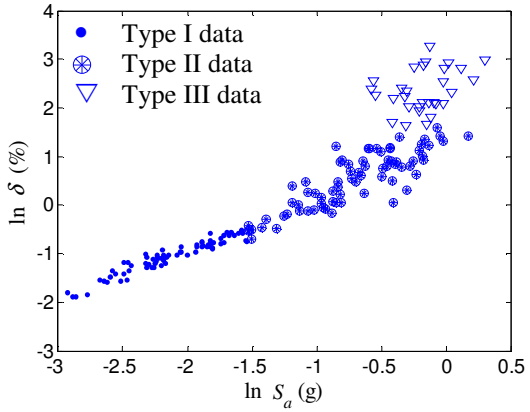

(a) 1 story

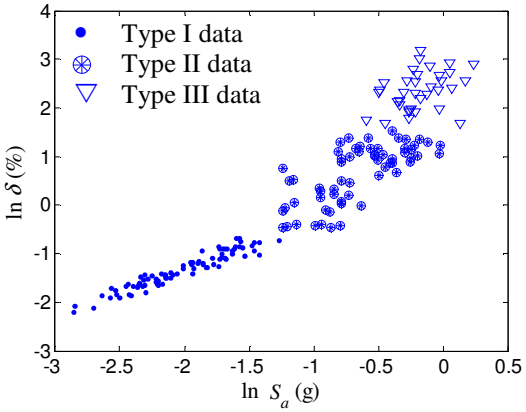

(b) 2 story

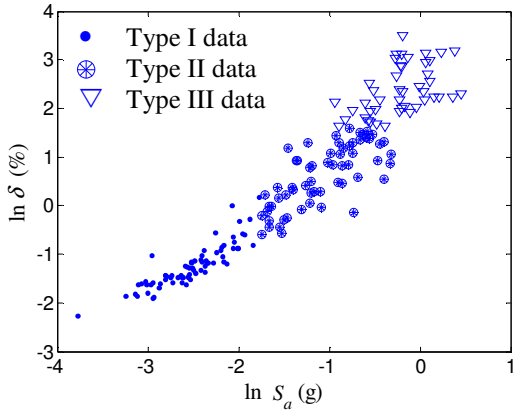

(c) 3 story

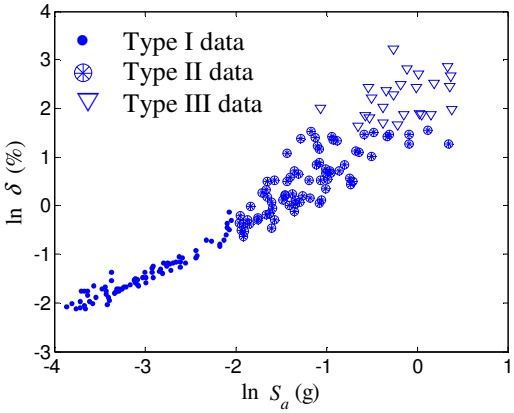

(d) 6 story

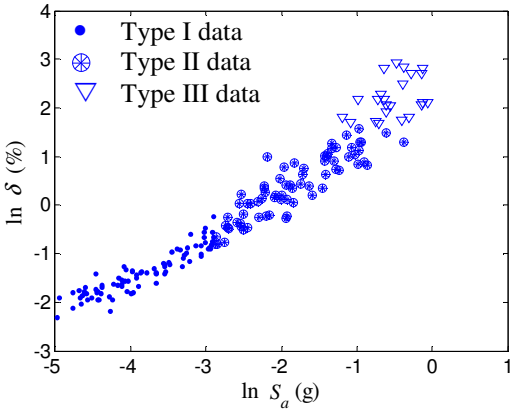

(e) 10 story

Figure 4.1 Peak inter story drift response data from nonlinear time history analysis

4.3 UNCERTAINTY IN MODELS AND PREDICTION

A large variety of uncertainties are involved in developing and assessing a probabilistic model. Some of these uncertainties are inherently random (or aleatoric) and cannot be reduced with further data or observation. Referring to the model formulations in the preceding section, this kind of uncertainty is present in the variable S_a and partly in the error term ε. Other uncertainties arise from a lack of data (statistical uncertainty) and ignorance or approximations in modeling (model inexactness), termed as epistemic uncertainty. This kind of uncertainty is reducible by using more accurate measurements and larger sample size. These uncertainty is present in the model parameters $\boldsymbol{\Theta}$ and partly in the error term ε. Further discussion and details of the uncertainties are presented in Wen and Ellingwood (2003) and Gardoni et al. (2002a)

4.4 BAYESIAN ESTIMATION OF PARAMETERS

The unknown parameters of the demand models given in Eq. (4.3) are determined by using the Bayesian methodology. Since no prior information is available for the parameters $\boldsymbol{\Theta} = (\boldsymbol{\theta}, \sigma_{D|S_a})$, a non-informative prior is selected. Following Gardoni et al. (2002b), for the linear model in Eq. (4.3) with negligible error in estimating S_a, and under the assumption of statistically independent observations, the likelihood has the general form:

$$L\left(\boldsymbol{\theta}, \sigma_{D|S_a}\right) \propto \prod_{\text{equality data}} p\left[\sigma_{D|S_a}\varepsilon_i = r_i\left(\boldsymbol{\theta}\right)\right] \times \prod_{\text{lower bound data}} p\left[\sigma_{D|S_a}\varepsilon_i > r_i\left(\boldsymbol{\theta}\right)\right] \tag{4.4}$$

where

$$r_i\left(\boldsymbol{\theta}\right) = D_{\text{simulated}} - D\left(S_a; \boldsymbol{\Theta}\right) \tag{4.5}$$

Since ε has the standard normal distribution, (4.4) can be written as

$$L\left(\boldsymbol{\theta}, \sigma_{D|S_a}\right) \propto \prod_{\text{equality data}} \left\{\frac{1}{\sigma_{D|S_a}} \varphi\left[\frac{r_i\left(\boldsymbol{\theta}\right)}{\sigma_{D|S_a}}\right]\right\} \times \prod_{\text{lower bound data}} \Phi\left[-\frac{r_i\left(\boldsymbol{\theta}\right)}{\sigma_{D|S_a}}\right] \tag{4.6}$$

where $\varphi(\cdot)$ and $\Phi(\cdot)$ denote the standard normal probability density function and the cumulative distribution function, respectively. In the above formulation for likelihood functions, equality data represents Types I and II response data and lower bound data represent the Type III response data classified earlier in Section 3.5.1.

The posterior distribution of the parameters is obtained using the importance sampling algorithm developed by Gardoni et al. (2002b). Table 4.1 lists the posterior statistics of the parameters in the demand models. The standard deviation, $\sigma_{D|S_a}$ of the model error reflects both the aleatory uncertainty inherent in the synthetic ground motions and the epistemic uncertainty in the demand model (Ramamoorthy et al. 2006a).

Table 4.1 Posterior statistics of parameters in single linear demand model for low-and mid-rise buildings

Building	Parameter	Mean	Standard deviation	Correlation coefficient		
				θ_o	θ_1	$\sigma_{D\|S_a}$
1 story	θ_o	1.9814	0.073	1		
	θ_1	1.4530	0.049	0.83	1	
	$\sigma_{D\|S_a}$	0.5631	0.035	0.12	0.09	1
2 story	θ_o	2.2595	0.086	1		
	θ_1	1.7736	0.055	0.85	1	
	$\sigma_{D\|S_a}$	0.5845	0.037	0.24	0.18	1
3 story	θ_o	2.7263	0.084	1		
	θ_1	1.5799	0.045	0.87	1	
	$\sigma_{D\|S_a}$	0.5335	0.034	0.24	0.19	1
6 story	θ_o	2.1123	0.066	1		
	θ_1	1.1639	0.029	0.86	1	
	$\sigma_{D\|S_a}$	0.4320	0.025	0.16	0.13	1
10 story	θ_o	2.4070	0.066	1		
	θ_1	0.9855	0.022	0.90	1	
	$\sigma_{D\|S_a}$	0.3825	0.023	0.06	0.04	1

Figures 4.2 and 4.3 show the plot of predicted demand and residuals of the demand models for sample buildings, respectively. Since the residuals are not randomly distributed, a single linear model (SLM) for the entire range of S_a is inadequate and does not provide a good fit of the response data. Therefore, to obtain a better prediction of inter story drift demand, a bilinear model is developed based on the observation of the transformed data.

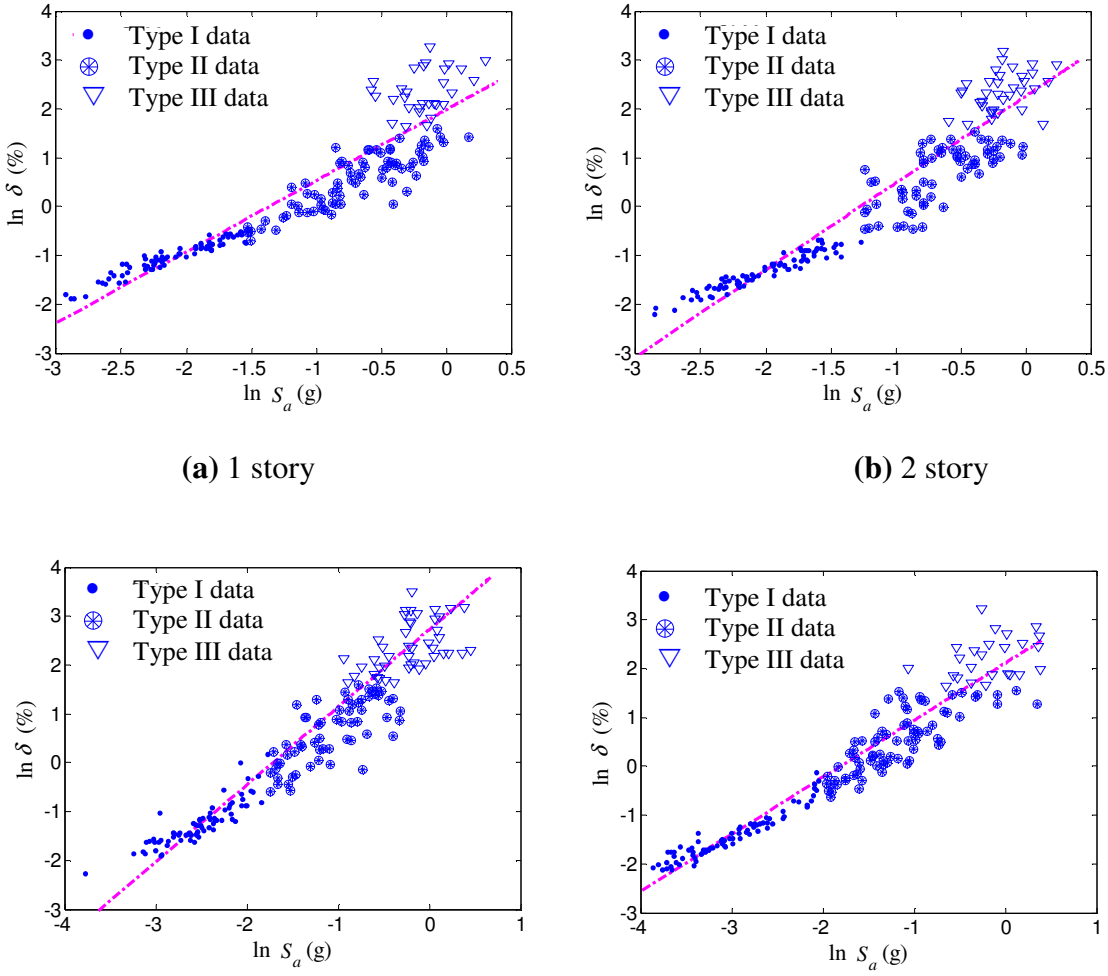

(a) 1 story

(b) 2 story

(c) 3 story

(d) 6 story

Figure 4.2 Probabilistic single linear model (SLM) for low- and mid-rise GLD RC frame buildings

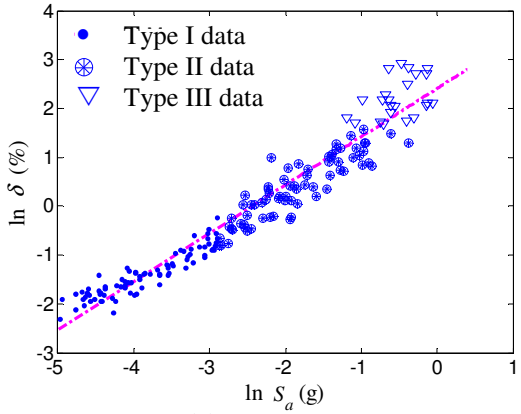

(e) 10 story

Figure 4.2 Continued

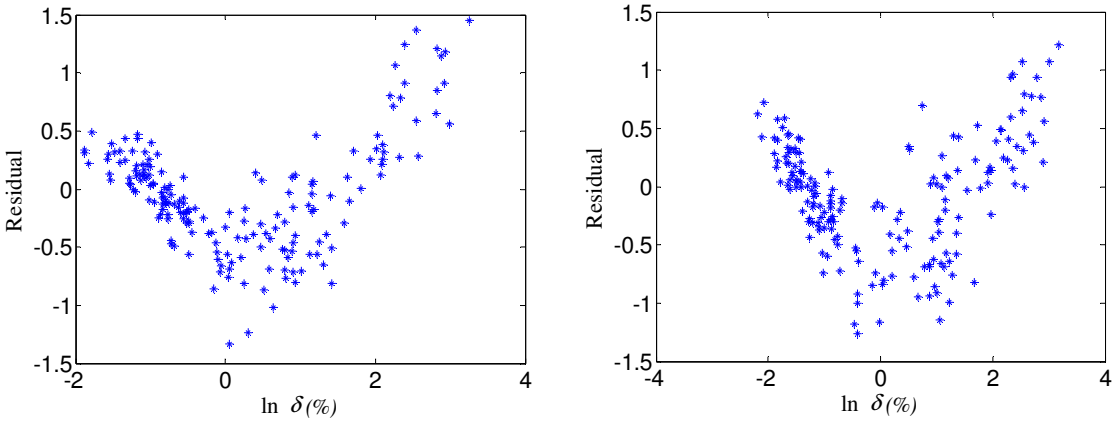

(a) 1 story **(b)** 2 story

Figure 4.3 Residual plots of single linear model (SLM) for GLD RC frame buildings

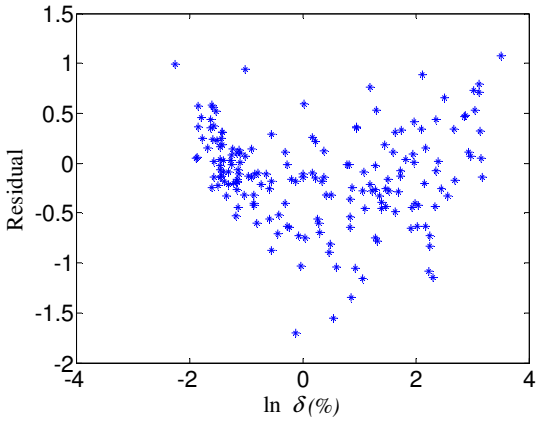

(c) 3 story

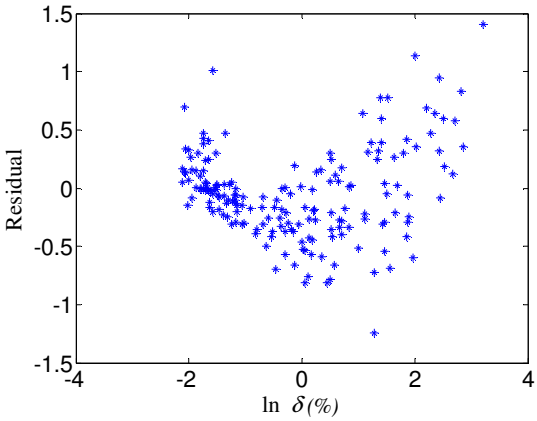

(d) 6 story

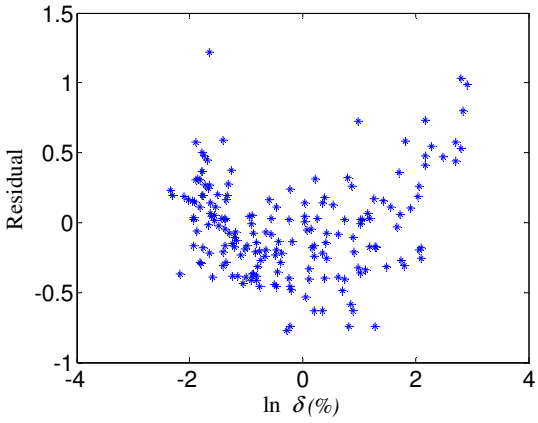

(e) 10 story

Figure 4.3 Continued

4.5 BILINEAR MODELS (BLM)

A bilinear demand model is developed to predict the seismic structural demands since a single linear demand model did not provide a good fit for the entire range of S_a. A first

linear model is developed for the elastic region using the Type I data ($\delta < 0.6\%$) and a second linear model is developed for the inelastic region using Types II and III data.

The posterior statistics of the parameters in the bilinear model, $\boldsymbol{\theta}_1 = (\theta_{10}, \theta_{11}, \sigma_{1D|S_a})$ and $\boldsymbol{\theta}_2 = (\theta_{21}, \sigma_{2D|S_a})$, are estimated using a Bayesian approach and is listed in Table 4.2. For all buildings, $\sigma_{1D|S_a}$ is larger in the inelastic range (higher S_a values) compared to the elastic range. While $\sigma_{2D|S_a}$ does not vary significantly for low- and mid-rise buildings in the elastic range, $\sigma_{2D|S_a}$ is larger in the inelastic range, for low-rise buildings than for the mid-rise buildings.

Figure 4.4 shows the predicted demand for all buildings (solid line) along with one standard deviation confidence interval (dotted lines) for low- and mid-rise buildings using the bilinear model. In addition, the dash-dot line represents the predicted demand obtained from a single linear model. Figure 4.5 shows the residual plot of the bilinear model for all buildings. It is clear, that the residuals of the bilinear model are randomly distributed compared to the residuals of the single linear model.

The bilinear model approaches the single linear model as the number of stories increase. This is consistent with the 'equal-displacement' rule proposed by Velestos and Newmark (1960), where the peak displacements from both elastic and inelastic analysis are similar for buildings with fundamental building period greater than about 1 sec.

Table 4.2 Posterior statistics of parameters in bilinear demand model for elastic and inelastic range for low-and mid-rise buildings

Building	Range	Parameter	Mean	Standard deviation	Correlation coefficient		
					θ_o	θ_1	σ
1 story	Elastic $\delta < 0.6\%$	θ_{10}	0.9015	0.067	1		
		θ_{11}	0.9142	0.032	0.99	1	
		$\sigma_{1D\|S_a}$	0.0988	0.005	0.01	0.01	1
	Inelastic $\delta > 0.6\%$	θ_{21}	1.8117	0.080	NA	1	
		$\sigma_{2D\|S_a}$	0.7724	0.071	NA	0.26	1
2 story	Elastic $\delta < 0.6\%$	θ_{10}	0.6148	0.065	1		
		θ_{11}	0.9600	0.032	0.98	1	
		$\sigma_{1D\|S_a}$	0.1086	0.008	–0.01	0.01	1
	Inelastic $\delta > 0.6\%$	θ_{21}	2.7576	0.123	NA	1	
		$\sigma_{2D\|S_a}$	0.8270	0.079	NA	0.37	1
3 story	Elastic $\delta < 0.6\%$	θ_{10}	1.2875	0.172	1		
		θ_{11}	0.9955	0.067	0.99	1	
		$\sigma_{1D\|S_a}$	0.2187	0.018	–0.01	–0.01	1
	Inelastic $\delta > 0.6\%$	θ_{21}	2.0913	0.084	NA	1	
		$\sigma_{2D\|S_a}$	0.7134	0.068	NA	0.40	1
6 story	Elastic $\delta < 0.6\%$	θ_{10}	1.1059	0.107	1		
		θ_{11}	0.8303	0.034	0.98	1	
		$\sigma_{1D\|S_a}$	0.1634	0.013	0.01	0.01	1
	Inelastic $\delta > 0.6\%$	θ_{21}	1.5281	0.056	NA	1	
		$\sigma_{2D\|S_a}$	0.5725	0.049	NA	0.25	1
10 story	Elastic $\delta < 0.6\%$	θ_{10}	1.1792	0.134	1		
		θ_{11}	0.6643	0.034	0.99	1	
		$\sigma_{1D\|S_a}$	0.1984	0.016	0.01	0.02	1
	Inelastic $\delta > 0.6\%$	θ_{21}	1.2453	0.034	NA	1	
		$\sigma_{2D\|S_a}$	0.4430	0.039	NA	0.25	1

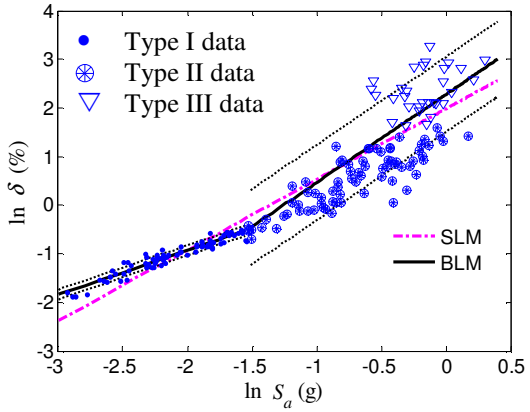

(a) 1 story

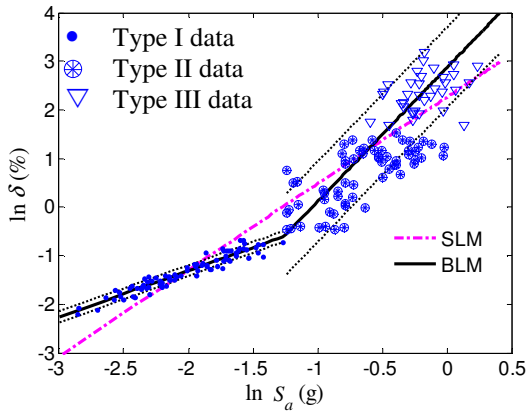

(b) 2 story

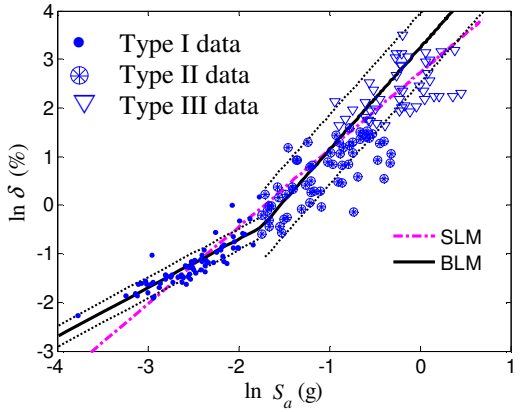

(c) 3 story

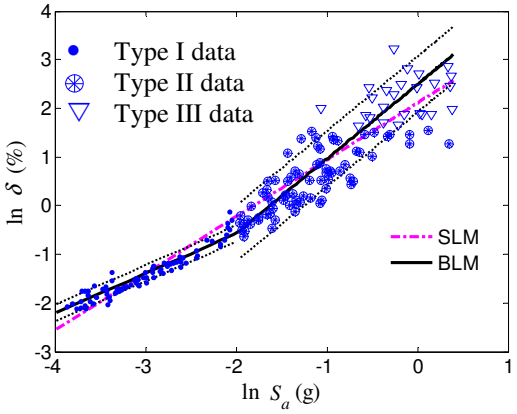

(d) 6 story

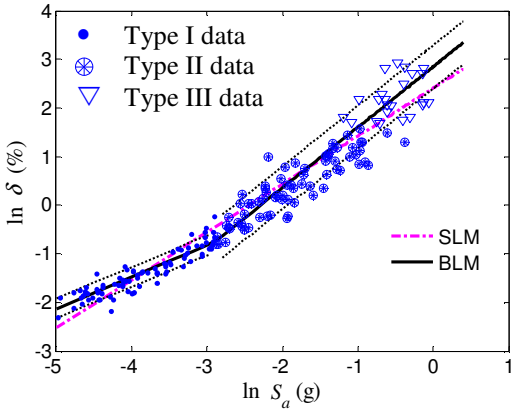

(e) 10 story

Figure 4.4 Probabilistic bilinear model (BLM) for low- and mid-rise GLD RC frame buildings

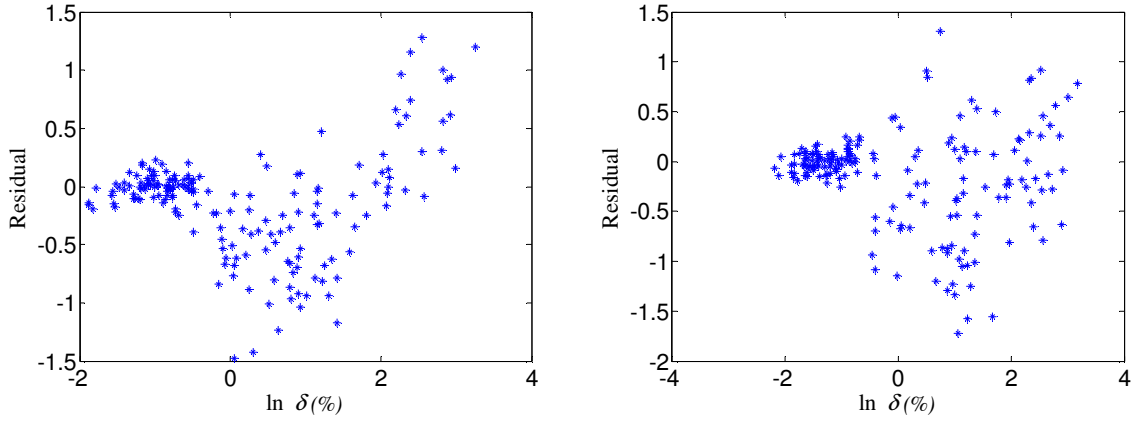

(a) 1 story **(b)** 2 story

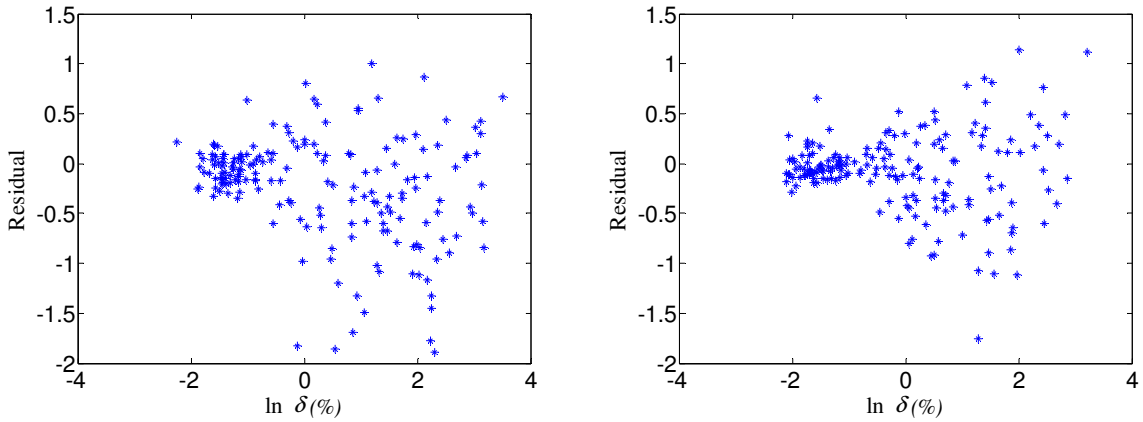

(c) 3 story **(d)** 6 story

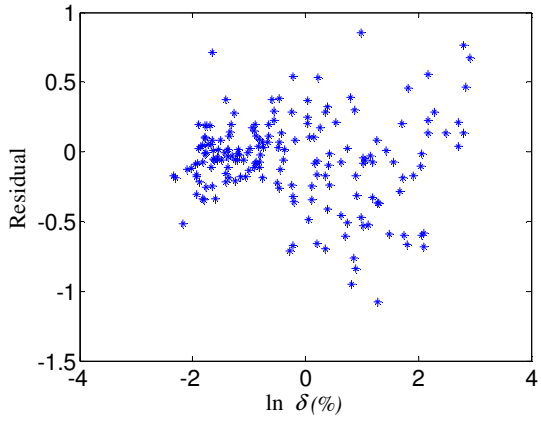

(e) 10 story

Figure 4.5 Residual plots for bilinear model (BLM) for GLD RC buildings

4.6 SUMMARY

Probabilistic demand models are developed to predict the peak inter story drift given the ground motion intensity measure. Following the Bayesian approach, the unknown parameters of the demand models are estimated using the simulated response data from the nonlinear time history analyses. The demand models are unbiased and explicitly account for the model error and statistical uncertainty.

CHAPTER V

PROBABILISTIC CAPACITY

5.1 SEISMIC STRUCTURAL CAPACITY

In general, structural capacity is defined as the maximum displacement, force, velocity, or acceleration that a member or a system can withstand without failure, or more specifically, without exceeding a prescribed performance level. These prescribed performance levels are discrete damage states that buildings could experience during an earthquake. In this study, inter story drift capacity corresponding to the desired performance level is used as the structural capacity. In general, probabilistic models to predict the structural capacity of building systems or components can be developed based on data obtained from previous seismic performance and from experimental testing of building systems and components (Gardoni et al. 2002a). In this study, due to the absence of such data, capacity values are considered corresponding to different performance levels as specified in FEMA-356 (2000) and those computed from nonlinear pushover analysis. In the followings sections inter story drift capacity value are identified for different performance levels.

5.2 CAPACITY VALUES FOR FEMA-356 PERFORMANCE LEVELS

Qualitative structural performance levels described in FEMA-356 (2000) are: Immediate Occupancy (IO), Life Safety (LS), and Collapse Prevention (CP). Table 5.1 lists the description of the IO, LS, and CP performance levels. For RC frame structures, these qualitative performance levels are represented by deterministic inter story drift limits of 1%, 2%, and 4% of the story height for IO, LS, and CP performance levels, respectively. Although these suggested limits are approximate, they are considered fairly accurate for buildings properly designed for seismic loading.

Table 5.1 Structural performance levels specified in FEMA-356 (2000)

Structure type	Structural performance levels	Description of structural performance level	Inter story drift capacity
Concrete Frame	Immediate Occupancy (IO)	Minimal damage and occupants would have access to the structure following the earthquake event	0.5%
	Life Safety (LS)	Significant damage, but the life safety of the occupants would be preserved	1.0%
	Collapse Prevention (CP)	Verge of structural collapse	2.0%

New RC frame buildings designed according to the current building codes should have the desired levels of seismic performance corresponding to different specified levels of earthquake ground motion. However, for existing GLD RC frame buildings, the drift limits for LS and CP performance levels are probably not representative, nor conservative due to insufficient column strength and lack of reinforcement detailing for ductility. Therefore, in this study for low- and mid-rise GLD RC frame buildings reduced drift capacity values of 0.5%, 1%, and 2% are used for IO, LS, and CP performance levels, respectively. These drift values are selected based on the approximate member level rotations for vertical elements suggested in FEMA-356 (2000). These reduced drift values are consistent with the experimental tests conducted by Bracci et al. (1992a) on a scaled model of GLD RC frame buildings.

5.3 PUSHOVER ANALYSIS TO IDENTIFY STRUCTURAL CAPACITY

Nonlinear static (pushover) analysis is used to quantify the resistance of the structure to lateral deformation. Pushover analyses are commonly used in seismic design and evaluation of structures as indicators of structural yielding and potential failure mechanisms (Mwafy and Elnashai 2001). The static pushover analyses procedure has been presented and developed by Saiidi and Sozen (1981), Fajfar and Gaspersic (1996), Bracci et al. (1997), and several other researchers. In general, a sequence of inelastic static analysis is performed on the structural model of the building by applying a predefined lateral load pattern which is distributed along the building height. The lateral forces are then monotonically increased until it becomes unstable and reaches the collapse state (force controlled) or its roof displacement reaches the predetermined limit (displacement controlled).

The pushover technique provides useful information on the overall characteristics of the structural system and allows tracing the sequence of yielding and failure of the members. Results of pushover analysis demonstrate resistance of the building in terms of story shear force versus top displacement, commonly referred to as the capacity curve of the building. Figure 5.1a shows the illustration of an inverted triangular force controlled pushover analysis to identify the critical response of a 3 story RC frame building. The yielding of members is represented by a solid dot (●).

The pushover method is also recommended as a tool for design and analysis purpose by the National Earthquake Hazard Reduction Program (NEHRP) guidelines for the seismic rehabilitation of existing buildings (FEMA-356 2000). Various techniques have been recommended in FEMA-356 (2000), including the use of constant lateral force profiles and the use of adaptive and multimodal approaches. Dooley and Bracci (2001) showed that critical drift capacity values for structural system performance levels can be identified using displacement controlled pushover analysis. The performance levels identified are First Yielding (FY), defined as the inter story drift at which a member of a story or of a structure initiates yielding under an imposed lateral loading and Plastic Mechanism Initiation (PMI), defined as the inter story drift at which a story mechanism

(column side sway mechanism) initiates under an imposed lateral loading. Although deformations beyond the PMI performance level may be possible provided

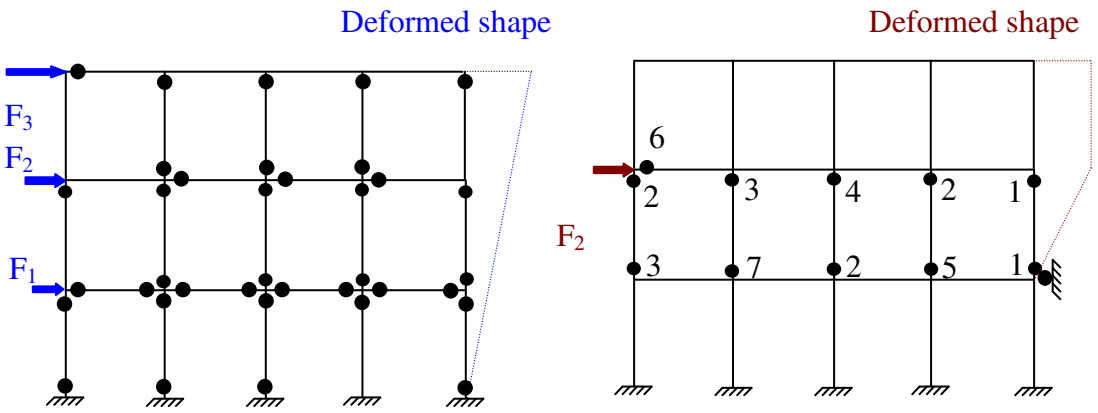

(a) Inverted triangular loading

(b) Critical 2nd story response

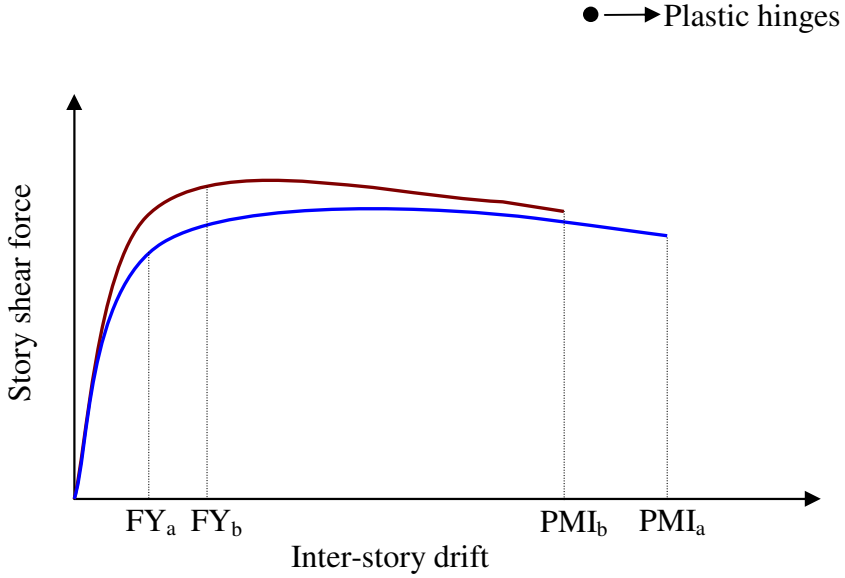

(c) Capacity diagram from pushover analysis

Figure 5.1 Pushover analysis to identify critical story response

plastic hinging behavior is in a ductile fashion, this behavior can not be guaranteed for GLD RC frames.

Figure 5.1b shows the illustration of displacement controlled pushover analysis procedure suggested by Dooley and Bracci (2001) to identify the critical response of a 3 story RC frame building. In order to identify the critical story mechanism of second story, the first story is held and the second story is given a target displacement of 10% drift. The yielding of members is represented by a solid dot (●) and the numbers next to the dots indicate the sequence of yielding. Based on the sequence of yielding of the members, the inter story drift capacity corresponding to the FY and PMI performance levels are identified. Figure 5.1c shows hypothetical capacity diagram for the force and displacement controlled pushover analysis shown in Figure 5.1a and 5.1b. It is clear from the capacity diagram that the inter story drift capacity for FY and PMI performance levels depend on the loading or deformation pattern.

Following the procedure suggested by Dooley and Bracci (2001), displacement controlled pushover analysis of sample buildings is performed in IDASS to identify the inter story drift capacity corresponding to FY and PMI performance levels. Figures 5.2 and 5.3 show the sequence of yielding of members along with the inter story drift capacity for FY and PMI performance levels for low- and mid-rise buildings, respectively. The drift values of pushover performance levels are comparable to the reduced drift values of 0.5%, 1%, and 2% for FEMA-356 IO, LS, and CP performance levels respectively.

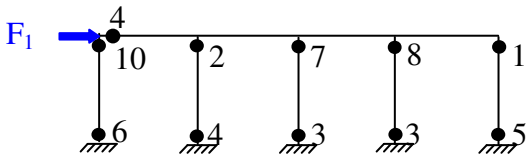

FY = 0.88% and PMI = 1.04%

(a) 1 story

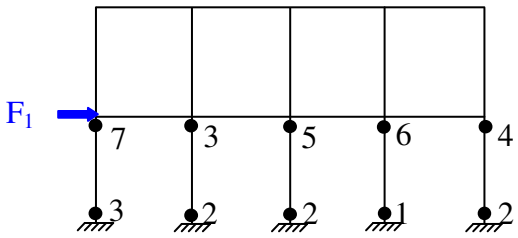

FY = 0.35% and PMI = 0.56%

(b) 2 story

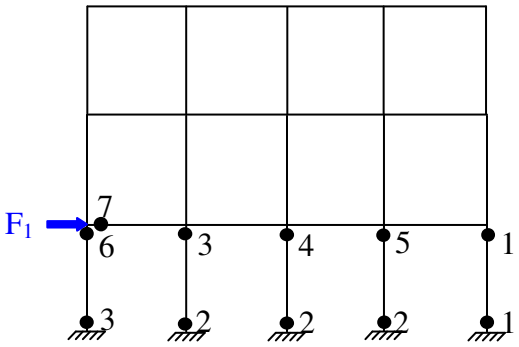

FY = 0.35% and PMI = 0.56%

(c) 3 story

Figure 5.2 Pushover analysis of low-rise buildings

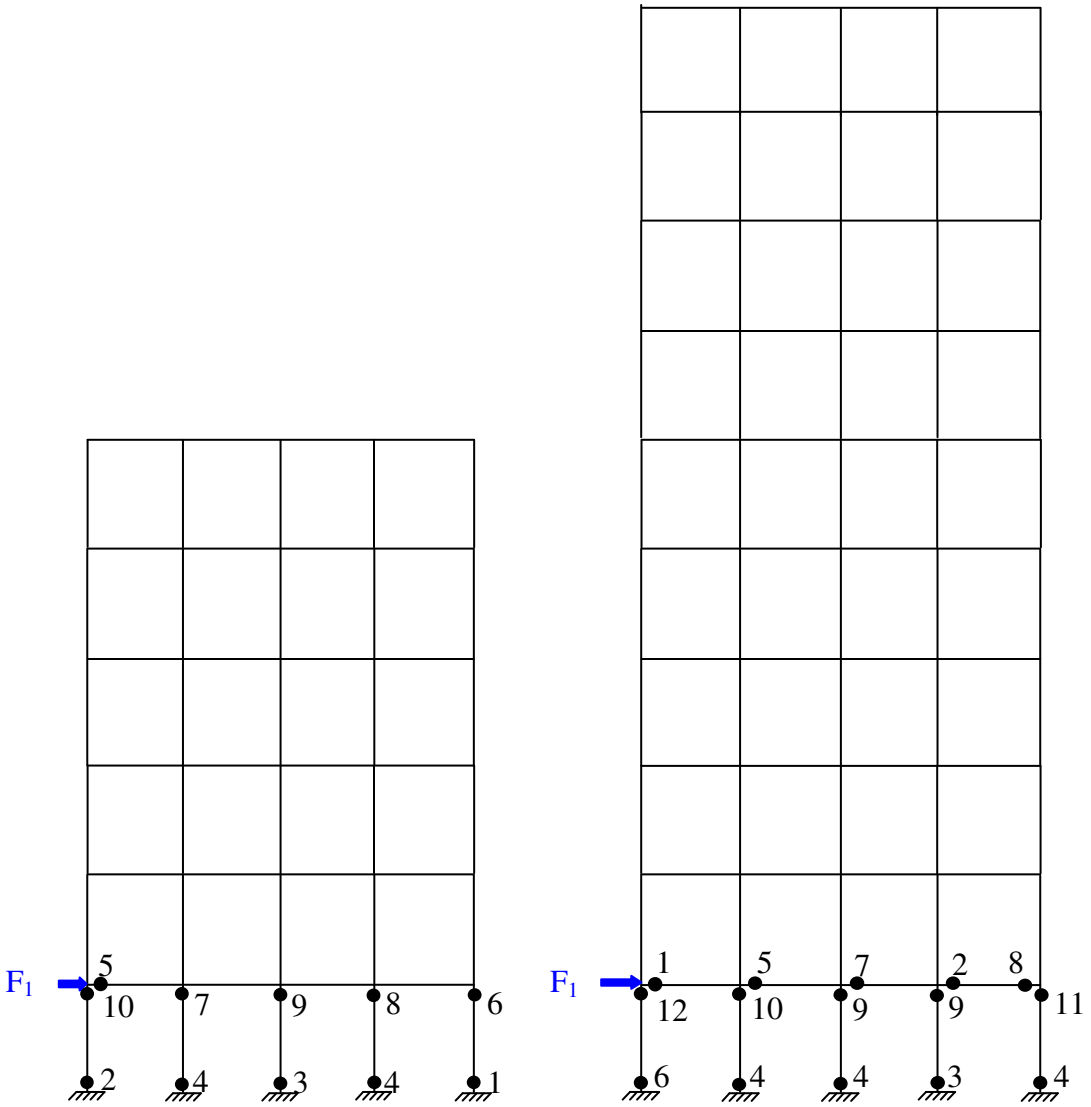

FY = 0.43% and PMI = 1.44%

(a) 6 story

FY = 0.67% and PMI = 1.92%

(b) 10 story

Figure 5.3 Pushover analysis of mid-rise buildings

5.4 PROBABILISTIC STRUCTURAL CAPACITY

To estimate the seismic fragility the capacity values must be specified in a probabilistic sense. The deterministic seismic structural capacity value corresponding to the performance levels specified in FEMA-356 (2000) or damage levels from nonlinear pushover analyses are considered as the median capacity value. Table 5.2 lists the median capacity values against each performance level for all buildings. Uncertainty in estimation of the structural capacity arises from uncertain material properties, geometry, quality of construction, and assumptions in structural models of buildings. In this study, the uncertainty in estimating the capacity is assumed to 0.30 (Wen et al. 2004).

Table 5.2 Median drift capacities (in % story height)

Performance level	Low-rise buildings			Mid-rise buildings	
	1 story	2 story	3 story	6 story	10 story
Immediate Occupancy (IO)	0.5	0.5	0.5	0.5	0.5
Life Safety (LS)	1	1	1	1	1
Collapse Prevention (CP)	2	2	2	2	2
First Yield (FY)	0.88	0.35	0.35	0.43	0.67
Plastic Mechanism Initiation (PMI)	1.04	0.56	0.56	1.44	1.92

5.5 SUMMARY

Structural capacity values are identified corresponding to the performance levels specified in FEMA-356 (2000) and damage levels from nonlinear pushover analysis. To estimate the seismic fragility, the capacity values must be specified in a probabilistic sense. Therefore, the deterministic capacity values are assumed as the median capacity and the standard deviation is assumed equal to 0.30 (Wen et al. 2004).

CHAPTER VI

FRAGILITY ESTIMATES

6.1 INTRODUCTION

As defined earlier, fragility is the conditional probability of a building reaching or exceeding a certain performance level for a given ground motion parameter. Following the conventional notation in structural reliability theory (Ditlevsen and Madsen 1996), the limit state function for the building is written as

$$g\left(C, S_a; \boldsymbol{\Theta}\right) = C - D\left(S_a; \boldsymbol{\Theta}\right) \tag{6.1}$$

where S_a represents the elastic 5% damped spectral acceleration at the fundamental time period of the building, which is used as the seismic intensity parameter, $\boldsymbol{\Theta}$ represents the vector of unknown parameters of the demand model, and C and D represents the capacity and demand of the building, respectively.

Using Eq. (6.1), the fragility for the building is written as

$$F\left(S_a; \boldsymbol{\Theta}\right) = P\left[\left\{g\left(C, S_a; \boldsymbol{\Theta}\right) \le 0\right\} \middle| S_a\right] \tag{6.2}$$

The uncertainty in the event $g(C, S_a; \boldsymbol{\Theta}) \le 0$ for given S_a arises from the inherent randomness in the capacity C, the inexact nature of the limit state function, and the uncertainty inherent in the parameters $\boldsymbol{\Theta}$ of the demand models.

6.2 ESTIMATION OF FRAGILITY

Depending on how the parameters $\boldsymbol{\Theta}$ are treated, different estimates of the fragility can be obtained (Der Kiureghian 2000 and Gardoni et al. 2002b). A point estimate of the fragility is obtained by using the point estimates of the parameters $\boldsymbol{\Theta}$, e.g., the mean values of $\overline{\boldsymbol{\Theta}} = (\overline{\theta}, \overline{\sigma})$. The corresponding point fragility estimates is given as

$$\overline{F}\left(S_a\right) = F\left(S_a; \overline{\boldsymbol{\Theta}}\right) \tag{6.3}$$

$\bar{F}(S_a)$ does not account for the epistemic uncertainties inherent in the model parameters. One way to account for the epistemic uncertainties in the fragility estimation is to treat $\boldsymbol{\Theta}$ as random variables. The corresponding fragility estimate, known as predictive fragility estimate is denoted by $\tilde{F}(S_a)$ and it is obtained by integrating $F(S_a;\boldsymbol{\Theta})$ over all the possible values of $\boldsymbol{\Theta}$ with the posterior density as weighing function, i.e.

$$\tilde{F}\left(S_a\right) = \int F\left(S_a;\boldsymbol{\Theta}\right) f\left(\boldsymbol{\Theta}\right) d\boldsymbol{\Theta} \tag{6.4}$$

where $f(\boldsymbol{\Theta})$ denote the posterior joint probability density function of $\boldsymbol{\Theta}$ obtained by the Bayesian analysis. The predictive fragility is the mean of the conditional fragility with respect to the uncertain parameters $\boldsymbol{\Theta}$. The predictive fragility estimates does not distinguish between the aleatory and epistemic uncertainties.

6.3 MEDIAN FRAGILITY ESTIMATES

Wen et al. (2004) developed a closed form approximation to estimate $F(S_a;\boldsymbol{\Theta})$ by assuming lognormal distribution for capacity and demand. The fragility formulation is given as

$$F\left(S_a;\boldsymbol{\Theta}\right) \cong 1 - \Phi\left(\frac{\lambda_C - \lambda_{D|S_a}}{\sqrt{\sigma_C^2 + \sigma_{D|S_a}^2 + \sigma_m^2}}\right) \tag{6.5}$$

where $\Phi(\cdot)$ denotes the standard normal cumulative distribution function, λ_C and $\lambda_{D|S_a}$ are the natural logarithm of the median capacity and demand of the structural system, respectively, σ_C represents the uncertainty in estimating the capacity, $\sigma_{D|S_a}$ represents the uncertainty in estimating the demand, and σ_m represents the uncertainty in structural modeling of buildings for nonlinear analysis.

Fragility estimates for sample buildings are obtained by using the probabilistic demand models developed in Chapter IV and the capacity values developed in Chapter V for FEMA-356 and pushover performance levels in Eq. (6.5). The dispersion of the

demand model $\sigma_{D|S_a}$ represents the uncertainty in estimating the demand. Following the recommendations of Wen et al. (2004), σ_C and σ_m are assumed to be equal to 0.3.

Figure 6.1 shows the median fragility estimates for a 1 story building corresponding to the FEMA-356 and pushover performance levels. The jump in the fragility estimates is due to the prediction of demand using the bilinear model. The dispersion in the inelastic range, $\sigma_{2D|S_a}$ has a larger value compared to the $\sigma_{1D|S_a}$ value in the elastic range. At the transition point from the elastic range to the inelastic range, due to a larger value of $\sigma_{2D|S_a}$, the value in the second term in Eq. (6.5) decreases for $(\lambda_c - \lambda_{D|S_a}) > 0$, leading to a sudden increase in fragility. Similarly, the value in the second term in Eq. (6.5) increases when $(\lambda_c - \lambda_{D|S_a}) < 0$ resulting in a decrease in fragility.

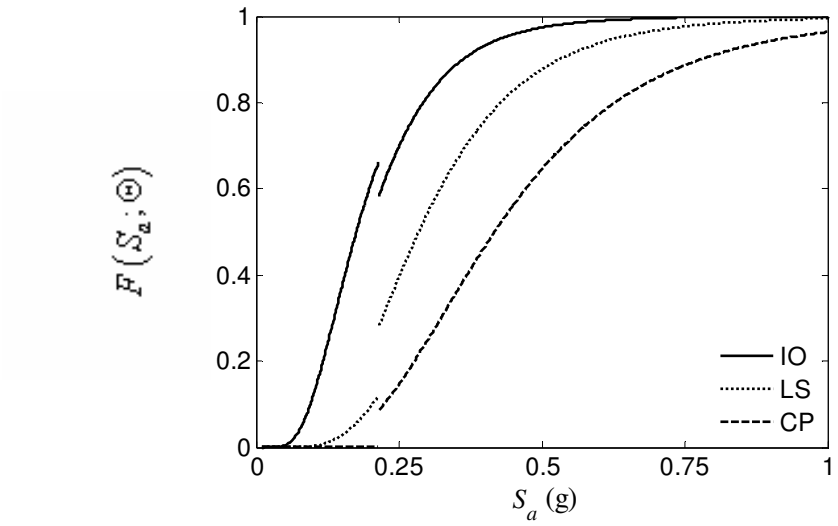

(a) FEMA-356 performance levels

(IO = 0.5%, LS =1%, and CP = 2%)

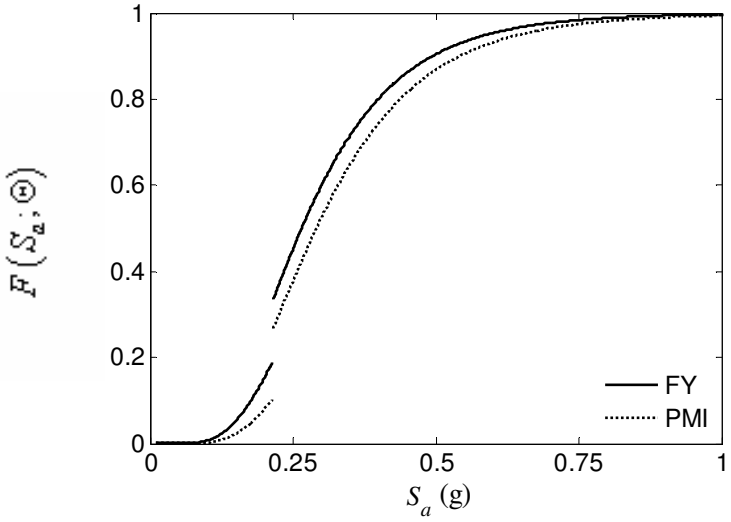

(b) Pushover performance levels

(FY = 0.88% and PMI =1.04%)

Figure 6.1 Median fragility estimates for 1 story building

6.3.1 Continuous Fragility Estimates

Since for practical applications a continuous fragility estimate is preferred, a lognormal function is selected to obtain continuous fragility estimates over the entire range of S_a. The lognormal function is given as:

$$\hat{F}\left(S_a;\boldsymbol{\Gamma}\right)=\Phi\left(\frac{\ln\left(S_a\right)-\gamma_1}{\gamma_2}\right) \tag{6.6}$$

where $\hat{F}(S_a;\boldsymbol{\Gamma})$ represents the continuous fragility and $\boldsymbol{\Gamma}=(\gamma_1,\gamma_2)$ denotes a vector of unknown parameters of the lognormal function. The parameters, γ_1 and γ_2 are determined by fitting $\hat{F}(S_a;\boldsymbol{\Gamma})$ on $F(S_a;\boldsymbol{\Theta})$ using a Bayesian approach. Tables 6.1 and 6.2 list the estimates of the parameters for all buildings.

Figure 6.2 shows the continuous fragility estimates for 1 story building. Figures 6.3 and 6.4 show the $\hat{F}(S_a;\boldsymbol{\Gamma})$ curves for FEMA-356 and pushover performance levels for sample buildings. Fragility curves for the mid-rise buildings are steeper than the low-rise buildings. For example, fragility estimates for IO performance level increases from 0 to 1 as S_a goes from about 0.1g to 0.25g for the 10 story building. To reach the same fragility values, the S_a goes from about 0.1g to 0.75g for the 1 story building. The increase in the range of S_a for the 1 story building is due to the larger value of $\sigma_{D|S_a}$ in the inelastic range.

Table 6.1 Estimates of the parameters for continuous fragility estimates (low-rise buildings)

Building	Performance level		Parameters	
			λ_1	λ_2
1 story	Immediate Occupancy	$+1\sigma$	–1.7555	0.4918
		Median	–1.7069	0.5422
		-1σ	–1.6454	0.5829
	Life Safety	$+1\sigma$	–1.3140	0.4064
		Median	–1.2224	0.4308
		-1σ	–1.1272	0.4299
	Collapse Prevention	$+1\sigma$	–0.9899	0.5022
		Median	–0.8697	0.4769
		-1σ	0.7619	0.4447
	First Yield	$+1\sigma$	–1.3727	0.3947
		Median	–1.2883	0.4273
		-1σ	–1.1974	0.4335
	Plastic Mechanism Initiation	$+1\sigma$	–1.2964	0.4115
		Median	–1.2027	0.4331
		-1σ	–1.1063	0.4299

Table 6.1 Continued

Building	Performance level		Parameters	
			λ_1	λ_2
2 story	Immediate Occupancy	$+1\sigma$	–1.4143	0.3775
		Median	–1.3638	0.4217
		-1σ	–1.2968	0.4557
	Life Safety	$+1\sigma$	–1.1045	0.2666
		Median	–1.0176	0.2976
		-1σ	–0.9265	0.2987
	Collapse Prevention	$+1\sigma$	–0.8975	0.3418
		Median	–0.7850	0.3294
		-1σ	–0.6849	0.3052
	First Yield	$+1\sigma$	–1.7443	0.4788
		Median	–1.7128	0.5285
		-1σ	–1.6696	0.5867
	Plastic Mechanism Initiation	$+1\sigma$	–1.3341	0.3360
		Median	–1.2780	0.3790
		-1σ	–1.2050	0.4056
3 story	Immediate Occupancy	$+1\sigma$	–2.0416	0.4338
		Median	–1.9858	0.4934
		-1σ	–1.9062	0.5503
	Life Safety	$+1\sigma$	–1.6294	0.3067
		Median	–1.5213	0.3579
		-1σ	–1.3990	0.3651
	Collapse Prevention	$+1\sigma$	–1.3601	0.3944
		Median	–1.2105	0.3875
		-1σ	–1.0742	0.3613
	First Yield	$+1\sigma$	–2.3820	0.4906
		Median	–2.3468	0.5395
		-1σ	–2.2996	0.6144
	Plastic Mechanism Initiation	$+1\sigma$	–1.9475	0.4026
		Median	–1.8838	0.4619
		-1σ	–1.7944	0.5096

Table 6.2 Estimates of the parameters for continuous fragility estimates (mid-rise buildings)

Building	Performance level		Parameters	
			λ_1	λ_2
6 story	Immediate Occupancy	$+1\sigma$	−2.2149	0.4866
		Median	−2.1513	0.5352
		-1σ	−2.0699	0.5730
	Life Safety	$+1\sigma$	−1.7324	0.4218
		Median	−1.6179	0.4396
		-1σ	−1.5011	0.4315
	Collapse Prevention	$+1\sigma$	−1.3173	0.4941
		Median	−1.1794	0.4653
		-1σ	−1.0575	0.4353
	First Yield	$+1\sigma$	−2.3738	0.5305
		Median	−2.3210	0.5804
		-1σ	−2.2529	0.6288
	Plastic Mechanism Initiation	$+1\sigma$	−1.5223	0.4696
		Median	−1.3905	0.4576
		-1σ	−1.2681	0.4335
10 story	Immediate Occupancy	$+1\sigma$	−2.9753	0.4947
		Median	−2.8796	0.5486
		-1σ	−2.7567	0.5736
	Life Safety	$+1\sigma$	−2.4370	0.4916
		Median	−2.2808	0.4871
		-1σ	−2.1312	0.4660
	Collapse Prevention	$+1\sigma$	−1.8903	0.5230
		Median	−1.7272	0.4930
		-1σ	−1.5819	0.4658
	First Yield	$+1\sigma$	−2.7300	0.4551
		Median	−2.6023	0.4899
		-1σ	−2.4602	0.4879
	Plastic Mechanism Initiation	$+1\sigma$	−1.9235	0.5228
		Median	−1.7600	0.4930
		-1σ	−1.6143	0.4658

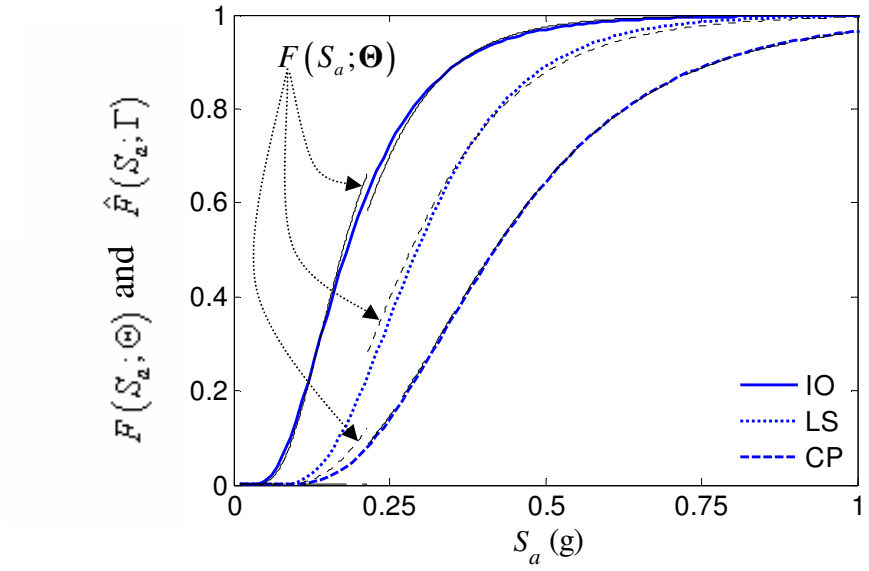

(a) FEMA-356 performance levels

(IO = 0.5%, LS =1%, and CP = 2%)

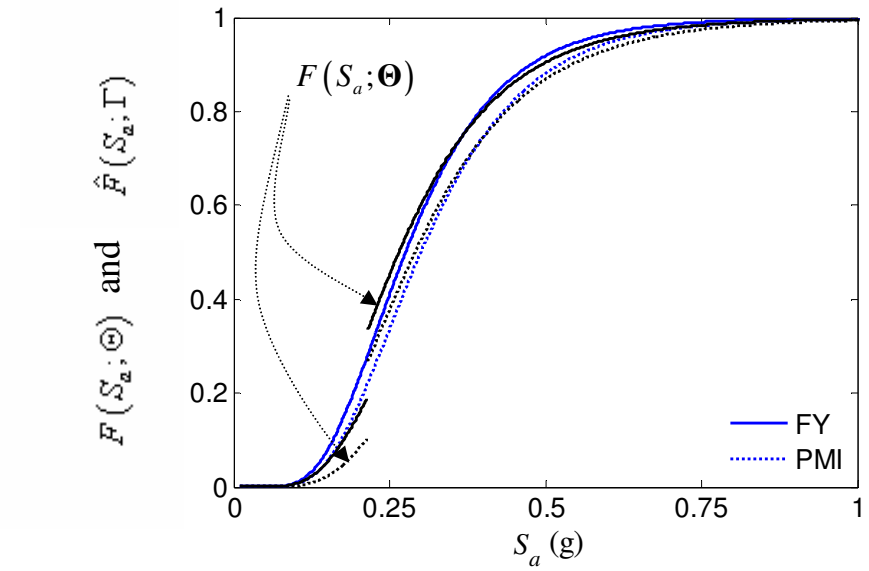

(b) Pushover performance levels

(FY = 0.88% and PMI =1.04%)

Figure 6.2 Continuous fragility estimates for 1 story building

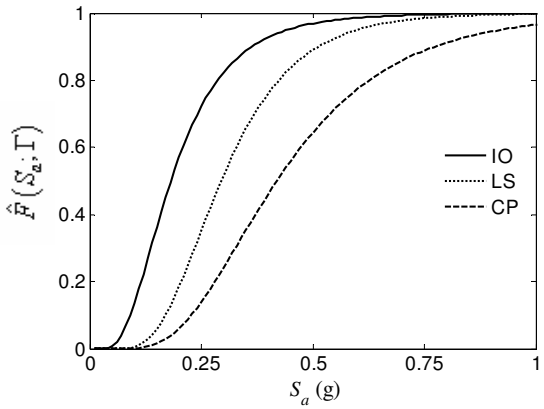

(a) 1 story

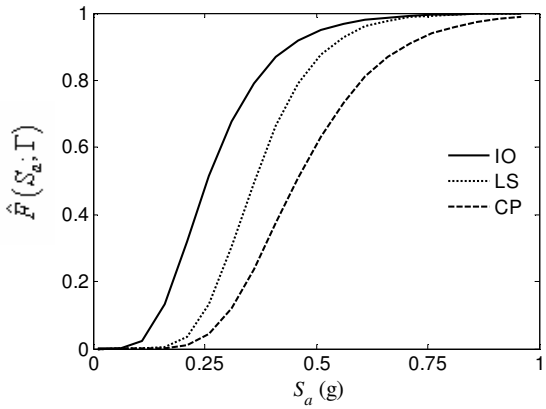

(b) 2 story

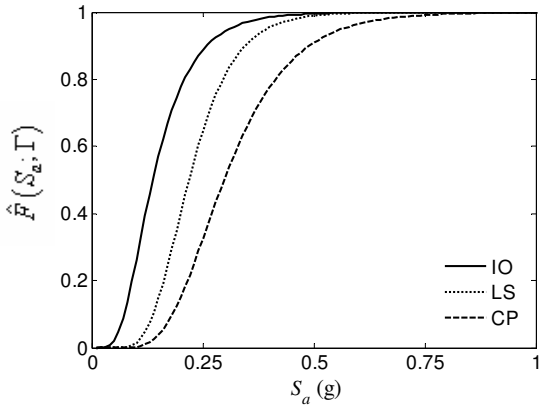

(c) 3 story

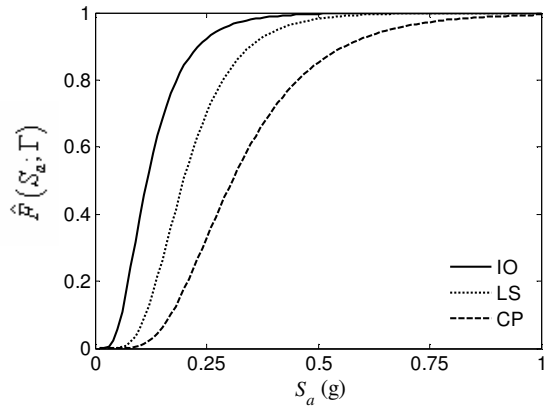

(d) 6 story

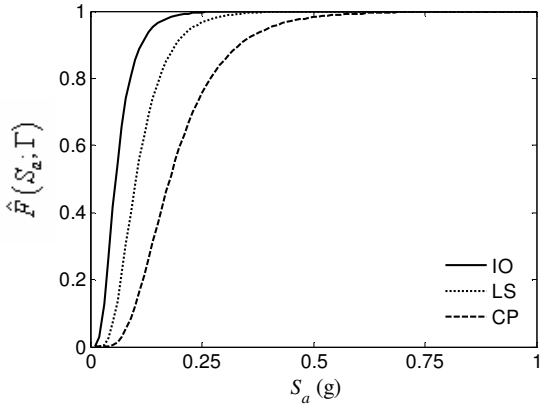

(e) 10 story

Figure 6.3 Fragility estimates for FEMA-356 performance levels for all buildings

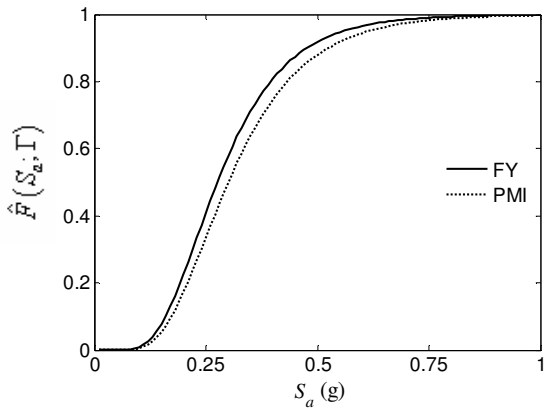

(a) 1 story

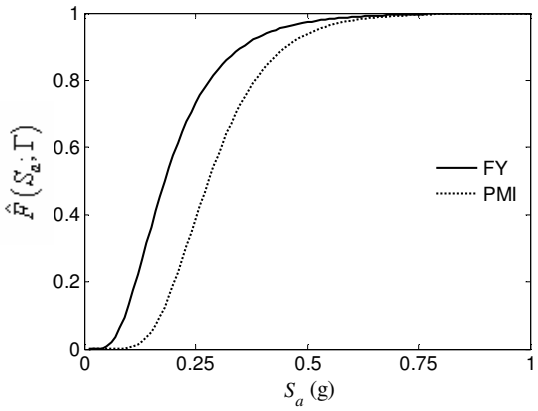

(b) 2 story

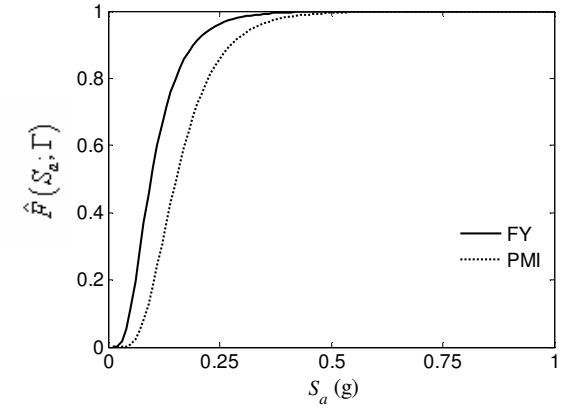

(c) 3 story

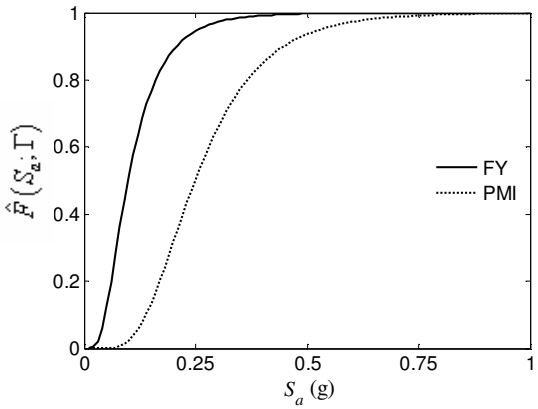

(d) 6 story

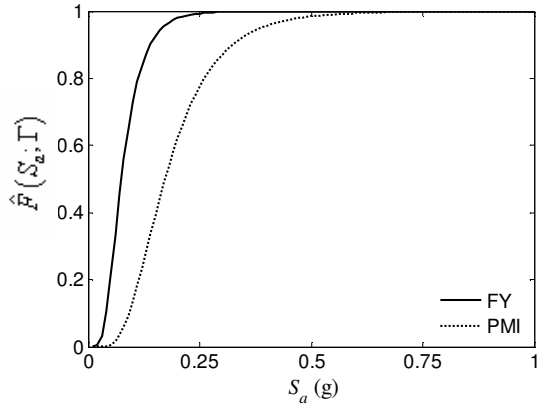

(e) 10 story

Figure 6.4 Fragility estimates for pushover performance levels for all buildings

6.3.2 Confidence Bounds for the Fragility Estimates

It is desirable to determine the epistemic uncertainty inherent in the fragility estimate, which is reflected in the probability distribution of $F(S_a;\boldsymbol{\Theta})$ relative to the parameters $\boldsymbol{\Theta}$. Exact evaluation of this distribution requires nested reliability calculations (Der Kiureghian 1989). Following Gardoni et al. (2002b), approximate confidence bounds are obtained using a first-order analysis. The reliability index corresponding to the conditional fragility in Eq. (6.5) is defined as:

$$\beta(S_a;\boldsymbol{\Theta}) = \left(\frac{\lambda_C - \lambda_{D|S_a}(S_a;\boldsymbol{\theta})}{\sqrt{\sigma_C^2 + \sigma_{D|S_a}^2 + \sigma_m^2}} \right) \tag{6.7}$$

The variance of $\beta(S_a;\boldsymbol{\Theta})$ can be approximated by using a first-order Taylor series expansion around the mean point $M_{\boldsymbol{\Theta}}$ as:

$$\sigma_\beta^2(S_a) \approx \nabla_{\boldsymbol{\Theta}}\beta(S_a)\,\Sigma_{\boldsymbol{\Theta}\boldsymbol{\Theta}}\,\nabla_{\boldsymbol{\Theta}}\beta(S_a)^T \tag{6.8}$$

where $\nabla_{\boldsymbol{\Theta}}\beta(S_a)$ is the gradient row vector of $\beta(S_a;\boldsymbol{\Theta})$ at the mean point and $\Sigma_{\boldsymbol{\Theta}\boldsymbol{\Theta}}$ denotes the posterior covariance matrix. Transforming these back into the probability space, one standard deviation bounds of the fragility estimate can be approximated as:

$$\left\{\Phi\left[-\beta(S_a)-\sigma_\beta(S_a)\right],\ \Phi\left[-\beta(S_a)+\sigma_\beta(S_a)\right]\right\} \tag{6.9}$$

These bounds approximately correspond to 15% and 85% confidence level on the fragility estimates. Figures 6.5 and 6.6 show the $\hat{F}(S_a;\boldsymbol{\Gamma})$ curves with confidence bounds for FEMA-356 and pushover performance levels for all buildings.

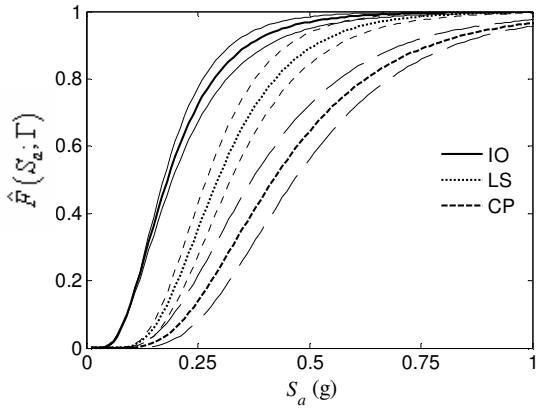

(a) 1 story

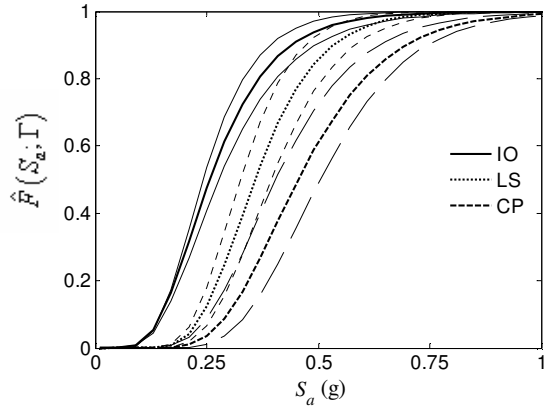

(b) 2 story

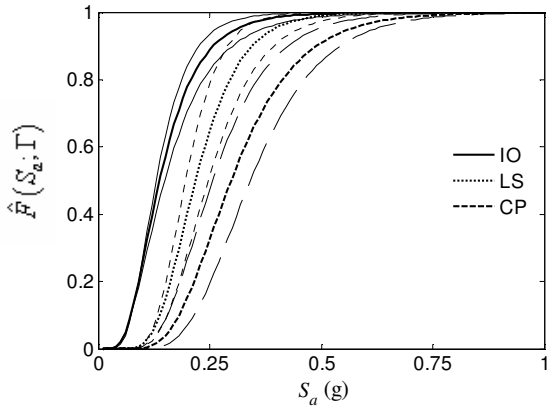

(c) 3 story

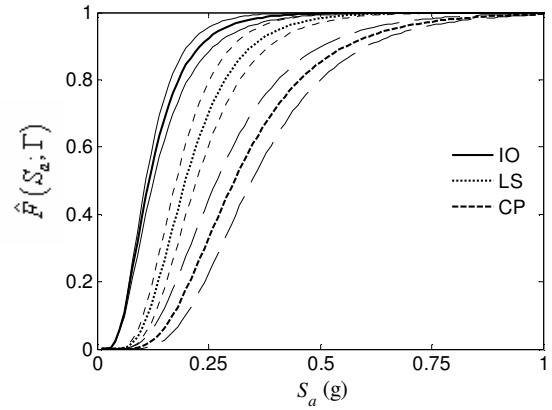

(d) 6 story

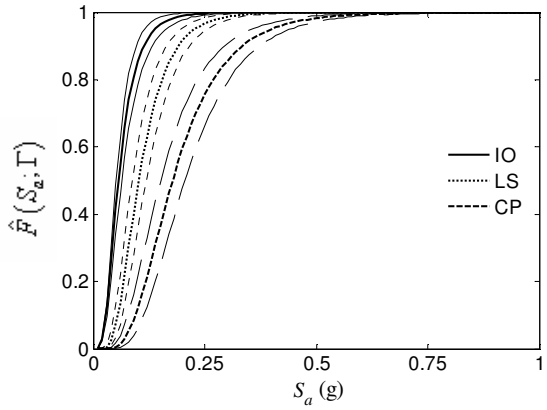

(e) 10 story

Figure 6.5 Fragility estimates for FEMA-356 performance levels with confidence bounds

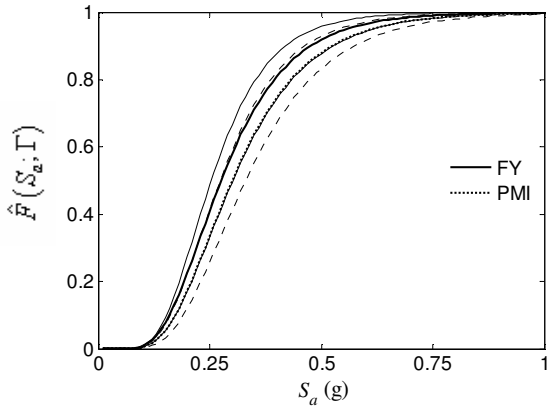

(a) 1 story

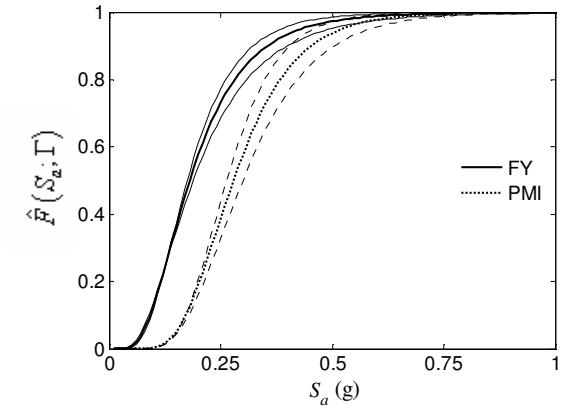

(b) 2 story

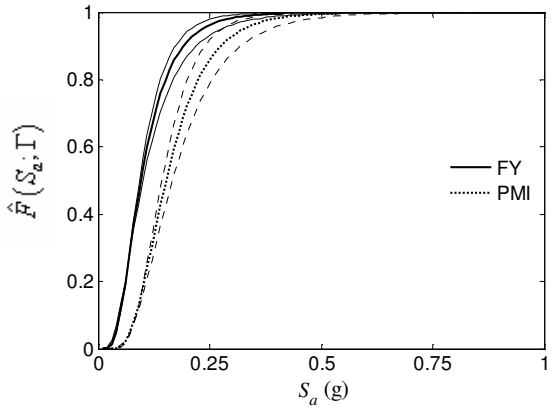

(c) 3 story

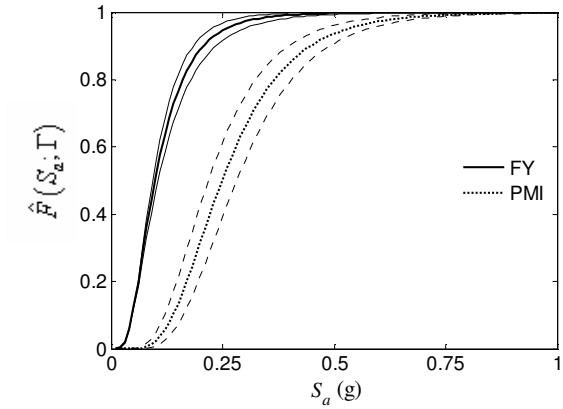

(d) 6 story

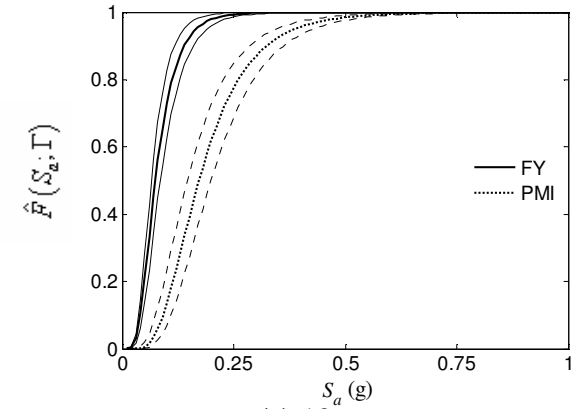

(e) 10 story

Figure 6.6 Fragility estimates for pushover performance levels with confidence bounds

Given the fragility estimates, the seismic vulnerability of low- and mid-rise buildings can be estimated for a given seismic event. For example according to the IBC (2003) the general design response spectrum for Memphis, Tennessee is shown in Figure 6.7. The design S_a corresponding to the fundamental time period for the 1, 2, 3, 6, and 10 story building is equal to 0.69 g, 0.73 g, 0.49 g, 0.31 g, and 0.18 g, respectively.

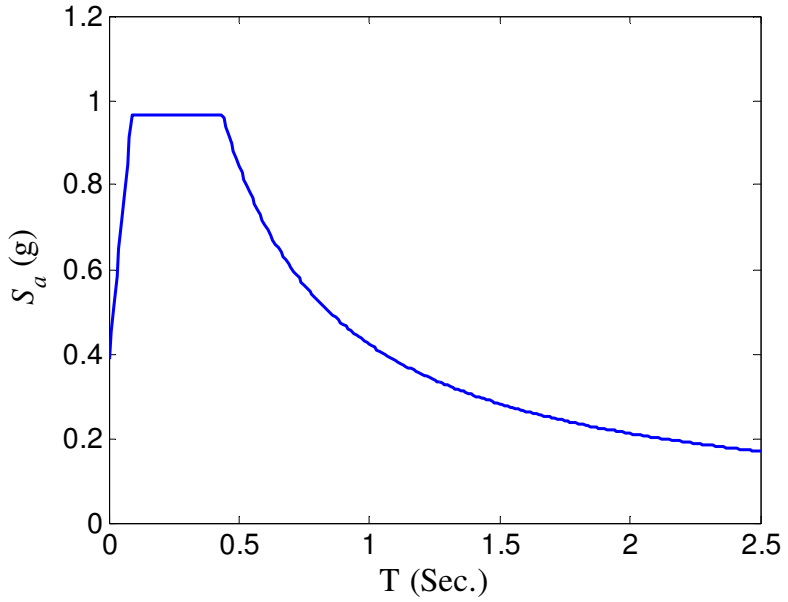

Figure 6.7 General design response spectrum for Memphis, TN based on IBC (2003)

The median fragility values corresponding to the design response spectrum for the 1, 2, 3, 6, and 10 story building are obtained from Figure 6.3 and are listed in Table 6.3. The results show that for life safety and collapse prevention performance levels, significant damage is expected for the low-rise buildings compared to the mid-rise buildings.

Table 6.3 Median fragility values for low- and mid-rise buildings (in %)

Performance level	Low-rise buildings			Mid-rise buildings	
	1 story	2 story	3 story	6 story	10 story
Immediate Occupancy	99.31	99.36	99.50	96.65	98.31
Life Safety	97.51	99.09	98.80	84.53	87.74
Collapse Prevention	85.21	92.33	90.02	50.71	51.00

6.4 VALIDATION OF ANALYTICAL FRAGILITY ESTIMATES

The validity of analytical fragility estimates should be determined using the observed damage data or experimental test data. Due to lack of actual earthquake damage data of buildings in the Mid-America Region the analytical fragility estimates cannot be directly validated.

As mentioned earlier in Chapter III, Section 3.4.2, the IDASS (Kunnath 2003) program was validated using the experimental test data on a GLD RC frame buildings and structural components by Bracci et al. (1992a) and Aycardi et al. (1992). In this study, the probabilistic demand models are developed using the simulated response data obtained using IDASS. Therefore, there is a higher confidence on the predicted inter story drift demands of sample buildings. These predicted demands are used to develop the analytical fragility estimates of sample buildings. Thus the developed analytical fragility estimates are party validated.

6.5 COMPARISON OF ANALYTICAL FRAGILITY ESTIMATES

In this section, the analytical fragility estimates developed for GLD RC frame buildings are compared with the analytical fragility estimates developed for similar buildings by Celik and Ellingwood (2006) and Hwang and Huo (1996). Celik and Ellingwood developed fragility curves for a 3 story GLD RC frame building located in Memphis, TN. Nonlinear time history analyses of a two-dimensional finite element model of an

interior frame in OpenSees (McKenna and Fenves 2006) was carried out by using 2% in 50 years probabilistic ground motions for soft soil developed by Wen and Wu (2001) for Memphis, TN. Using the simulated response data, probabilistic demand model in power form was developed.

Figure 6.8 shows the comparison of median fragility estimates for 3 story building obtained in this study with the fragility estimates obtained by Celik and Ellingwood (2006). The solid line represents the fragility estimate developed in this study using the predicted demand from bilinear demand model along with confidence bounds for the fragility estimates. The dashed line represents the fragility estimates form Celik and Ellingwood study using the rigid joint model. In general the fragility estimates are not in good agreement. This may be due to the difference in idealization and assumption in structural models, ground motions, analysis software, and demand model form in each study.

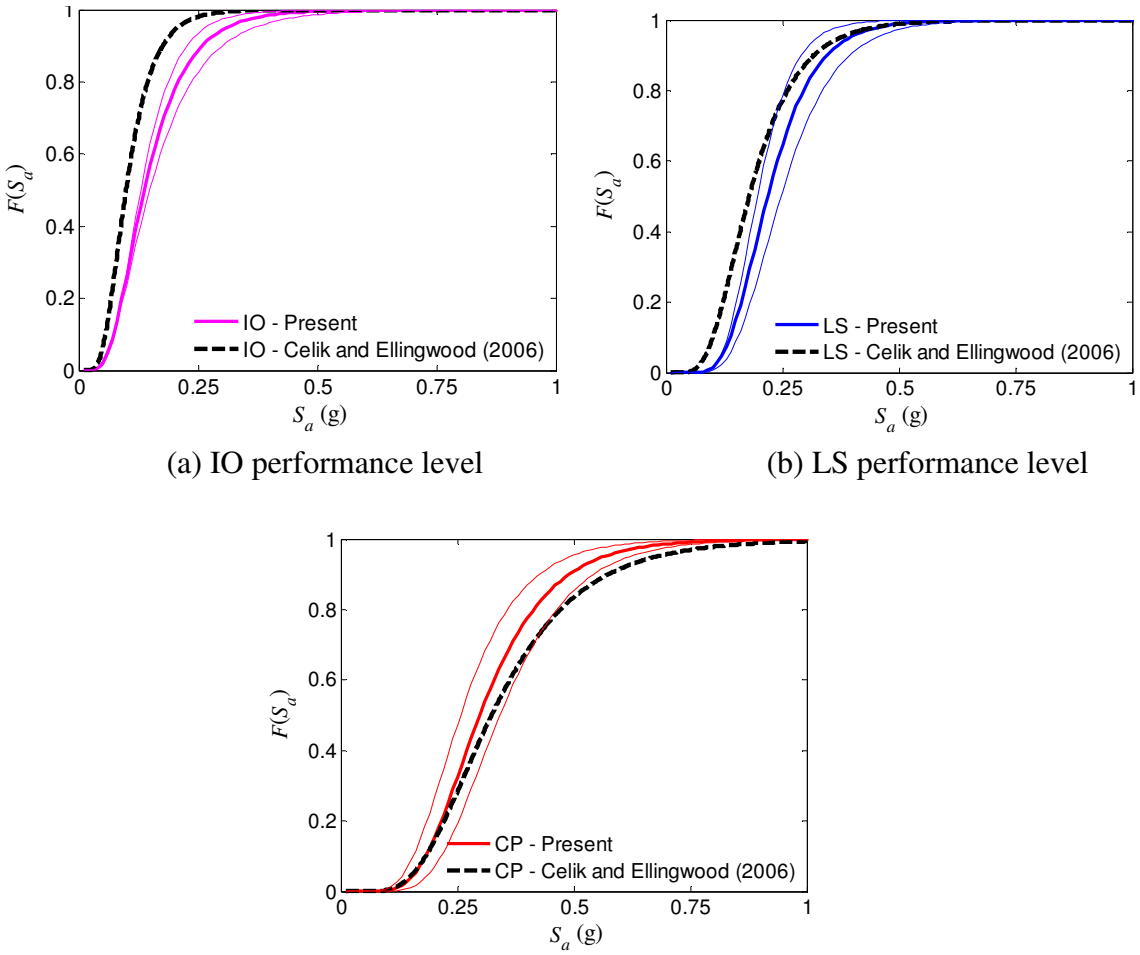

(a) IO performance level

(b) LS performance level

(c) CP performance level

Figure 6.8 Fragility estimates for 3 story RC frame building with confidence bounds for FEMA-356 performance levels (Demand is predicted using bilinear model)

For example, Celik and Ellingwood (2006) used only 2% in 50 years probabilistic ground motion records for Memphis, TN, developed by Wen and Wu (2001) compared to 180 ground motions used in this study. In addition, Celik and Ellingwood used a simple power model to develop the demand models. Figure 6.9 shows the comparison of the analytical fragility estimates developed in this study using the predicted demand from single linear model with the Celik and Ellingwood (2006) fragility estimates.

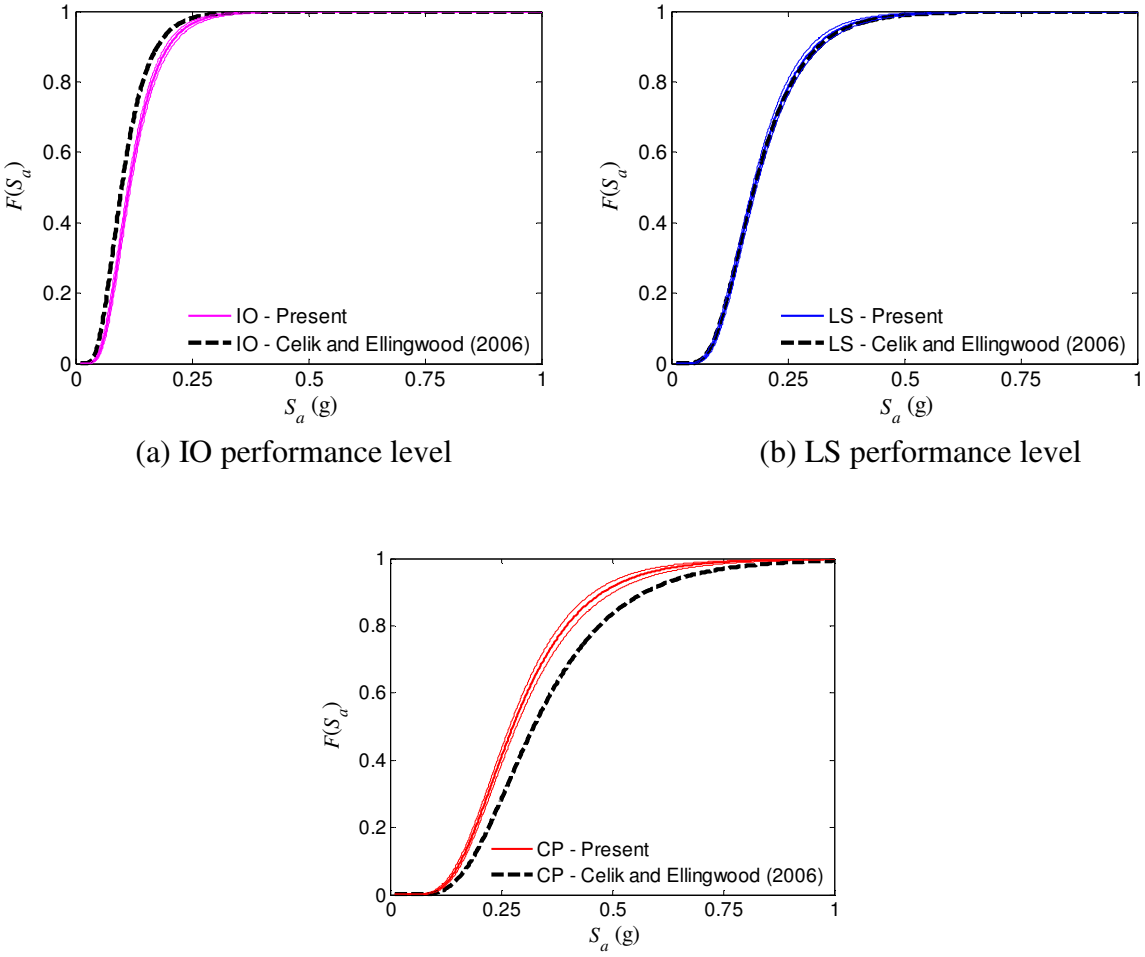

(a) IO performance level

(b) LS performance level

(c) CP performance level

Figure 6.9 Fragility estimates for 3 story RC frame building with confidence bounds for FEMA-356 performance levels (Demand is predicted using single linear model)

It is clear that the fragility estimates obtained using single linear model compare well with fragility estimates developed by Celik and Ellingwood (2006) than the fragility estimates obtained using the bilinear model.

Hwang and Huo (1996) selected a 2 story RC frame building to represent the generic low-rise (1 to 3 story) RC frame buildings. Nonlinear analysis of the structural models was carried out using two different ground motions in IDARC (Kunnath et al. 1991). Using the simulated response data, analytical fragility estimates for 2 story RC frame building were obtained for slight, moderate, extensive, and complete damage states. These damage states were defined using the damage index proposed by Park and Ang (1985).

For comparison, slight, moderate, and extensive damage levels are related to FEMA-356 IO, LS, and CP performance levels. Figures 6.10 and 6.11 show the comparison of analytical fragility estimates with confidence bounds for 2 story building obtained in this study using predicted demand from bilinear and single linear demand models, respectively with the fragility estimates obtained by Hwang and Huo (1996). The solid line represents the fragility estimates developed in this study and the dotted line represents the fragility estimates developed by Hwang and Huo (1996). In general, the fragility estimates developed by Hwang and Huo (1996) are not in good agreement with the fragility estimates developed in this study. This may be due to the difference in the in the inter story drift capacity values for the FEMA-356 performance levels used in this study compared to the damage levels used in Hwang and Huo study.

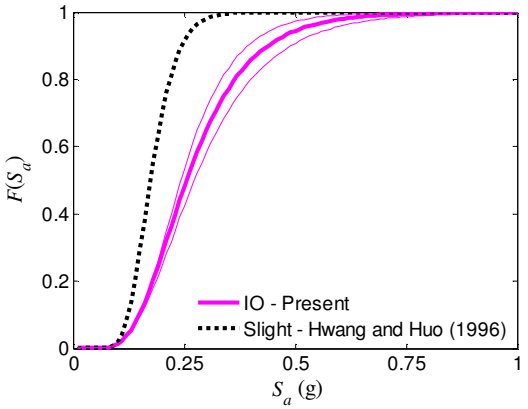

(a) IO performance level

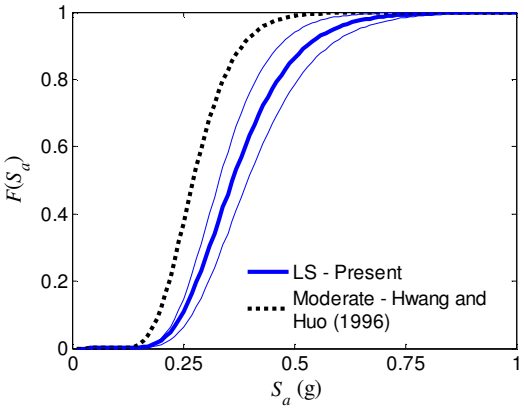

(b) LS performance level

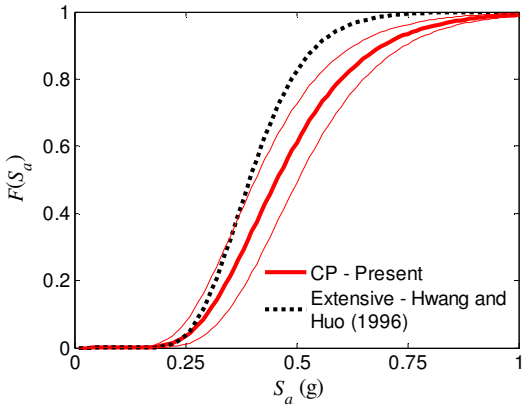

(c) CP performance level

Figure 6.10 Fragility estimates for 2 story RC frame building with confidence bounds for FEMA-356 performance levels (Demand is estimated using bilinear model)

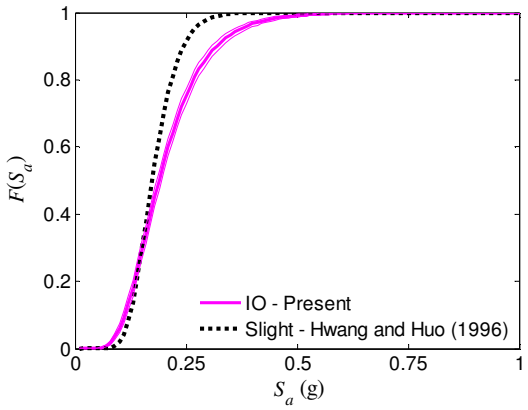

(a) IO performance level

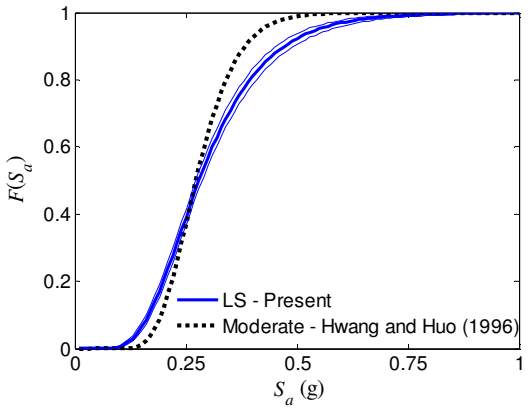

(b) LS performance level

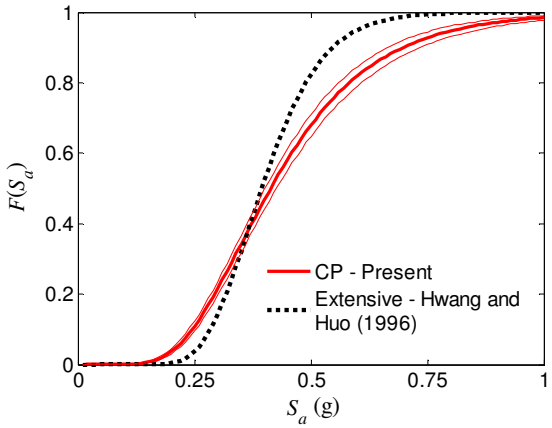

(c) CP performance level

Figure 6.11 Fragility estimates for 2 story RC frame building with confidence bounds for FEMA-356 performance levels (Demand is estimated using single linear model)

6.6 BIVARIATE FRAGILITY ESTIMATES

It is well known that the seismic response of buildings is sensitive to the frequency content of the earthquake and the fundamental period of the building, T_1. Therefore it is

important that the seismic fragility estimates account for the building period, even for rapid vulnerability assessment (Ramamoorthy et al. 2006b). In general, for a single demand variable, the plot of fragility estimates as a function of the single demand variable is referred as the fragility curve. When several variables are used to define the demand on the structural system or component, then $F(\mathbf{S})$ defines a fragility surface over the space of demand variables, $\mathbf{S}$. In this study, bivariate fragility estimates, defined as the conditional probability of attaining or exceeding a specified performance level for given values of S_a and T_1 are developed using the fragility estimates of the sample buildings. In Figure 6.12, corresponding to the T_1 of each of the five buildings considered, dots (•) identify the values of S_a that corresponds to a fragility value from 0.1 to 0.9 with a step of 0.1 (nine dots for each value of T_1) for FEMA-356 IO performance level.

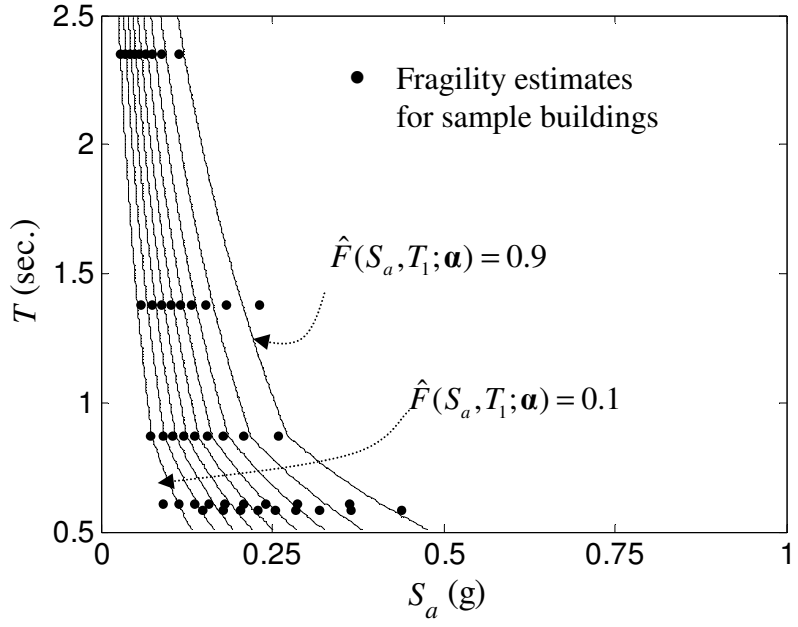

Figure 6.12 Contour plots of bivariate fragility estimates for FEMA-356 IO performance level (IO = 0.5% Inter story drift)

Fragility estimates of any 1 to 10 story building of general height (h) can be obtained by using a logarithmic interpolation function with S_a and T_1 as regressors. In order to obtain continuous bivariate fragility estimates, two interpolation functions are developed. The first interpolation function, developed for $T_1 \geq 0.87$ sec., is written as:

$$\hat{F}_1\left(S_a, T_1; \boldsymbol{\alpha}_1\right) = \Phi\left(\frac{\log\left(S_a\right) - \left(\alpha_{11} + \alpha_{12} T_1\right)}{\left(\alpha_{13} + \alpha_{14} T_1\right)}\right) \tag{6.10}$$

where $\boldsymbol{\alpha}_1 = (\alpha_{11}, \alpha_{12}, .., \alpha_{14})$ is a vector of unknown parameters that are estimated using the Bayesian approach. Data from the $\hat{F}(S_a; \boldsymbol{\Gamma})$ estimates for 3, 6, and 10 story buildings are used for the statistical analysis. A second interpolation function, developed for $0.00 < T_1 < 0.87$ sec., is written as:

$$\hat{F}_2\left(S_a, T_1; \boldsymbol{\alpha}_2\right) = \Phi\left(\frac{\log\left(S_a\right) - \left(\hat{\alpha}_{11} + \hat{\alpha}_{12} 0.87\right)}{\left(\hat{\alpha}_{13} + \hat{\alpha}_{14} 0.87\right)} + \left(0.87 - T_1\right)\frac{\log\left(S_a\right) - \alpha_{21}}{\alpha_{22}}\right) \tag{6.11}$$

where $\hat{\boldsymbol{\alpha}}_1 = (\hat{\alpha}_{11}, \ldots, \hat{\alpha}_{14})$ represents the mean of $\boldsymbol{\alpha}_1$ in the first interpolation function and $\boldsymbol{\alpha}_2 = (\alpha_{21}, \alpha_{22})$ is a vector of unknown parameters. Vector $\boldsymbol{\alpha}_2$ is estimated by using data from the $\hat{F}(S_a; \boldsymbol{\Gamma})$ estimates of 1 and 2 story buildings ($T_1 < 0.87\,\text{sec.}$). Tables 6.4 and 6.5 list the point estimates of the parameters for FEMA-356 and pushover performance levels. The lines in Figure 6.12 represent the contour lines of the bivariate fragility estimates. Each contour line in this plot connects pairs of values of S_a and T_1 that correspond to a level of fragility in the range 0.1-0.9. Figures 6.13-6.16 show the contour lines of the bivariate fragility estimates for LS, CP, FY, and PMI performance levels, respectively. The probability of reaching or exceeding a particular performance level (for example CP performance level) of a RC frame building (1 to 10 story) for a given T_1 and S_a can be obtained by using the contour plots of the bivariate fragility estimates or the interpolation functions.

The contour lines of the bivariate fragility estimates shown in Figures 6.12-6.16 are obtained by using the fragility estimates of the sample buildings. While the sample building configurations, member sizes, and joint details are chosen such that they are

representative of the GLD RC frame building inventory in the Mid-America Region, other options are also possible. The bivariate fragility estimates in an average sense account for such variability because they are developed using five different realizations (one for each of the selected building height). For this reason, the bivariate fragility estimates are believed to provide an accurate assessment of the seismic vulnerability of GLD RC frame buildings in the Mid-America Region.

Table 6.4 Estimates of the unknown parameters of the bivariate fragility function (FEMA-356 performance levels)

Performance level	Parameter		Mean values
Immediate Occupancy	$\hat{\boldsymbol{\alpha}}_1$	$\hat{\alpha}_{11}$	−1.4297
		$\hat{\alpha}_{12}$	−0.5882
		$\hat{\alpha}_{13}$	0.4863
		$\hat{\alpha}_{14}$	0.0237
	$\hat{\boldsymbol{\alpha}}_2$	$\hat{\alpha}_{21}$	33.6713
		$\hat{\alpha}_{22}$	11.7658
Life Safety	$\hat{\boldsymbol{\alpha}}_1$	$\hat{\alpha}_{11}$	−1.0435
		$\hat{\alpha}_{12}$	−0.5021
		$\hat{\alpha}_{13}$	0.3111
		$\hat{\alpha}_{14}$	0.0851
	$\hat{\boldsymbol{\alpha}}_2$	$\hat{\alpha}_{21}$	12.533
		$\hat{\alpha}_{22}$	3.892
Collapse Prevention	$\hat{\boldsymbol{\alpha}}_1$	$\hat{\alpha}_{11}$	−0.8408
		$\hat{\alpha}_{12}$	−0.3500
		$\hat{\alpha}_{13}$	0.3651
		$\hat{\alpha}_{14}$	0.0631
	$\hat{\boldsymbol{\alpha}}_2$	$\hat{\alpha}_{21}$	6.4062
		$\hat{\alpha}_{22}$	2.6323

Table 6.5 Estimates of the unknown parameters of the bivariate fragility function (Pushover performance levels)

Performance level	Parameter		Mean values
First Yield	$\hat{\boldsymbol{\alpha}}_1$	$\hat{\alpha}_{11}$	–2.1432
		$\hat{\alpha}_{12}$	–0.1848
		$\hat{\alpha}_{13}$	0.6018
		$\hat{\alpha}_{14}$	–0.0405
	$\hat{\boldsymbol{\alpha}}_2$	$\hat{\alpha}_{21}$	4.3385
		$\hat{\alpha}_{22}$	1.1316
Plastic Mechanism Initiation	$\hat{\boldsymbol{\alpha}}_1$	$\hat{\alpha}_{11}$	–1.7001
		$\hat{\alpha}_{12}$	0.0141
		$\hat{\alpha}_{13}$	0.5338
		$\hat{\alpha}_{14}$	–0.0102
	$\hat{\boldsymbol{\alpha}}_2$	$\hat{\alpha}_{21}$	0.2450
		$\hat{\alpha}_{22}$	0.4854

-

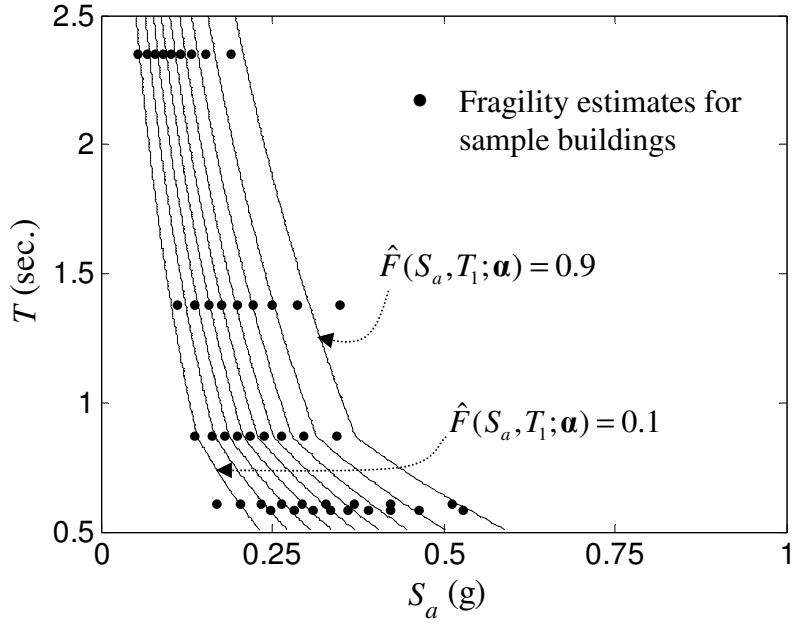

Figure 6.13 Contour plots of bivariate fragility estimates for FEMA-356 LS performance level (LS = 1% Inter story drift)

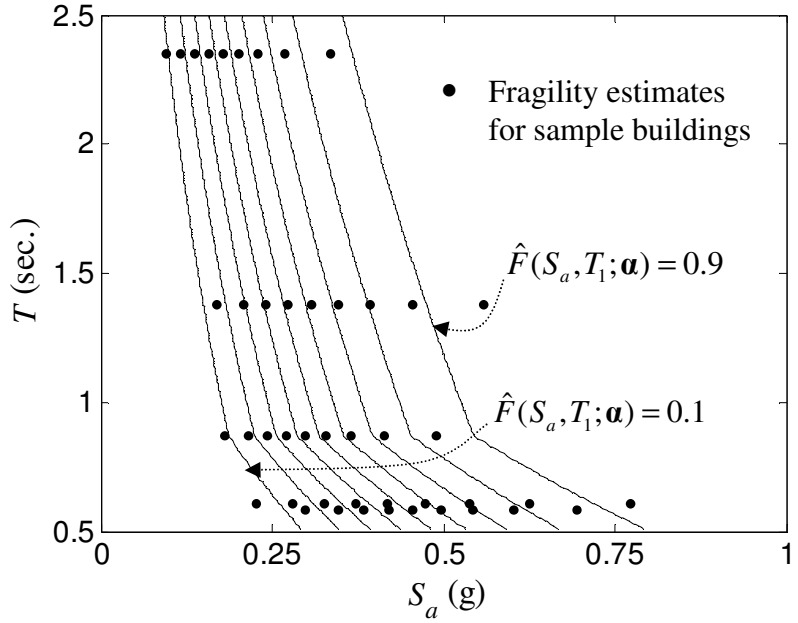

Figure 6.14 Contour plots of bivariate fragility estimates for FEMA-356 CP performance level (CP = 2% Inter story drift)

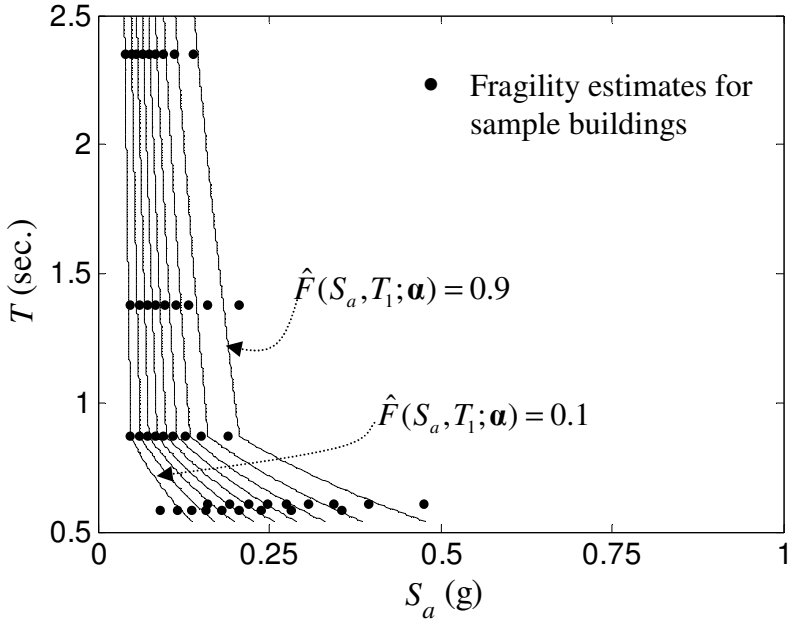

Figure 6.15 Contour plots of bivariate fragility estimates for pushover performance level (First Yield)

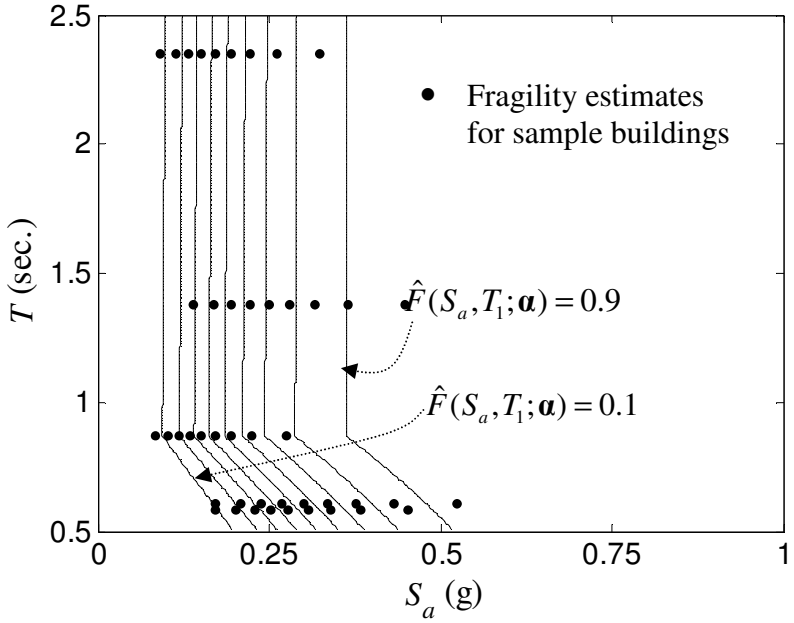

Figure 6.16 Contour plots of bivariate fragility estimates for pushover performance level (Plastic Mechanism Initiation)

6.7 SUMMARY

Fragility estimates are developed for GLD RC frame buildings using the probabilistic demand models and capacity values corresponding to FEMA-356 (2000) performance levels and damage levels obtained form pushover analysis. Approximate confidence bounds are developed to represent the inherent epistemic uncertainties in the fragility estimates.

The analytical fragility estimates developed in this study are compared with the fragility estimates developed for GLD RC frame buildings from previous studies by Celik and Ellingwood (2006) and Hwang and Huo (1996). Bivariate fragility estimates are formulated as a function of spectral acceleration and fundamental building period. Fragility estimates of the sample buildings are used to estimate the unknown parameters of the bivariate fragility function. The bivariate fragility estimates and can be used for rapid seismic vulnerability assessment of 1 to 10 story GLD RC frame buildings.

CHAPTER VII

BAYESIAN UPDATING OF ANALYTICAL FRAGILITY ESTIMATES USING OBSERVED DAMAGE DATA

7.1 INTRODUCTION

To develop more robust fragility estimates, the analytical fragility estimates should be updated by using earthquake damage data or experimental test data of building systems and components if and when they become available. This chapter presents a framework for updating the analytical fragility estimates with the observed damage data or experimental test data using the Bayesian methodology. As an illustration of the framework, analytical bivariate fragility estimates developed in Chapter VI for 1 to 10 story GLD RC frame buildings are updated by using the damage data of similar buildings from 1994 Northridge, California Earthquake (Ramamoorthy et al. 2006c).

7.2 FRAMEWORK FOR UPDATING THE ANALYTICAL FRAGILITY ESTIMATES

The Bayes' updating rule given in Eq. (2.5) is used to develop a framework for updating the analytical fragility estimates. Figure 7.1 shows the schematics of the updating framework. Let $\boldsymbol{\alpha} = (\alpha_1, \alpha_2, \ldots, \alpha_k)$ represent the parameters of an analytical fragility function. The analytical fragility parameters $\boldsymbol{\alpha}$, are updated by using the observed damage data or experimental test data. The details of the updating framework are presented in the following sections.

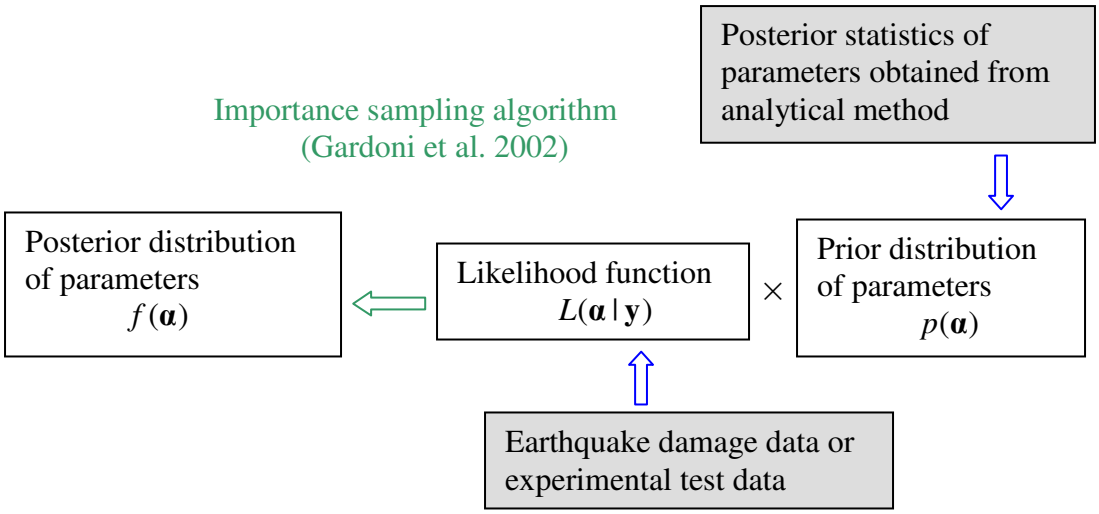

Figure 7.1 Schematics of the Bayesian updating framework

7.2.1 Prior Distribution

The posterior statistics of the parameters $\boldsymbol{\alpha} = (\alpha_1, \alpha_2, \ldots, \alpha_k)$, of the analytical fragility estimates are used to obtain the marginal distribution for α_1, α_2, or α_k. Liu and Der Kiureghian (1986) developed two multi-variate joint distribution models that are consistent with the marginal distributions and covariance matrix of random variables. In this study, the prior joint probability density function, $p(\boldsymbol{\alpha})$ of $\boldsymbol{\alpha}$ is constructed using the Nataf multi-variate distribution model developed by Liu and Der Kiureghian (1986). Thus, $p(\boldsymbol{\alpha})$ represents the existing knowledge obtained from the analytical fragility estimates.

7.2.2 Likelihood Function

The earthquake damage data or the experimental test data, $\mathbf{y}$ enter the updating framework through the likelihood function. Following Shinozuka et al. (2000), the likelihood function for updating the analytical fragility estimates is written as

$$L(S_{ai}, T_{1i}) = \prod_{i=1}^{n} \left[F(S_{ai}, T_{1i}) \right]^{x_i} \left[1 - F(S_{ai}, T_{1i}) \right]^{1-x_i} \quad (7.1)$$

where n represents the sample size of the structural system or components in the surveyed damage data, $F(\square)$ represents the fragility estimates for a specific state of damage that are obtained by relating the observed damage level with the structural performance level of buildings, and x_i represents the realizations of the Bernoulli random variable X_i with, x_i = 0 or 1 depending on whether or not the structural system or component sustains a particular damage level for given S_a and T_1.

7.2.3 Posterior Distribution

Posterior joint probability density function, $f(\boldsymbol{\alpha})$ of the parameters is obtained by combining the prior distribution and the likelihood functions. $f(\boldsymbol{\alpha})$ incorporates both the previous information about $\boldsymbol{\alpha}$ included in $p(\boldsymbol{\alpha})$ and the new data included in L. Point estimates of the updated parameters are obtained using the importance sampling algorithm developed by Gardoni et al. (2002b).

7.3 APPLICATION OF BAYESIAN UPDATING TO RC FRAMES

This section presents an illustration of the Bayesian updating framework developed in Section 7.2. The analytical bivariate fragility estimates for GLD RC frame buildings presented in Chapter VI are updated using damage data of similar buildings during the 1994 Northridge, California Earthquake.

7.3.1 Damage Data of RC Frame Buildings

The Applied Technology Council (ATC) conducted building surveys to consistently gather and document building characteristics and performance during the 1994 Northridge, California Earthquake. The results of this survey were documented in the ATC-38 report (ATC 2000). A total of 530 buildings were surveyed in the vicinity of

the 31 strong-motion stations in the Los Angeles area. California division of mines and geology (CDMG) operated 18 stations, University of Southern California (USC) operated 7 stations, and U.S. Geological Survey (USGS) operated 6 stations. Strong motion records and response spectra were available for 30 of the 31 recording sites where buildings were surveyed. Figure 7.2 shows an example response spectra plots for the earthquake ground motions recorded at CDMG 24322.

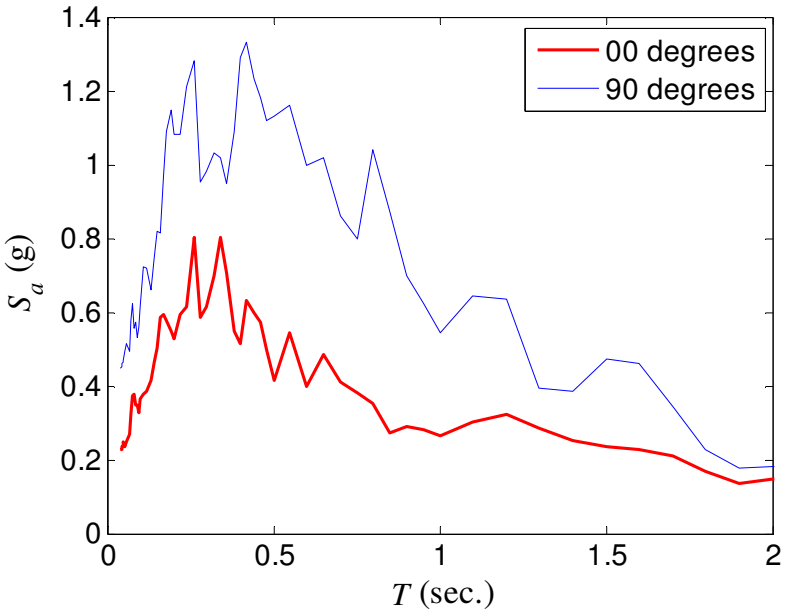

Figure 7.2 Response spectra for earthquake ground motion recorded at recording station operated by California division of mines and geology (CDMG 24322) during the 1994 Northridge, California earthquake (ATC-38)

Based on structural materials and load resistance system, the surveyed buildings were categorized in terms of 15 model building types. These model building types were considered to represent the entire building inventory in the United States. The overall damage to the buildings was classified using four damage levels: None, Insignificant,

Moderate, and Heavy. Table 7.1 lists the description of the damage observed corresponding to the four damage levels.

Table 7.1 Damage state classification in ATC-38 (ATC 2000)

General damage state	Description
None (N)	No damage is visible either cosmetic or structural.
Insignificant (I)	Damage requires no more than cosmetic repair. No structural repairs are necessary.
Moderate (M)	Repairable structural damage has occurred. The existing elements can be repaired essentially in place, without substantial demolition or replacement of elements.
Heavy (H)	Damage is so extensive that repair of elements is either not feasible or requires major demolition or replacement.

In this study, the damage data of RC frame buildings with rigid diaphragm is used for updating the analytical fragility estimates. Table 7.2 lists the summary of damage data from ATC-38 for 1 to 10 story RC frame buildings. For all buildings listed in Table 7.2, fundamental building period, $\hat{T}_1$ is estimated using Eq. (3.3) by assuming a uniform story height of 12 feet. The maximum of the two horizontal S_a corresponding to $\hat{T}_1$ is used as the seismic intensity measure.

Table 7.2 Earthquake damage data for low- and mid-rise RC frame buildings with rigid diaphragm (adapted from ATC-38)

Building ID	Number of stories	Design date	General damage state	$\hat{T}_1$ (sec)	S_a (g)
CDMG 231-GZ-16	6	1966	M	1.40	0.21
CDMG 231-GZ-17	8	1967	I	1.67	0.18
CDMG 231-GZ-18	6	1963	M	1.40	0.21
CDMG 322-SH-03	1	1965	I	0.46	1.18
CDMG 322-SH-04	1	1960	H	0.46	1.18
CDMG 385-MF-08	1	1970	M	0.46	0.60
CDMG 386-SH-18	7	1965	H	1.54	0.43
CDMG 463-AC-01	5	1971	I	1.25	0.11
CDMG 567-GZ-05	9	1993	I	1.80	0.09
CDMG 567-GZ-10	5	1980	M	1.25	0.11
CDMG 579-S1-01	9	1924	I	1.80	0.09
CDMG 688-RE-03	5	1965	I	1.25	0.23

As discussed earlier in Chapter I, buildings in Western, Central, and Eastern United States are constructed following different building codes and construction practices. However, in general, GLD buildings that were designed and constructed before 1976 are considered to have similar characteristics across the different regions of United States. For example, non-ductile reinforcement details discussed in Chapter I were typical of old GLD buildings constructed across the United States. Therefore, it is appropriate to update the fragility estimates of GLD buildings in the Mid-America Region using damage data of similar buildings from 1994 Northridge, California Earthquake. It should be mentioned that the earthquake ground motions associated with the above damage data might not be representative for the Mid-America Region.

7.3.2 Estimates of Updated Parameters

The prior joint distribution of the parameters $\boldsymbol{\alpha}_1 = (\alpha_{11}, \alpha_{12}, .., \alpha_{14})$ and $\boldsymbol{\alpha}_2 = (\alpha_{21}, \alpha_{22})$ in Eq. (6.10) and Eq. (6.11), respectively, is constructed using the Nataf multi-variate distribution model developed by Liu and Der Kiureghian (1986). The posterior statistics

of the parameters listed in Tables 6.3 and 6.4 are used to construct the marginal distributions of $\alpha_{11}, \alpha_{12}, .., \alpha_{14}$ and α_{21}, α_{22}.

As mentioned earlier in Section 7.2.2, to estimate the likelihood value, the general damage state used for classifying the damaged buildings should be related to the structural performance level of buildings. In this study, the damage levels (None, Insignificant, Moderate, and Heavy) are related to IO, LS, and CP performance levels specified in FEMA-356 (2000). Table 7.3 shows the suggested relation between the damage levels specified in ATC-38 and FEMA-356 performance levels. Using the relationship between the damage level and performance level given in Table 7.3, for each performance level, x_i is assigned 0 or 1 based on the level of damage sustained by each building. For example, for IO performance level, $x_i = 0$ if building sustains the 'None' damage level, otherwise $x_i = 1$. Since all buildings have damage levels higher than 'None', $x_i = 1$ for IO performance level. Similarly, for LS performance level $x_i = 0$ if the building sustains the up to the 'Insignificant' damage level, otherwise $x_i = 1$. Thus, X_i will have different realizations based on the performance levels. Table 7.4 lists the input data used for updating the parameters of bivariate fragility function corresponding to IO, LS, and CP performance levels.

Point estimates of the updated parameters of bivariate fragility function for IO, LS, and CP performance levels are obtained using importance sampling algorithm developed by Gardoni et al. (2002a) and are listed in Table 7.5. The estimates now include the information content of the damage data. The updated posterior means of the parameters are similar to the ones estimated based on the simulated data.

Table 7.3 Relationship between the ATC-38 damage state and FEMA-356 performance level and classification of damage based on $\hat{T}_1$

General damage state	FEMA-356 performance level
None	←Immediate Occupancy (IO)
Insignificant	←Life Safety (LS)
Moderate	←Collapse Prevention (CP)
Heavy	

Table 7.4 Damage data for calculating the likelihood value

Building ID	General damage state	$\hat{T}_1$ (sec)	S_a (g)	x_i		
				IO	LS	CP
CDMG 231-GZ-16	M	1.40	0.21	1	1	0
CDMG 231-GZ-17	I	1.67	0.18	1	0	0
CDMG 231-GZ-18	M	1.40	0.21	1	1	0
CDMG 322-SH-03	I	0.46	1.18	1	0	0
CDMG 322-SH-04	H	0.46	1.18	1	1	1
CDMG 385-MF-08	M	0.46	0.60	1	1	0
CDMG 386-SH-18	H	1.54	0.43	1	1	1
CDMG 463-AC-01	I	1.25	0.11	1	0	0
CDMG 567-GZ-05	I	1.80	0.09	1	0	0
CDMG 567-GZ-10	M	1.25	0.11	1	1	0
CDMG 579-S1-01	I	1.80	0.09	1	0	0
CDMG 688-RE-03	I	1.25	0.23	1	0	0

7.4 UPDATED BIVARIATE FRAGILITY ESTIMATES

Bivariate fragility estimates for GLD RC frame buildings are obtained by using the mean values of the updated parameters listed in Table 7.5. Figures 7.3-7.5 compare the contour plots of updated bivariate fragility estimates (thick lines) and analytical bivariate fragility estimates (thin lines) for IO, LS, and CP performance levels, respectively. Even

for the limited sample of observed damage data, the updated fragility estimates and the analytical fragility estimates are almost identical.

Table 7.5 Point estimates of the updated parameters

Performance level	Parameter		Mean values of parameters	
			Prior values	Updated values
Immediate Occupancy	$\hat{T}_1 > 0.87$	$\hat{\alpha}_{11}$	−1.4297	−1.4458
		$\hat{\alpha}_{12}$	−0.5882	−0.5779
		$\hat{\alpha}_{13}$	0.4863	0.4753
		$\hat{\alpha}_{14}$	0.0237	0.0254
	$\hat{T}_1 \le 0.87$	$\hat{\alpha}_{21}$	33.6713	32.4183
		$\hat{\alpha}_{22}$	11.7658	11.3726
Life Safety	$\hat{T}_1 > 0.87$	$\hat{\alpha}_{11}$	−1.0435	−1.0406
		$\hat{\alpha}_{12}$	−0.5021	−0.5008
		$\hat{\alpha}_{13}$	0.3111	0.3129
		$\hat{\alpha}_{14}$	0.0851	0.0983
	$\hat{T}_1 \le 0.87$	$\hat{\alpha}_{21}$	12.533	12.747
		$\hat{\alpha}_{22}$	3.892	3.937
Collapse Prevention	$\hat{T}_1 > 0.87$	$\hat{\alpha}_{11}$	−0.8408	−0.8366
		$\hat{\alpha}_{12}$	−0.3500	−0.3537
		$\hat{\alpha}_{13}$	0.3651	0.3647
		$\hat{\alpha}_{14}$	0.0631	0.0672
	$\hat{T}_1 \le 0.87$	$\hat{\alpha}_{21}$	6.4062	6.8502
		$\hat{\alpha}_{22}$	2.6323	2.8243

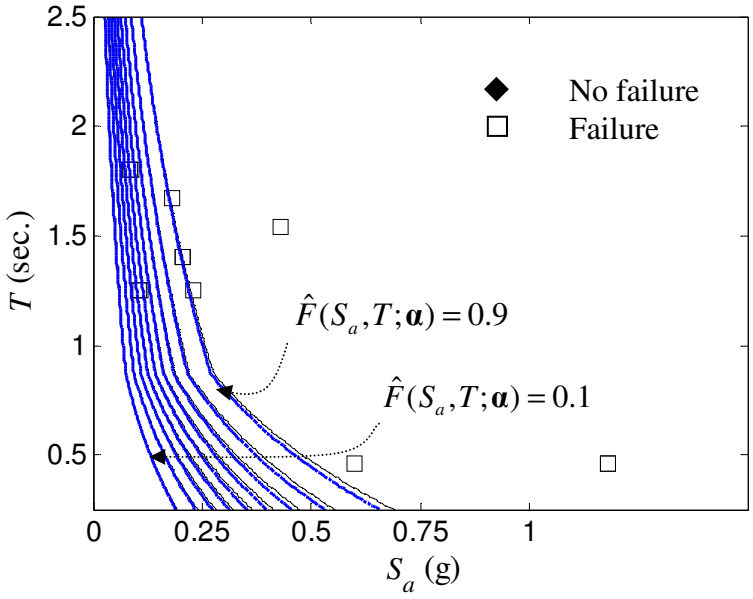

Figure 7.3 Contour plots of updated fragility estimates for FEMA-356 IO performance level (IO =0.5% inter story drift)

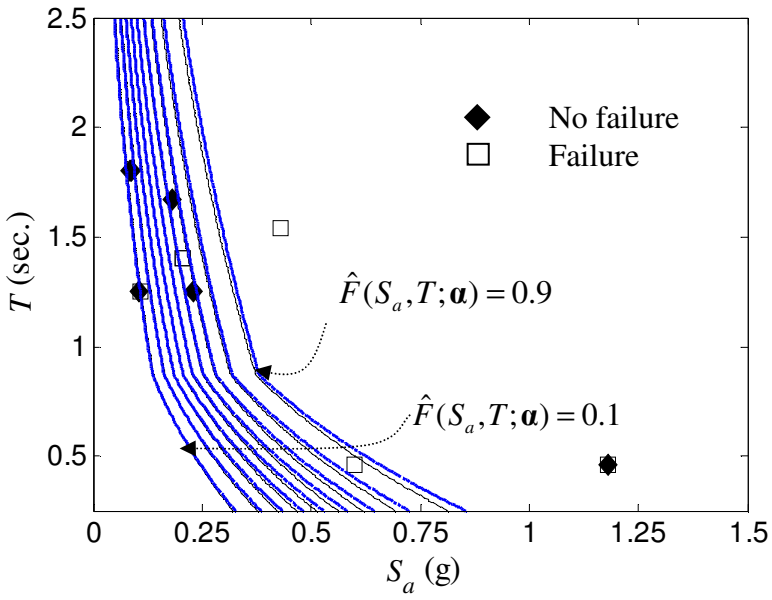

Figure 7.4 Contour plots of updated fragility estimates for FEMA-356 LS performance level (LS =1% inter story drift)

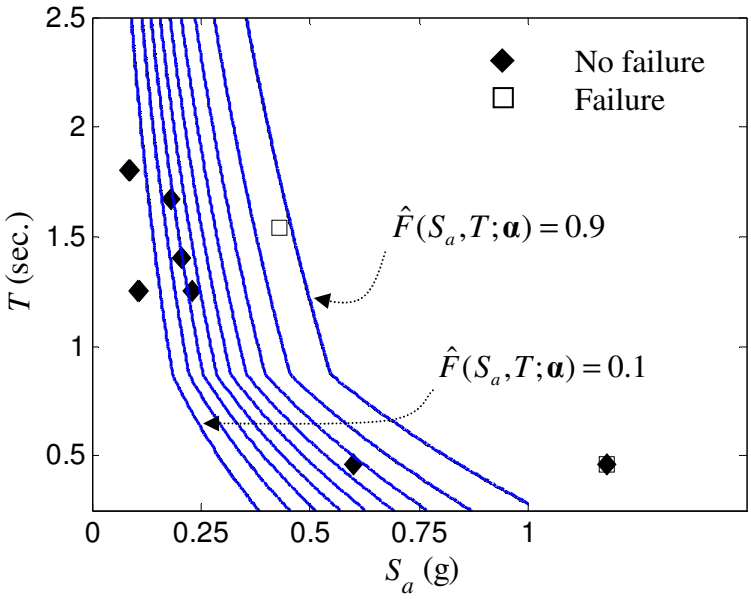

Figure 7.5 Contour plots of updated fragility estimates for FEMA-356 CP performance level (CP =2% inter story drift)

Table 7.6 lists the mean S_a for the 1994 Northridge, California Earthquake and the synthetic ground motions for Memphis, TN, used for developing the analytical fragility estimates. It is clear that the information content of the damage data used for updating are consistent with the simulated response data used for developing the analytical fragility estimates.

As mentioned earlier in Section 7.1, to develop more robust fragility estimates, the fragility estimates should be updated as and when new damage data or experimental data are available. To reduce error and inconsistency in the observed damage data, surveying methods should also be improved and standardized. Furthermore different relations between the damage states and performance levels can lead to different fragility estimates.

Table 7.6 Comparison of S_a for the 1994 Northridge, California Earthquake and synthetic ground motions for Memphis, TN

Building ID	$\hat{T}_1$ (sec)	S_a (g)	Wen and Wu (2001)	Rix and Fernandez (2004)			
			2% in 50 yrs.	6.5d10ab*	6.5d10fa†	7.5d20ab	7.5d20fa
CDMG 231-GZ-16	1.40	0.21	0.40	0.22	0.60	0.32	0.99
CDMG 231-GZ-17	1.67	0.18	0.37	0.19	0.56	0.27	0.93
CDMG 231-GZ-18	1.40	0.21	0.40	0.22	0.60	0.32	0.99
CDMG 322-SH-03	0.46	1.18	0.86	0.44	0.71	0.56	0.85
CDMG 322-SH-04	0.46	1.18	0.86	0.44	0.71	0.56	0.85
CDMG 385-MF-08	0.46	0.60	0.86	0.44	0.71	0.56	0.85
CDMG 386-SH-18	1.54	0.43	0.37	0.20	0.58	0.30	0.97
CDMG 463-AC-01	1.25	0.11	0.45	0.24	0.67	0.36	0.96
CDMG 567-GZ-05	1.80	0.09	0.32	0.15	0.52	0.25	0.90
CDMG 567-GZ-10	1.25	0.11	0.45	0.24	0.67	0.36	0.96
CDMG 579-S1-01	1.80	0.09	0.32	0.15	0.52	0.25	0.90
CDMG 688-RE-03	1.25	0.23	0.45	0.24	0.68	0.36	0.96

* represents moment magnitude 6.5, hypo-central distance of 10 km and Atkinson and Boore (1995) model

† represents moment magnitude 6.5, hypo-central distance of 10 km and Frankel et al. (1996) model

7.5 SUMMARY

In this chapter, a Bayesian framework is presented to update the existing analytical fragility estimates using observed damage data or experimental test data. The updating process enables the incorporation of different types of information, including experimental test data and damage data as new data become available. With the availability of new data, the posterior statistics of the parameters of the previously updated fragility estimates can be used as the prior estimates in the Bayesian updating framework. As an illustration of the updating framework the analytical bivariate fragility estimates for GLD RC frame buildings are updated using the damage data of similar buildings during the 1994 Northridge, California Earthquake. The updated fragility estimates and the analytical fragility estimates are almost identical.

CHAPTER VIII

FRAGILITY ESTIMATES FOR RETROFITTED BUILDINGS

8.1 INTRODUCTION

It was shown in Chapter VI that existing GLD RC frame buildings in the Mid-America Region are vulnerable to moderate and high intensity seismic events. Several retrofit strategies are available to enhance the seismic performance of these existing buildings. Selection of a particular retrofit strategy is a complex process and depends on several factors that include technical, financial, and sociological considerations.

Previous work by Bracci et al. (1992b and 1995b) and Dooley and Bracci (2001) on GLD RC frame buildings identified that the column-to-beam strength ratio at beam-column joints is a key structural parameter in controlling seismic damage. As mentioned earlier, GLD RC frame buildings are prone to sidesway mechanisms due to low moment capacity of columns as compared to the beams at a beam-column joint. Since these buildings are not designed and detailed for lateral loads, during moderate to severe seismic events they will exhibit story mechanism. For low-rise RC frame buildings designed in Chapter III, the average column-to-beam strength ratio is in the range of 0.5 to 0.8. This is significantly less than the current ACI-318 (2005) recommended value of 1.2. In an effort to enhance the seismic performance of the low-rise GLD RC frame buildings, and evaluate effectiveness of structural retrofitting, fragility estimates are developed based on a structural model with column-to-beam strength ratios of 1.2 and 1.8 for 2- and 3 story buildings.

8.2 RETROFIT STRATEGY

Out of several retrofit strategies, column strengthening leads to a significant increase in seismic lateral loading capability for moment resisting frame structures. An efficient and modest retrofit technique based on column strengthening can be accomplished by column jacketing, where an existing column section is enlarged with new concrete and additional reinforcement is used in the new concrete (Bracci et al. 1992b and 1995b).

The column-to-beam strength ratio of mid-rise buildings is significantly higher than the low-rise buildings. Furthermore, it is unrealistic to increase the column size for 1 story moment frame buildings. Therefore, in this study, only 2- and 3 story buildings retrofitted by column-to-beam strength ratios of 1.2 and 1.8 are used to are investigated to study the influence of column strengthening on the seismic performance.

For the analytical models of the retrofitted buildings in IDASS (Kunnath 2003), the increase in column-to-beam strength ratio is achieved by altering the column moment strength versus curvature. Figure 8.1 shows the moment-curvature relationship for columns of 2 story building with column-to-beam strength ratio of 0.5, 1.2 and 1.8, respectively. It is important to note that the initial stiffness of the retrofitted column response is unchanged compared to the original column in order to evaluate the influence of increased column strength on the fragility estimates. In general, this is a conservative assumption for design considerations.

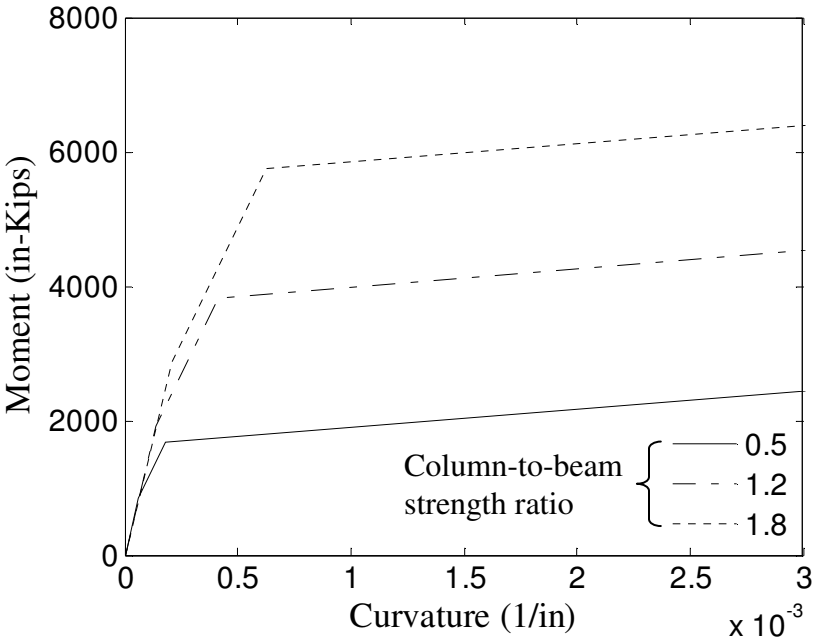

Figure 8.1 Moment-curvature relationship of columns in original and retrofitted 2 story building

8.3 PROBABILISTIC DEMAND MODELS AND CAPACITY VALUES FOR RETROFITTED BUILDINGS

Nonlinear time history analysis of the retrofitted buildings is carried out in IDASS using the synthetic ground motions described in Chapter IV. Figures 8.2 and 8.3 show the plots of response data in logarithmic space, $\ln(\delta)$ versus $\ln(S_a)$ for 2- and 3 story buildings with column-to-beam strength ratios of 1.2 and 1.8, respectively. Comparison of the transformed response data for the retrofitted buildings (Figures 8.2 and 8.3) with the original buildings (Figure 4.1) show that the there is a significant reduction in the scatter of the response data. The solid dots (•) represent Type I data, the stars (⊛) represent Type II data, and the triangles (▽) represent the 'lower bound' data (Type III). Dispersion of the simulated response data is significantly less for retrofitted buildings compared to the original buildings.

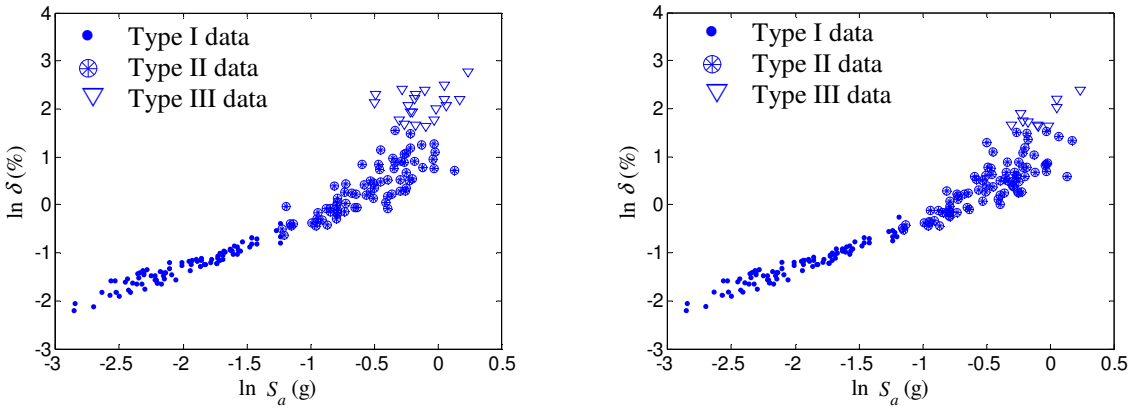

(a) Column-to-beam strength ratio =1.2 **(b)** Column-to-beam strength ratio =1.8

Figure 8.2 Peak inter story drift response data from nonlinear time history analysis of retrofitted 2 story building

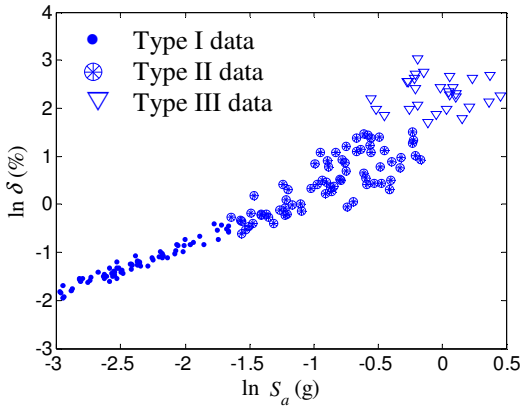

(a) Column-to-beam strength ratio =1.2

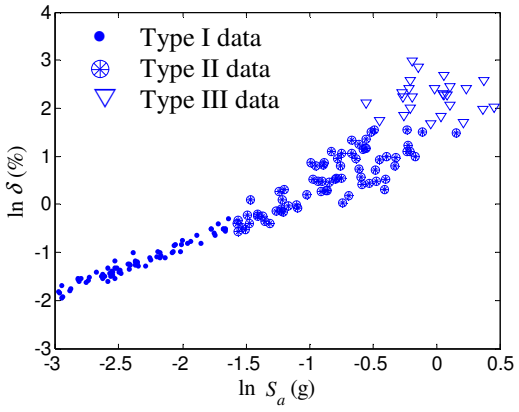

(b) Column-to-beam strength ratio =1.8

Figure 8.3 Peak inter story drift response data from nonlinear time history analysis of retrofitted 3 story building

Using the simulated response data, probabilistic bilinear demand models of the form given in Eq. (4.3) are developed for the retrofitted buildings. Using a Bayesian statistical analysis, the posterior statistics of the unknown parameters, $\boldsymbol{\theta}_1 = (\theta_{10}, \theta_{11}, \sigma_{1D|S_a})$ and $\boldsymbol{\theta}_2 = (\theta_{21}, \sigma_{2D|S_a})$, of the demand models for the retrofitted 2- and 3 story are obtained and are listed in Tables 8.1 and 8.2, respectively. Comparison of the parameters of the bilinear model for the retrofitted buildings (Tables 8.1 and 8.2) with the original buildings (Table 4.2) show that the there is a significant reduction in the seismic demand for the same set of ground motion records. In addition, for retrofitted buildings, the standard deviation of the model error in the elastic and inelastic range is significantly less compared to the original buildings. Figures 8.4 and 8.5 show predicted drift demand (solid lines) using the bilinear models along with the one standard deviation confidence interval (dotted lines)for the retrofitted 2- and 3 story buildings, with column-to-beam strength ratios of 1.2 and 1.8, respectively.

Table 8.1 Posterior statistics of parameters in bilinear demand model for retrofitted 2 story building

Column-to-beam strength ratio	Range	Parameter	Mean	Standard deviation	Correlation coefficient		
					θ_o	θ_1	σ
1.2	Elastic $\delta < 0.6\%$	θ_{10}	0.4883	0.0618	1		
		θ_{11}	0.8895	0.0306	0.98	1	
		$\sigma_{1D\|S_a}$	0.1110	0.0082	0.04	0.03	1
	Inelastic $\delta > 0.6\%$	θ_{21}	1.8905	0.0863	NA	1	0.17
		$\sigma_{2D\|S_a}$	0.6759	0.0594	NA	0.17	1
1.8	Elastic $\delta < 0.6\%$	θ_{10}	0.5137	0.0577	1	0.98	
		θ_{11}	0.9004	0.0290	0.98	1	
		$\sigma_{1D\|S_a}$	0.1110	0.0087	–0.01	–0.02	1
	Inelastic $\delta > 0.6\%$	θ_{21}	1.5598	0.0580	NA	1	0.04
		$\sigma_{2D\|S_a}$	0.4387	0.0353	NA	0.04	1

Table 8.2 Posterior statistics of parameters in bilinear demand model for retrofitted 3 story building

Column-to-beam strength ratio	Range	Parameter	Mean	Standard deviation	Correlation coefficient		
					θ_o	θ_1	σ
1.2	Elastic $\delta < 0.6\%$	θ_{10}	1.0360	0.0609	1		
		θ_{11}	0.9452	0.0245	0.98	1	
		$\sigma_{1D\|S_a}$	0.0960	0.0079	–0.01	–0.02	1
	Inelastic $\delta > 0.6\%$	θ_{21}	1.7123	0.0624	NA	1	
		$\sigma_{2D\|S_a}$	0.6097	0.0546	NA	0.25	1
1.8	Elastic $\delta < 0.6\%$	θ_{10}	1.0826	0.0566	1		
		θ_{11}	0.9620	0.0229	0.98	1	
		$\sigma_{1D\|S_a}$	0.0956	0.0074	0.02	0.02	1
	Inelastic $\delta > 0.6\%$	θ_{21}	1.6340	0.0590	NA	1	
		$\sigma_{2D\|S_a}$	0.5506	0.0472	NA	0.26	1

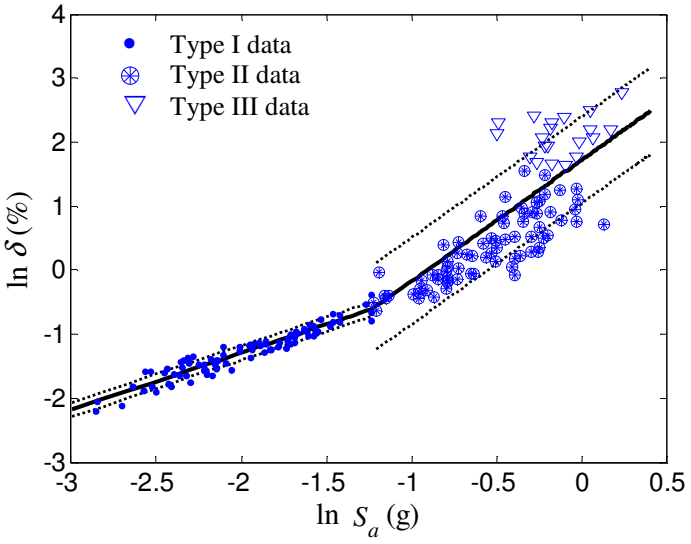

(a) Column-to-beam strength ratio =1.2

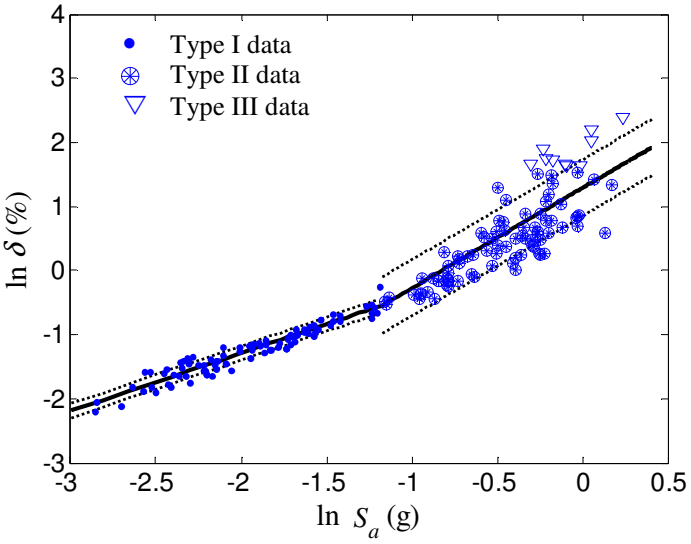

(b) Column-to-beam strength ratio =1.8

Figure 8.4 Probabilistic bilinear model (BLM) for retrofitted 2 story building

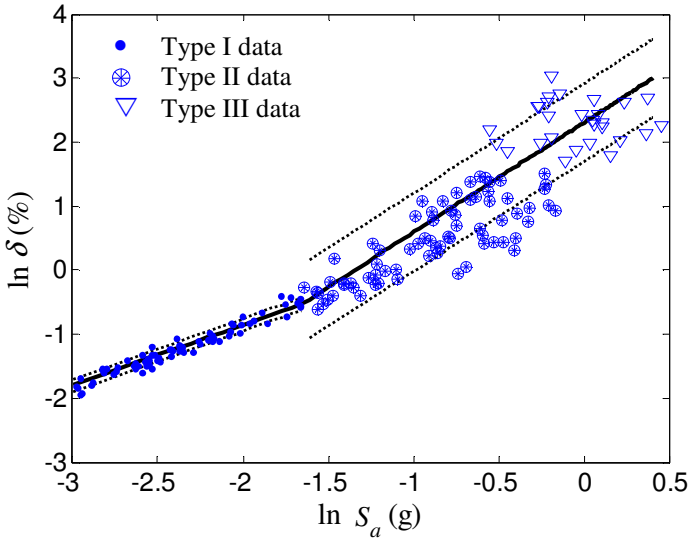

(a) Column-to-beam strength ratio =1.2

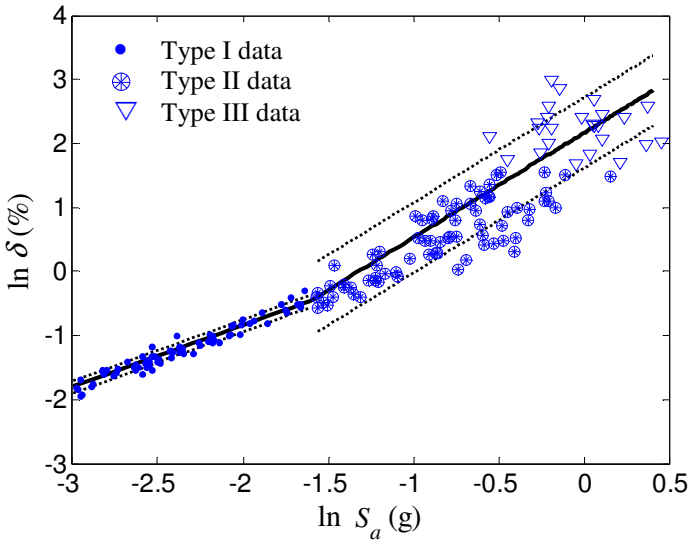

(b) Column-to-beam strength ratio =1.8

Figure 8.5 Probabilistic bilinear model (BLM) for retrofitted 3 story building

For the retrofitted buildings, inter story drift capacity values of 1%, 2%, and 4% are used for FEMA-356 IO, LS, and CP performance levels, respectively. These capacity values are probably more representative for the retrofitted structure since it is expected that the increased moment capacity of the retrofitted columns will deter the story mechanisms. In addition, inter story drift capacity values are also identified from displacement controlled pushover analysis. Table 8.3 lists the drift capacity values for FEMA-356 and for pushover performance levels.

Table 8.3 Median drift capacity values for retrofitted low-rise buildings (in % story height)

Buildings	Column-to-beam strength ratio	Performance levels				
		IO	LS	CP	FY	PMI
2 story	1.2	1	2	4	0.83	1.61
	1.8	1	2	4	1.29	3.55
3 story	1.2	1	2	4	0.83	1.45
	1.8	1	2	4	1.34	4.06

8.4 FRAGILITY ESTIMATES FOR RETROFITTED BUILDINGS

Fragility estimates for the retrofitted buildings are developed in a way similar to the original buildings. The estimates of the parameters of the continuous fragility estimates, $\hat{F}(S_a)$ for retrofitted 2- and 3 story buildings are listed in Tables 8.4 and 8.5, respectively. Figures 8.6 and 8.7 show the $\hat{F}(S_a)$ estimates with confidence bounds for the retrofitted 2- and 3- story buildings, with column-to-beam strength ratios of 1.2 and 1.8, respectively.

Comparison of the fragility estimates for the retrofitted buildings (Figures 8.6 and 8.7) with the original buildings (Figures 6.3 and 6.4) show that the probability of attaining or exceeding a performance level for a given level of seismic demand is improved for buildings retrofitted by column strengthening. For example, Table 8.6 summarizes the

fragility estimates for CP performance level for the unretrofitted and retrofitted 2 and 3 story buildings.

Table 8.4 Estimates of the parameters of continuous fragility estimates for retrofitted 2 story building

Column-to-beam strength ratio	Performance level		Parameters	
			λ_1	λ_2
1.2	Immediate Occupancy	$+1\sigma$	–0.9604	0.3805
		Median	–0.8875	0.3860
		-1σ	–0.8152	0.3776
	Life Safety	$+1\sigma$	–0.6281	0.4457
		Median	–0.5399	0.4184
		-1σ	–0.4622	0.3907
	Collapse Prevention	$+1\sigma$	–0.2611	0.4553
		Median	–0.1749	0.4220
		-1σ	–0.1006	0.3939
	First Yield	$+1\sigma$	–1.0461	0.3655
		Median	–0.9801	0.3804
		-1σ	–0.9917	0.3796
	Plastic Mechanism Initiation	$+1\sigma$	–0.7375	0.4324
		Median	–0.6518	0.4126
		-1σ	–0.5740	0.3882
1.8	Immediate Occupancy	$+1\sigma$	–0.8700	0.3829
		Median	–0.8182	0.3774
		-1σ	–0.7680	0.3668
	Life Safety	$+1\sigma$	–0.4356	0.4103
		Median	–0.3812	0.3908
		-1σ	–0.3319	0.3730
	Collapse Prevention	$+1\sigma$	0.0112	0.4088
		Median	0.0630	0.3913
		-1σ	0.1105	0.3758
	First Yield	$+1\sigma$	–0.7142	0.3990
		Median	–0.6596	0.3850
		-1σ	–0.6086	0.3692
	Plastic Mechanism Initiation	$+1\sigma$	–0.0655	0.4092
		Median	–0.0135	0.3913
		-1σ	–0.0341	0.3754

Table 8.5 Estimates of the parameters of continuous fragility estimates for retrofitted 3 story building

Column-to-beam strength ratio	Performance level		Parameters	
			λ_1	λ_2
1.2	Immediate Occupancy	$+1\sigma$	−1.4134	0.3738
		Median	−1.3222	0.3957
		-1σ	−1.2276	0.3944
	Life Safety	$+1\sigma$	−1.0548	0.4545
		Median	−0.9382	0.4300
		-1σ	−0.8345	0.4024
	Collapse Prevention	$+1\sigma$	−0.6500	0.4681
		Median	−0.5351	0.4337
		-1σ	−0.4361	0.4042
	First Yield	$+1\sigma$	−1.5056	0.3585
		Median	−1.4260	0.3927
		-1σ	−1.3381	0.4025
	Plastic Mechanism Initiation	$+1\sigma$	−1.2290	0.4252
		Median	−1.1201	0.4187
		-1σ	−1.2290	0.4252
1.8	Immediate Occupancy	$+1\sigma$	−1.3816	0.3705
		Median	−1.3013	0.3904
		-1σ	−1.2175	0.3909
	Life Safety	$+1\sigma$	−0.9995	0.4450
		Median	−0.8968	0.4220
		-1σ	−0.8047	0.3968
	Collapse Prevention	$+1\sigma$	−0.5735	0.4561
		Median	−0.4742	0.4254
		-1σ	−0.3875	0.3988
	First Yield	$+1\sigma$	−1.2273	0.4076
		Median	−1.1335	0.4064
		-1σ	−1.0431	0.3921
	Plastic Mechanism Initiation	$+1\sigma$	−0.5642	0.4561
		Median	−0.4650	0.4254
		-1σ	−0.3785	0.3989

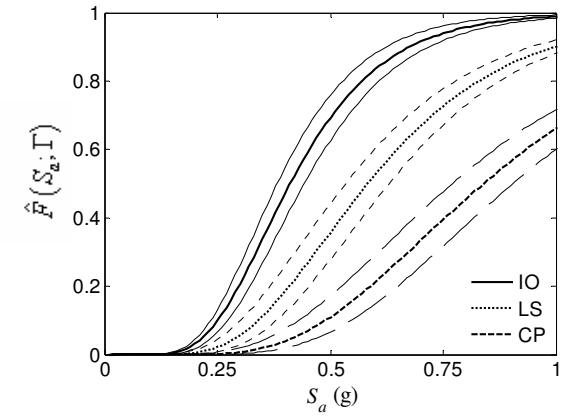

FEMA-356 performance levels

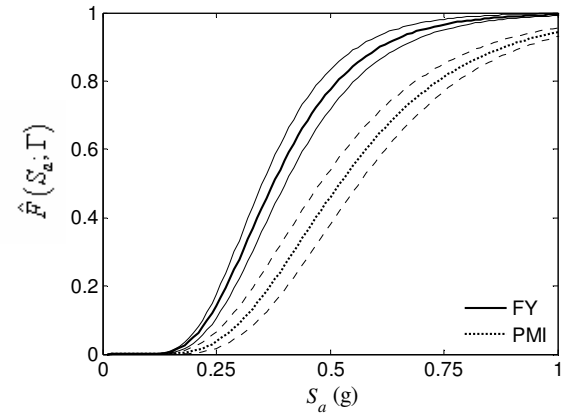

Pushover performance levels

(a) Column-to-beam strength ratio =1.2

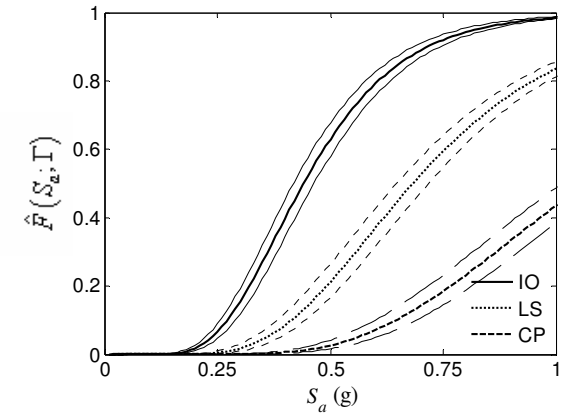

FEMA-356 performance levels

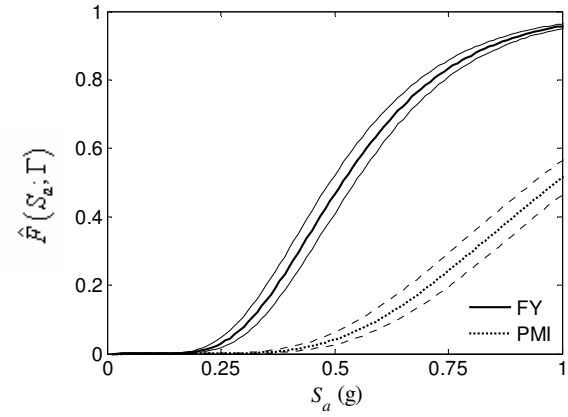

Pushover performance levels

(b) Column-to-beam strength ratio =1.8

Figure 8.6 Fragility estimates with confidence bounds for retrofitted 2 story building

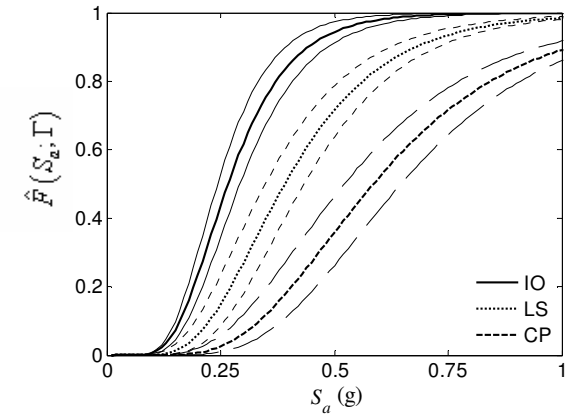

FEMA-356 performance levels

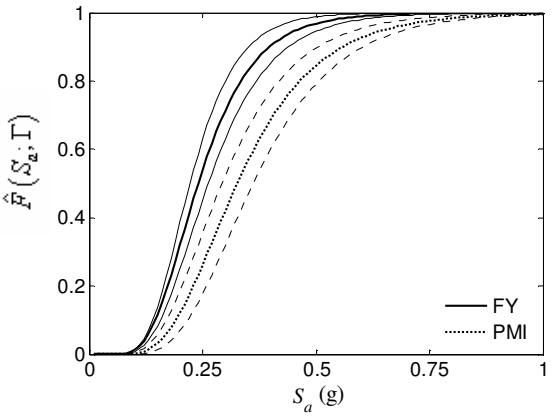

Pushover performance levels

(a) Column-to-beam strength ratio =1.2

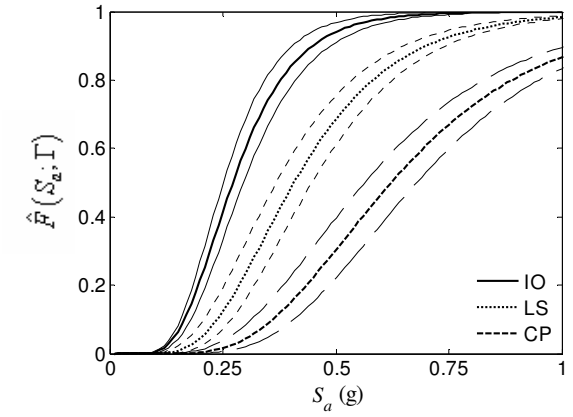

FEMA-356 performance levels

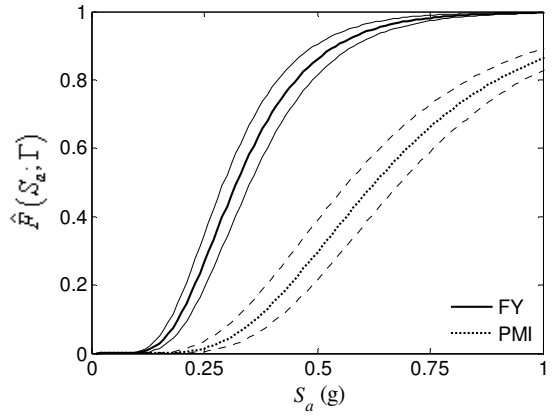

Pushover performance levels

(b) Column-to-beam strength ratio =1.8

Figure 8.7 Fragility estimates with confidence bounds for retrofitted 3 story building

Table 8.6 Fragility estimates for CP performance levels for original and retrofitted buildings

Buildings	Column-to-beam strength ratio	$S_a(g)$					
		0.0	0.2	0.4	0.6	0.8	1.0
2 story	0.5 (unretrofitted)	0.000	0.006	0.345	0.797	0.956	0.991
	1.2	0.000	0.003	0.040	0.213	0.455	0.661
	1.8	0.000	0.000	0.006	0.071	0.232	0.436
3 story	0.6 (unretrofitted)	0.000	0.152	0.776	0.965	0.995	0.999
	1.2	0.000	0.007	0.190	0.522	0.764	0.891
	1.8	0.000	0.004	0.149	0.466	0.722	0.868

8.5 SUMMARY

The existing GLD RC frame buildings in the Mid-America Region are vulnerable for moderate to severe seismic event. To mitigate the economic loss and human casualties due to structural failure of GLD RC frame buildings, it is desired to improve the seismic performance of these buildings. In general, the column-to-beam strength of GLD RC frame buildings is less than the current ACI 318 recommendation of 1.2. For an imposed lateral load, these buildings are prone to sidesway mechanism. By increasing the moment capacity of these columns the sidesway mechanism can be avoided.

To demonstrate the effectiveness of a simple retrofit strategy for 2- and 3 story building, the columns of these buildings are retrofitted by strengthening the columns. In the analytical models, the increase in column strength is achieved by changing the trilinear moment versus curvature relationship of the retrofitted columns so as to achieve column-to-beam strength ratios of 1.2 and 1.8.

Probabilistic demand models and capacity values for various performance levels are obtained for the retrofitted buildings. The fragility estimates of the retrofitted building are obtained in a way similar to the unretrofitted buildings. From the plot of fragility

estimates, it is clear that there is a significant increase in the seismic performance of the retrofitted buildings compared to the unretrofitted buildings.

CHAPTER IX

CONCLUSIONS

9.1 SUMMARY AND MAJOR FINDINGS

The Mid-America Region is susceptible to infrequent, but high intensity, earthquakes. However, most of the existing building and bridge infrastructure in this region was not designed to withstand for these high intensity earthquake events. Therefore it is necessary to assess the seismic vulnerability of this infrastructure to develop appropriate hazard mitigation techniques.

The focus of this dissertation is to quantify the seismic vulnerability of low- and mid-rise gravity load designed (GLD) reinforced concrete (RC) frame buildings, which make a significant population of the inventory in this region. To quantify the seismic vulnerability of buildings in this region, fragility estimates are developed for typical buildings that represent, in an average sense, the building inventory. In the context of this study, fragility is defined as the probability of a building reaching or exceeding a certain performance level given a specific ground motion intensity parameter. Fragility estimates developed from the observed damage data from previous earthquake ground motions are more representative of the building inventory and soil characteristics of that region. However, in the absence of such data fragility estimates are developed using the simulated response data of the structural models of the generic buildings. The key steps in the simulation procedure are: selection of ground motions, definition of generic buildings, and nonlinear analysis of structural models of generic buildings.

In this study, fragility estimates are developed for generic RC frame buildings of 1, 2, 3, 6, and 10 stories tall that are representative of the Mid-America region. A Bayesian methodology is used to develop probabilistic demand models to predict the drift demand. Performance levels specified in FEMA-356 and as computed by nonlinear pushover analyses are used as mean drift capacity values. Approximate confidence bounds are developed to represent the epistemic uncertainties inherent in the fragility estimations.

The analytical fragility estimates developed in this study are compared with the fragility estimates developed for similar RC frame buildings by other researchers.

Bivariate fragility estimates are formulated as a function of spectral acceleration and fundamental building period, which is a function of building height. The bivariate fragility estimates, in an average sense, account for the variability in building configurations, member sizes, and joint details, because they are developed using five different realizations (one for each of the selected building height). For this reason, the bivariate fragility estimates are believed to provide an accurate assessment of the seismic vulnerability of GLD RC frame buildings in the Mid-America Region. A framework is developed to update the analytical fragility estimates using damage data or experimental test data of building systems and components. As an illustration of the updating framework, the bivariate fragility estimates obtained for GLD RC frame buildings were updated using the damage data from the 1994, Northridge, California Earthquake.

The fragility estimates indicate that low- and mid-rise GLD RC frame buildings are vulnerable to damage for a moderate to strong seismic events. In order to minimize the economic and human loss, it is desired to mitigate the seismic vulnerability of these buildings. In general, the GLD buildings have low column capacity compared to beams at a beam-column joint. Due to low column-to-beam strength ratio, these buildings are prone to softstory mechanisms for an imposed lateral load. In this study, it is shown that increasing the column strength of these buildings deterred the softstory mechanisms. The fragility estimates of the retrofitted buildings quantify the increase in the seismic performance compared to the original buildings.

9.2 SIGNIFICANT CONTRIBUTIONS

Important contributions identified in this study are listed below;

1. Developed bi-linear probabilistic demand models that can properly account for inelastic and higher mode effects in RC frame buildings using the simulated response data. These data were classified into equality and lower bound data based on the 5% inter story drift value used for validation of IDASS. In addition

a Bayesian methodology was used for developing the probabilistic demand models.

2. To quantify the seismic vulnerability of GLD RC frame buildings that are representative of the Mid-America Region, analytical fragility estimates were developed for generic RC frame buildings of 1, 2, 3, 6 and 10 story tall. Since the seismic response of buildings is sensitive to the frequency content of the earthquake and the fundamental building period, bivariate fragility estimates, defined as the conditional probability of attaining or exceeding a specified performance level for given values of spectral acceleration and fundamental building period, were developed using the fragility estimates of the generic buildings. The bivariate fragility estimates can be used to quantify the seismic vulnerability of 1 to 10 story GLD RC frame buildings in the Mid-America Region.
3. Approximate confidence bounds on the fragility estimates are developed to reflect the inherent epistemic uncertainty in the predicted values.
4. Following the Bayesian methodology, a framework was developed to update the analytical fragility estimates with damage data and experimental test data, as they become available. As an application of the framework, the bivariate fragility estimates developed for GLD RC frame buildings were updated using the damage data from 1994, Northridge, California Earthquake.

9.3 FUTURE RESEARCH

Some of the future research needs related to the assessment of seismic vulnerability of buildings are listed below:

1. A parametric study can be conducted to study the effect of different idealizations and assumptions involved in developing the structural models of buildings. This study can help in estimating the epistemic uncertainty involved in structural modeling.

2. To obtain more robust estimates of demand and capacity, it is required to reduce the epistemic uncertainties. Component and sub-assembly experimental test data of buildings can be used to quantify the epistemic uncertainties. Furthermore, the experimental test data will help to validate and update the capacity and demand models. The Bayesian methodology adopted in this work is suitable for this purpose.
3. As explained earlier, to obtain more robust analytical fragility estimates, the observed damage data of similar buildings should be used. However, there is considerable subjectivity involved in the survey of damage data of buildings and essential facilities. Therefore there is a need to develop a systematic approach in surveying the damage data.

REFERENCES

American Concrete Institute (ACI) (2005). "Building code requirements for structural concrete and commentary." *ACI-318,* American Concrete Institute, Farmington Hills, Mich.

Alire, D. A. (2002). "Seismic evaluation of existing unconfined reinforced concrete beam-column joints." MS Thesis, Univ. of Washington, Seattle.

American Society of Civil Engineers (ASCE) (2002). "Minimum design loads for buildings and other structures." *ASCE 7-02*, ASCE, Reston, Va.

Applied Technology Council (ATC) (1985). "Earthquake damage evaluation data for California." *ATC-13 Report*, Applied Technology Council, Redwood City, Calif.

Applied Technology Council (ATC) (1996). "Seismic evaluation and retrofit of concrete buildings." *ATC-40 Report*, Applied Technology Council, Redwood City, Calif.

Applied Technology Council (ATC) (2000). "Database on the performance of structures near strong-motion recordings: 1994 Northridge, California, earthquake." *ATC-38 Report*, Applied Technology Council, Redwood City, CA.

Atkinson, G., and Boore, D. (1995). "New ground motions relations for eastern North America." *Bull. Seismol. Soc. Am.*, 85, 17-30.

Aycardi, L. E., Mander, J. B., and Reinhorn, A. M. (1992). "Seismic resistance of reinforced concrete frame structures designed only for gravity loads: Part II-Experimental performance of subassemblages." *NCEER-92-0028*, National Center for Earthquake Engineering Res., State Univ. of New York, Buffalo.

Beres, A., White, R. N., and Gergerly, P. (1992). "Seismic behavior of reinforced concrete frame structures with nonductile details: Part I- Summary of experimental findings of full scale beam-column joint tests." *NCEER-92-0024*, National Center for Earthquake Engineering Res., State Univ. of New York, Buffalo.

Beres, A., Pessiki, S. P., White, R. N., and Gergerly, P. (1996). "Implications of experiments on the seismic behavior of gravity load designed RC beam-to-column connections." *Earthquake Spectra*, 12(2), 185-198.

Box, G. E. P., and Tiao, G. C. (1992). *Bayesian inference in statistical analysis,* Addison-Wesley, Reading, Mass.

Bracci, J. M., Reinhorn, A. M., and Mander, J. B. (1992a). "Seismic resistance of reinforced concrete frame structures designed only for gravity loads: Part III-Experimental performance and analytical study of a structural model." *NCEER -92-0029*, National Center for Earthquake Engineering Res., State Univ. of New York, Buffalo.

Bracci, J. M., Reinhorn, A. M., and Mander, J. B. (1992b). "Evaluation of seismic retrofit of reinforced concrete frame structures designed only for gravity loads: Part II-Experimental performance and analytical study of a retrofitted structural model." *NCEER -92-0031*. National Center. for Earthquake Engineering Res., State Univ. of New York, Buffalo.

Bracci, J.M., Reinhorn, A.M., and Mander, J.B. (1995a). "Seismic resistance of reinforced concrete frame structures designed for gravity loads: Performance of structural system." *ACI Structural Journal*, 92(5), 597-609.

Bracci, J. M., Reinhorn, A. M., and Mander, J. B. (1995b). "Seismic retrofit of reinforced concrete buildings designed for gravity loads: Performance of structural model." *ACI Structural Journal*, 92(6), 711-723.

Bracci, J. M., Kunnath, S. M., and Reinhorn, A. M. (1997). "Seismic performance and retrofit evaluation of reinforced structures." *J. Struct. Engrg.*, 123(1), 3-10.

Building Officials and Code Administrators (BOCA) (1984). *Basic/National Code/1984*, Building Officials and Code Administrators International, Inc., County Club Hills, ILL.

Celik, O. C., and Ellingwood, B. R. (2006). "Modeling beam-column joints in fragility assessment of gravity load designed reinforced concrete frames." *Journal of Earthquake Engineering* submitted for publication.

Cornell, C. A. (1968). "Engineering seismic risk analysis", *Bull. Seismol. Soc. Am.*, 58, 1583-1606.

Cornell, C. A., Jalayer, F., Hamburger, R.O., and Foutch, D.A. (2002). "Probabilistic basis for the 2000 SAC Federal Emergency Management Agency steel moment frame guidelines." *J. Struct. Eng.*, 128(4), 526-533.

Der Kiureghian, A. (1989). "Measures of structural safety under imperfect states of knowledge." *J. Struct. Engrg.*, 115(5), 1119-40.

Der Kiureghian, A. (2000). "A Bayesian framework for fragility assessment." *Proc., 8th Int. Conf. on Applications of Statistics and Probability in Civil Engineering,* Sydney, Australia, Vol. 2, 1003-1010.

Ditlevsen, O., and Madsen, H. O. (1996). *Structural reliability methods,* J. Wiley, New York.

Dooley, K. L., and Bracci, J. M. (2001). "Seismic evaluation of column to beam strength ratios in RC frames." *ACI Structural Journal*, 99(6), 843-851.

Fajfar, P., and Gaspersic, P. (1996). "The N2 method for the seismic damage analysis of RC buildings." *Journal of Earthquake Engrg. and Structural Dynamics*, 25, 1-46.

Federal Emergency Management Association (FEMA). (2000). "Prestandard and commentary for the seismic rehabilitation of buildings." *FEMA 356,* ASCE, Reston, Va.

Fisher, R. A. (1922). "On the mathematical formulation of theoretical statistics". Phil. Trans. Roy.Soc., Series A 222: 309.

Frankel, A., Mueller, C., Barnhard, T., Perkins, D., Leyendecker, E., Dickman, N., Hanson, S., and Hopper, M. (1996). National seismic hazard maps: Documentation. *USGS Open-File Report 96-532*, USGS, Denver, Colo.

French, S. (2004). "Memphis Test-Bed project summer report", *Mid-America Earthquake Center Project DS-2 Report*, University of Illinois at Urbana-Champaign.

Gardoni, P., Der Kiureghian, A., and Mosalam, K. M. (2002a). "Probabilistic models and fragility estimates for bridge components and systems." *PEER Report 2002/13*, Pacific Earthquake Engineering Research Center, University of California, Berkeley, CA.

Gardoni, P., Der Kiureghian, A., and Mosalam, K. M. (2002b). "Probabilistic capacity models and fragility estimates for RC columns based on experimental observations." *J. Engrg Mech.*, 128(10), 1024-1038.

Gardoni, P., Mosalam, K. M., and Der Kiureghian, A. (2003). "Probabilistic seismic demand models and fragility estimates for RC bridges." *J. Earthquake Engrg.* 7(1), 79-106.

Hoffmann, G. W., Kunnath, S. K., Mander, J. B., and Reinhorn, A. M. (1992). "Gravity-load-designed reinforced concrete buildings: Seismic evaluation of existing construction and detailing strategies for improved seismic resistance." *Technical Report NCEER-92-0016*, National Center for Earthquake Engineering Res., State Univ. of New York Buffalo.

Hwang, H. H. M., and Huo, J-R. (1994). "Generation of hazard consistent fragility curves." *Soil Dyn. Earthquake Engrg.,* 13, 345-354.

Hwang, H. H. M., and Huo, J-R. (1996). "Generation of fragility curves for RC buildings in the Memphis areas." *Technical Report,* Center for Earthquake Research and Information, The University of Memphis, Memphis.

International Building Code (IBC). (2005). *International Building Code*, International Code Council, Inc., Fall Church, Va.

International Conference of Building Officials (ICBO). (1997). *1997 Uniform Building Code*, Vol. 2, Whittier, Calif.

Kunnath, S.K. (2003). "Inelastic Dynamic Analysis of Structural Systems (IDASS)." <http://cee.engr.ucdavis.edu/faculty/kunnath>.

Leyendecker, E. V., Hunt, R. J., Frankel, A. D. and Rukstakes, K. S. (2000). "Development of maximum considered earthquake ground motion maps." *Earthquake Spectra*, 16(1), 21-40.

Liu, P.-L., and Der Kiureghian, A. (1986). "Multivariate distribution models with prescribed marginals and covariances." *Probabilistic Engrg. Mechanics*, 1(2), 105-112.

Luco, N., and Cornell, C. A. (2000). "Effects of connection fractures on SMRF seismic drift demands." *J. Struct. Engrg.*, 126(1), 127-136.

Mackie, K., and Stojadinovic, B. (2001). "Probabilistic seismic demand model for California highway bridges." *J. Bridge. Engrg*. 6(6), 468-481.

McKenna, F., and Fenves, G. L. (2006). "Open system for earthquake engineering simulation (OpenSees) user Manual." Univ. of California, Berkeley <http://opensees.berkeley.edu.>.

Mosalam, K. M. (1996). "Experimental and computational strategies for the seismic behavior evaluation of frames with infill walls." PhD. Dissertation, Cornell Univ., Ithaca, N.Y.

Mosalam, K. M., Ayala, G., White, R. N., and Roth, C. (1997). "Seismic fragility of LRC frames with and without masonry infill walls." *J. Earthq. Engrg.* 1(4), 693-719.

Mosteller, F., and Wallance, D. L. (1964). *Inference and disputed authorship: The federalist*. Addison-Wesley, Reading, Massachusetts.

Mwafy, A. M., and Elnashai, A. S. (2001). "Static pushover versus dynamic collapse analysis of RC buildings." *Engineering Structures*. 23, 407–424.

Nuttli, O. W. (1973). "The Mississippi Valley earthquakes of 1811 and 1812: Intensities, ground motion and magnitudes." *Bull. Seismol. Soc. Am.*, 63(1), 227-248.

Office of Emergency Services (OES) (1995). "The Northridge earthquake of January 17, 1994: Report of data collection and analysis, part A: Damage and inventory data." Governor's Office of Emergency Services of the State of California, Sacremento.

Pantelides, C. P., Clyde, C., and Reaveley, L. D. (2002). "Performance-based evaluation of reinforced concrete building exterior joints for seismic excitation." *Earthquake Spectra*, 18(3), 449-480.

Priestley, M. J. N. (1998). "Displacement –based approaches to rational limit states design of new structures." Keynote address, *Proc., 11th European Conf. on Earthquake Engineering*. Paris,

Ramamoorthy, S. K., Gardoni, P. and Bracci, J. M. (2006a). "Probabilistic demand models and fragility curves for reinforced concrete frames." *J. Struct. Engrg.*, 132(10), 1563-1572.

Ramamoorthy, S. K., Gardoni, P. and Bracci, J. M. (2006b). "Seismic fragility and confidence bounds for gravity load designed reinforced concrete frames of varying height." *J. Struct. Engrg,* under review.

Ramamoorthy, S. K., Gardoni, P. and Bracci, J. M. (2006c). "A Bayesian approach to update analytical fragility estimates using field data." under preparation, August 2006.

Rao, C. R., and Toutenburg, H. (1997). *Linear models, least squares and alternatives*, Springer, New York.

Rix, G. J., and Fernandez, L. A. (2004). Earthquake ground motion simulation. http://www.ce.gatech.edu/research/mae_ground_motion/, September 2004.

Saidii, M., and Sozen, M. A. (1981). "Simple nonlinear seismic analysis of R/C structures." *J. Struct. Engrg.*, 107, 937-952.

Shinozuka, M., Feng, M. Q., Lee, J., and Naganuma, T. (2000). "Statistical analysis of fragility curves." *J. Eng. Mech.*, 126(12), 1224-1231.

Singhal, A., and Kiremidjian, A. S. (1996). "Method for probabilistic evaluation of seismic structural damage." *J. Struct. Engrg.*, 122(12), 1459-1467.

Singhal, A., and Kiremidjian, A. S. (1998). "Bayesian updating of fragilities with application to RC frames." *J. Struct. Engrg.*, 124(8), 922-929.

Southern Building Code Congress International (SBCCI). (1997). *Standard building code*, Birmingham, Ala.

Velestos, A. S., and Newmark, N. M. (1960). "Effect of inelastic behavior on the response of simple systems to Earthquake motion." *Proc., 2nd World Conf. on Earthquake Engineering*, Tokyo and Kyoto, Japan, Vol. 2, 895-912.

Walker, S. G. (2001). "Seismic performance of existing reinforced concrete beam-column joints." MS Thesis, Univ. of Washington, Seattle.

Wen, Y. K., and Wu, C. L. (2001). "Uniform hazard ground motions for Mid-America cities." *Earthquake Spectra*, 17(2), 359-383.

Wen, Y. K., and Ellingwood, B. R. (2003). "The role of fragility assessment in consequence-based engineering." *Proc., 9th Int. Conf. on Applications of Statistics and Probability in Civil Engineering,* San Francisco,Vol. 1, 1573-1579.

Wen, Y. K., Ellingwood, B. R., and Bracci, J. M. (2004). "Vulnerability functions." *Technical Rep. DS-4,* Mid-America Earthquake Center, Univ. of Illinois at Urbana-Champaign.

Yamazaki, F., and Murao, O. (2000). *Vulnerability functions for Japanese buildings based on damage data from the 1995 Kobe earthquake. Implication of recent earthquakes on seismic risk: Series on Innovation and Construction*, Vol. 2, Imperial College Press, London, 91-102.

VITA

Name: Sathish Kumar Ramamoorthy

Address: Department of Civil Engineering
Texas A&M University
3136 TAMU
College Station, Texas 77843-3136

Email: sathish@tamu.edu

Education: B.E., Civil Engineering, University of Madras, India, 1995
M.E., Structural Engineering, Indian Institute of Science, India, 1999
M.S., Engineering Mechanics, University of Nebraska, Lincoln, 2003
Ph.D., Civil Engineering, Texas A&M University, College Station, 2006